Government of Western Australia

Department of
Mines and Petroleum

REPORT
168

CRUSTAL DIFFERENTIATION IN THE PROTEROZOIC CAPRICORN OROGEN

by SP Johnson, FJ Korhonen, CL Kirkland, JA Cliff, EA Belousova and S Sheppard

EXPLORATION INCENTIVE SCHEME

GEMOC

CCFS

John de Laeter Centre

Curtin University

Geological Survey of Western Australia

Government of **Western Australia**
Department of **Mines and Petroleum**

REPORT 168

CRUSTAL DIFFERENTIATION IN THE PROTEROZOIC CAPRICORN OROGEN

by
SP Johnson, FJ Korhonen, CL Kirkland[1], JA Cliff[2], EA Belousova[3] and S Sheppard[4]

1 Centre for Exploration Targeting – Curtin, Department of Applied Geology, Western Australian School of Mines, Curtin University, Bentley WA 6102, Australia
2 Environmental Molecular Sciences Laboratory, Pacific Northwest National Laboratory, 3335 Innovation Boulevard, Richland, WA 99354, US
3 GEMOC, Department of Earth and Planetary Sciences, Macquarie University, Sydney NSW 2109, Australia
4 Department of Applied Geology, Curtin University, Bentley WA 6102, Australia

Perth 2017

Geological Survey of Western Australia

MINISTER FOR MINES AND PETROLEUM
Hon Bill Johnston MLA

ACTING DIRECTOR GENERAL, DEPARTMENT OF MINES AND PETROLEUM
David Smith

EXECUTIVE DIRECTOR, GEOLOGICAL SURVEY OF WESTERN AUSTRALIA
Rick Rogerson

REFERENCE
The recommended reference for this publication is:
Johnson, SP, Korhonen, FJ, Kirkland, CL, Cliff, JA, Belousova, EA and Sheppard, S 2017, Crustal differentiation in the Proterozoic Capricorn Orogen: Geological Survey of Western Australia, Report 168, 22p.

National Library of Australia Cataloguing-in-Publication entry:

Creator:	Johnson, S. P., author.
Title:	Crustal differentiation in the proterozoic capricorn orogen / SP Johnson, FJ Korhonen, CL Kirkland, JA Cliff, EA Belousova and S Sheppard.
ISBN:	9781741687378 (ebook)
Subjects:	Geological surveys--Western Australia--Capricorn Region. Geology, Stratigraphic--Proterozoic. Capricorn Region (W.A.)
Other Creators/Contributors:	Korhonen, F. J., author. Kirkland, C. L., author. Cliff, J. A., author. Belousova, E. A., author. Sheppard, S., author. Geological Survey of Western Australia, issuing body.

ISSN 0508–4741

Grid references in this publication refer to the Geocentric Datum of Australia 1994 (GDA94). Locations mentioned in the text are referenced using Map Grid Australia (MGA) coordinates, Zone 50. All locations are quoted to at least the nearest 100 m.

Copy editor: SR White
Cartography: J Peng
Desktop publishing: RL Hitchings

Published 2017 by Geological Survey of Western Australia
This Report is available online at <www.dmp.wa.gov.au/GSWApublications>.

Further details of geological publications and maps produced by the Geological Survey of Western Australia are available from:
Information Centre
Department of Mines and Petroleum
100 Plain Street
EAST PERTH WESTERN AUSTRALIA 6004
Telephone: +61 8 9222 3459 Facsimile: +61 8 9222 3444
www.dmp.wa.gov.au/GSWApublications

Cover photograph: Granite tor comprising coarse-grained porphyritic biotite monzogranite of the 1680–1620 Ma Durlacher Supersuite

Contents

Appendix

Figures

Tables

* Table 3 can be found as an Excel spreadsheet on the accompanying USB.

Crustal differentiation in the Proterozoic Capricorn Orogen

by

SP Johnson, FJ Korhonen, CL Kirkland[1], JA Cliff[2], EA Belousova[3] and S Sheppard[4]

Abstract

The in situ chemical differentiation of continental crust ultimately leads to the long-term stability of continents. This process, more commonly known as 'cratonization', is driven by deep crustal melting with the transfer of melts to shallower regions, resulting in a strongly chemically stratified crust in which a refractory, dehydrated lower portion is overlain by a complementary enriched upper portion. Because the lower to middle levels of continental crust are rarely exposed, investigation of the cratonization process must be through indirect methods. In this Report, we use in situ hafnium and oxygen isotope compositions of both magmatic and inherited zircons from several well-dated felsic magmatic suites in the Capricorn Orogen of Western Australia to highlight the differentiation history (i.e. cratonization) of this portion of late Archean to Proterozoic orogenic crust. The Capricorn Orogen shows a distinct tectono-magmatic history that evolved from an active continental margin through to intraplate reworking, ultimately leading to thermally stable crust that responded similarly to the adjacent Archean Pilbara and Yilgarn Cratons. The data define not only the source components from which the magmas were derived, but a range of physical and chemical processes that operated during magma transport and emplacement. These data also identify a previously unknown crustal reservoir in the Capricorn Orogen that may represent the remnants of an Ophthalmian-age magmatic arc.

KEYWORDS: continental crust, cratons, hafnium isotopes, magmatic differentiation, oxygen isotopes, zircon

Introduction

The continental crust is strongly heterogeneous, in terms of both its chemical composition and its physical properties (e.g. Rudnick and Taylor, 1987; Brown and Rushmer, 2006). This is due to differentiation processes whereby magmas generated by partial melting in the deep crust and upper mantle are transported to shallower levels, resulting in a chemically stratified crust in which a refractory, dehydrated lower portion is overlain by a complementary enriched upper portion (e.g. Rudnick, 1995). This process greatly alters the thermal structure and rheology of the crust, ultimately promoting the long-term stability of the continents (Sandiford and McLaren, 2002, Afonso and Ranalli, 2004; McKenzie and Priestley, 2008). Importantly, the differentiation process leads to the heterogeneous distribution of metalliferous ore deposits throughout the lithosphere and so understanding this process has important implications for an understanding of mineral systems (McCuaig et al., 2010; Joly et al., 2012; McCuaig and Hronsky, 2014).

The chemical and isotopic composition of continental crust in most Precambrian cratons and orogens is strongly heterogeneous, indicating that the majority of continental crust on Earth has a long and complicated differentiation history. The differentiation has resulted from the large-scale recycling of pre-existing crust, either in the deep crustal source region or by assimilation of crust during the transport and emplacement of magmas (Hawkesworth and Kemp, 2006b; Iizuka et al., 2010; Cawood et al., 2013). Therefore, understanding the differentiation process not only requires information on source components, including the proportion of mantle-derived material and the composition of the deep crustal source region, but also the chemical and physical history of magmas during their ascent and emplacement (Fisher et al., 2017; Johnson et al., 2017). Routine whole-rock analytical techniques, such as major and trace element chemistry and isotope signatures, provide only an average 'snapshot' of these individual components and, even within large datasets, these components may not always be revealed. However, over the past decade the isotopic compositions

1 Centre for Exploration Targeting – Curtin, Department of Applied Geology, Western Australian School of Mines, Curtin University, Bentley WA 6102, Australia

2 Environmental Molecular Sciences Laboratory, Pacific Northwest National Laboratory, 3335 Innovation Boulevard, Richland, WA 99354, US

3 GEMOC, Department of Earth and Planetary Sciences, Macquarie University, Sydney NSW 2109, Australia

4 Department of Applied Geology, Curtin University, Bentley WA 6102, Australia

of accessory phases such as zircon have proved to be significant tracers for identifying the various isotopic and chemical components in magma generation (e.g. Amelin et al., 2000; Kemp et al., 2007; Iizuka et al., 2010; Hiess et al., 2011; Kirkland et al., 2013).

Zircon is particularly useful in elucidating the chemical and isotopic history of the crust because:

- it is readily formed during the crystallization of silicic magmas (Kelsey et al., 2008; Yakymchuk and Brown, 2014)
- it may not completely dissolve during melting, and can survive multiple melting and melt extraction events (Yakymchuk and Brown, 2014)
- due to its very low lutetium–hafnium (Lu/Hf) ratio and high Hf content, its Lu–Hf composition can be precisely determined, which is a reflection of these components in the melt phase (Kemp et al., 2007; Payne et al., 2016)
- its physical and chemical robustness make it averse to isotopic resetting, even during multiple melting events
- it can preserve an oxygen isotope composition that was in equilibrium with the magma from which it crystallized, due to the slow diffusion of O in zircon (e.g. Cherniak and Watson, 2003; Peck et al., 2003; Page et al., 2007).

Furthermore, since zircon may crystallize over a wide range of temperatures, pressures and physical and chemical conditions, the isotopic data preserved as the crystal grows may retain evidence of both physical and chemical processes that occurred during the transport and emplacement of magmas to form plutons and batholiths in the upper crust (Kemp et al., 2007).

The Proterozoic Capricorn Orogen of Western Australia is ideally suited for an isotopic study of crustal differentiation and stabilization processes because it preserves a long history of magmatism that records a progressive evolution from subduction and continental convergence to intracontinental reworking and eventual cratonization (Sheppard et al., 2010a; Korhonen and Johnson, 2015; Johnson et al., 2017). This Report presents samarium–neodymium (Sm–Nd) whole-rock data, and Lu–Hf and oxygen ($\delta^{18}O$) isotopic data, from previously well-dated magmatic and inherited zircons from the four main felsic magmatic suites of the western Capricorn Orogen. These are used to highlight the differentiation and thermal history of this tract of orogenic crust.

Geological setting

The Proterozoic Capricorn Orogen is a geologically complex region that records the punctuated assembly of the Pilbara and Yilgarn Cratons with the Glenburgh Terrane to form the West Australian Craton (Fig. 1, inset; Cawood and Tyler, 2004). Collisional orogenesis was followed by more than one billion years of crustal reworking in an intraplate setting (Fig. 2; Sheppard et al., 2010a; Johnson et al., 2013; Korhonen and Johnson, 2015). The architecture of the orogen and the location of major crustal structures are generally well understood from deep crustal seismic data (Johnson et al., 2013), and the tectono-magmatic history of the orogen is particularly well known from geochemical, geochronological and isotopic studies (e.g. Sheppard et al., 2004, 2005, 2007, 2010b; Occhipinti et al., 2004; Johnson et al., 2011a, 2013).

The oldest component of the orogen is the Glenburgh Terrane (Fig. 1), which is interpreted to be an exotic microcontinent within the Capricorn Orogen (Occhipinti et al., 2004; Johnson et al., 2011b). The terrane is composed of heterogeneous granitic gneisses of the 2555–2430 Ma Halfway Gneiss (Fig. 2) and voluminous intermediate to granitic rocks of the 2005–1975 Ma Dalgaringa Supersuite (Fig. 2), which form an extensive granitic batholith along the southern margin of the terrane. These units represent the two oldest magmatic events. The Glenburgh Terrane is interpreted to have collided with the Pilbara Craton during the 2215–2145 Ma Ophthalmia Orogeny (Occhipinti et al., 2004; Johnson et al., 2011a), although an associated magmatic arc on either the Pilbara Craton or Glenburgh Terrane margin has yet to be identified. Collision of the combined Pilbara Craton – Glenburgh Terrane with the Yilgarn Craton took place during the latter part (1965–1950 Ma) of the Glenburgh Orogeny (Occhipinti et al., 2004; Johnson et al., 2011a) to form the West Australian Craton (Fig. 2). The whole-rock major, trace, rare earth element, and Sm–Nd composition of the Dalgaringa Supersuite rocks (Sheppard et al., 2004), as well as the Lu–Hf composition of magmatic zircons (Johnson et al., 2011a), indicate those magmas were generated in a continental margin arc setting along the southern margin of the Glenburgh Terrane. This has been interpreted to imply that subduction of oceanic crust was northwards beneath the combined Pilbara Craton – Glenburgh Terrane (Sheppard et al., 2004; Johnson et al., 2011a, 2013).

Following the final assembly of the West Australian Craton, the orogen was structurally and thermally reworked during at least five punctuated, intraplate orogenic events (Fig. 2), with deformation partitioned into discrete tectonic corridors or zones (Fig. 1a; Sheppard et al., 2010a). Many of the events, particularly the older ones, were accompanied by the intrusion of voluminous syntectonic felsic magmatic rocks (Figs 1a and 2), which show similar ‘calc-alkaline’ major, trace and rare earth element whole-rock chemistry (Sheppard et al., 2010b). Cogenetic mafic igneous rocks are rare components of these supersuites, implying that juvenile mantle-derived material does not form a significant component of the exposed magmatic rocks. The whole-rock chemistries of the mafic and felsic magmatic rocks indicate that they were generated and emplaced entirely within an intraplate tectonic setting (Sheppard et al., 2010b). The reworking events include:

- the 1820–1770 Ma Capricorn Orogeny and associated voluminous granite stocks and batholiths of the Moorarie Supersuite (Fig. 2), including the Minnie Creek batholith in the centre of the orogen (Fig. 1a; Sheppard et al., 2010b)

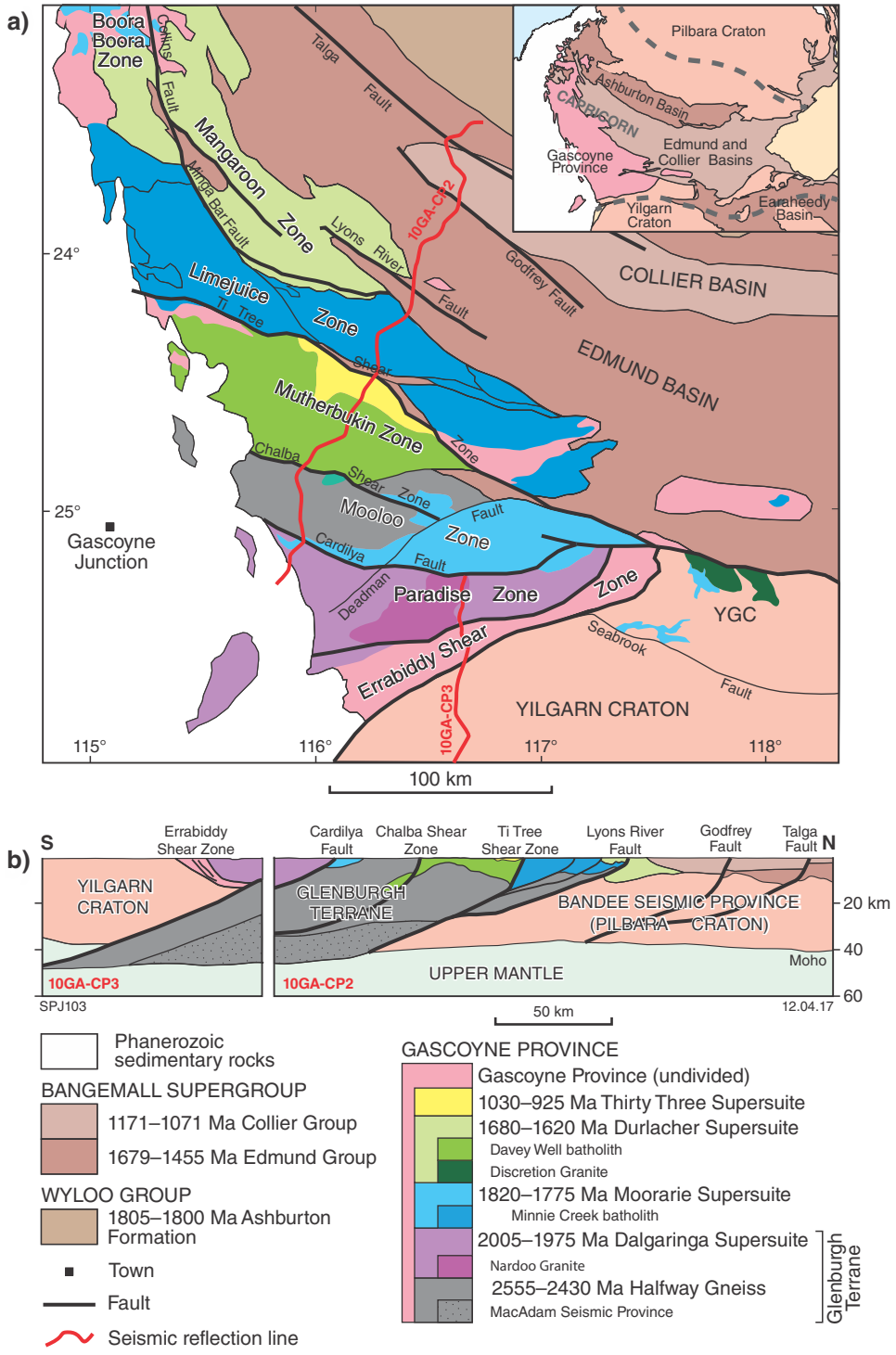

Figure 1. Geology of the western Capricorn Orogen showing the Glenburgh Terrane within the Gascoyne Province, adjacent sedimentary basins, and the Pilbara and Yilgarn Cratons: a) simplified geological map of the Gascoyne Province showing the distribution of magmatic rocks divided into the major magmatic events (see Fig. 2). Inset map shows the location of the province within the Capricorn Orogen (the limits of which are shown by dashed grey lines); b) geological cross-section though the Gascoyne Province, combining the interpretation of deep crustal seismic lines 10GA-CP2 and 10GA-CP3 (Johnson et al., 2013). Abbreviation: YGC, Yarlarweelor Gneiss Complex

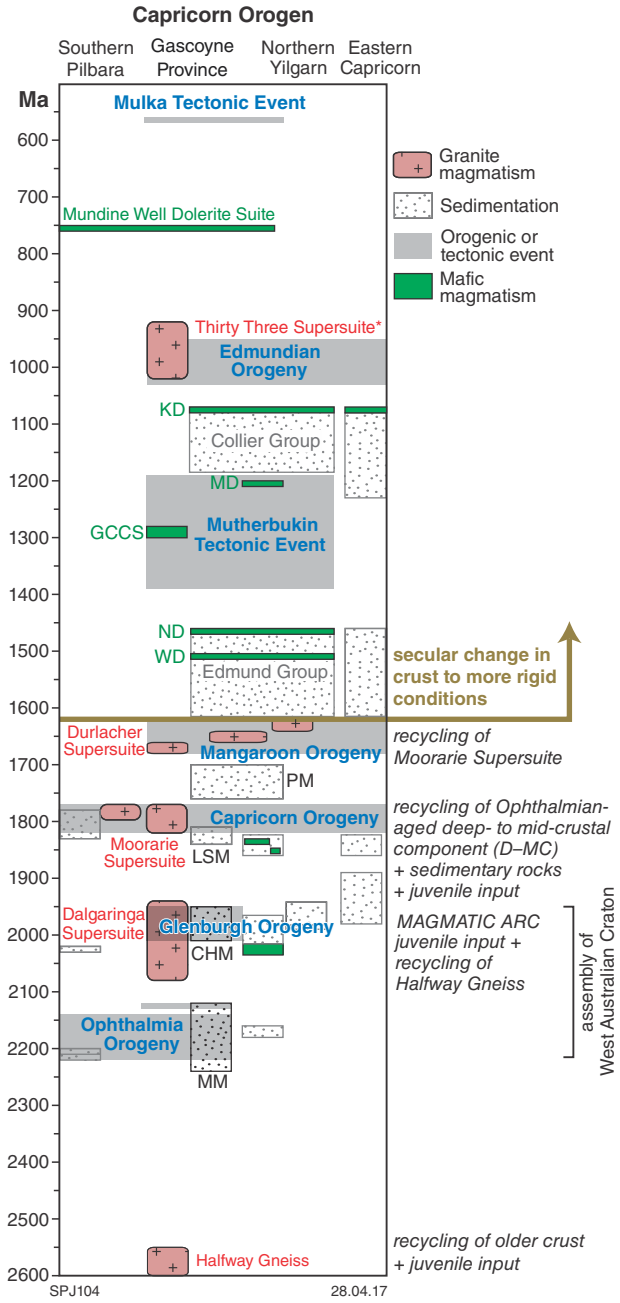

Figure 2. Time–space event summary of the Capricorn Orogen (after Korhonen and Johnson, 2015). Magmatic events shown in red; * denotes minor, localized intrusions. Magmatic evolution models from Johnson et al. (2011a,b, 2013); see text for details. Abbreviations: CHM, Camel Hills Metamorphics; GCCS, Gifford Creek Carbonatite Suite; KD, Kulkatharra Dolerite; LSM, Leake Spring Metamorphics; MD, Muggamurra Dolerite; MM, Moogie Metamorphics; ND, Narimbunna Dolerite; PM, Pooranoo Metamorphics; WD, Waldburg Dolerite

- the 1680–1620 Ma Mangaroon Orogeny (Sheppard et al., 2005) with the intrusion of the Durlacher Supersuite (Fig. 2), including the Davey Well batholith and the Discretion Granite
- the 1321–1171 Ma Mutherbukin Tectonic Event (Korhonen et al., 2015) with no associated magmatism
- the 1030–955 Ma Edmundian Orogeny (Martin and Thorne, 2004; Sheppard et al., 2007), accompanied by the intrusion of volumetrically minor, leucocratic, tourmaline-bearing granite stocks and sheets, and rare earth element-bearing pegmatites, of the Thirty Three Supersuite (Fig. 1a; Sheppard et al., 2007)
- the c. 570 Ma Mulka Tectonic Event (Sheppard et al., 2010a).

Granitic magmas generated during the intraplate magmatic events (Moorarie and Durlacher Supersuites) show a progressive enrichment in the heat-producing elements (HPE; e.g. U–Th–K; Korhonen and Johnson, 2015), demonstrating progressive fractionation of Capricorn Orogen crust with the production of an enriched, silicic, HPE-rich shallow crust. Following the generation of the Durlacher Supersuite, the orogenic crust underwent a broad secular change to more rigid behaviour (Fig. 2), allowing the emplacement of abundant mafic dykes and sills into the shallow crust (Wingate 2003; Morris and Pirajno, 2005), and the formation of thick intracontinental sedimentary basins (Cutten et al., 2016).

Isotope datasets

We present new whole-rock Sm–Nd, and zircon Lu–Hf and $^{18}O/^{16}O$, data and integrate these new data with previously collated Sm–Nd and Lu–Hf datasets to provide a comprehensive compilation of isotope data for felsic rocks from the four main, pre-1600 Ma magmatic events (Sheppard et al., 2004, 2010b; Johnson et al., 2011a). A summary of the analysed samples, including lithology, location, crystallization age, and available isotopic information is provided in Table 1. Lu–Hf and $^{18}O/^{16}O$ isotope analyses were conducted on previously dated magmatic and inherited zircon grains. These zircons were dated by U–Pb secondary ion mass spectrometry (SIMS) with the sensitive high-resolution ion microprobe (SHRIMP II) at the John de Laeter Centre at Curtin University, Perth, Western Australia, following analytical methods described in Wingate and Kirkland (2015). U–Pb zircon age data for samples are provided in GSWA (2016). A description of detailed analytical techniques is provided in the Appendix, tabulated results for whole-rock Sm–Nd are given in Table 2, and zircon Lu–Hf and $^{18}O/^{16}O$ results are presented in Table 3.

Table 1. Locations and ages of felsic and mafic magmatic rocks used in this study, and types of data collected; – indicates no data

Sample	*Sample description*	*Rock name*	*MGA Zone 50 grid coordinate*		*Igneous crystallization age (Ma)*		*Sm–Nd data*	*Lu–Hf data*	*Oxygen data*
			Easting	*Northing*	*age*	*±*			
northen Yilgarn Craton									
139459	foliated porphyritic biotite monzogranite	–	571145	7199919	**2738**	**5**	Y	–	–
168942	porphyritic biotite–muscovite monzogranite gneiss	–	433770	7167639	**2711**	**13**	Y	–	–
139467	pegmatite-banded grey monzogranitic gneiss	–	577945	7208062	**2700**	**6**	Y	–	–
142913	foliated biotite monzogranite	–	509800	7164500	**2687**	**5**	Y	–	–
142902	foliated biotite monzogranite dyke	–	544074	7170960	**2661**	**2**	Y	–	–
142906	coarse porphyritic monzogranite	–	508200	7181000	**2630**	**4**	Y	–	–
142914	porphyritic biotite–hornblende monzogranite	–	513970	7153751	**2615**	**2**	Y	–	–
142907	biotite monzogranite dyke	–	504168	7181129	**2608**	**3**	Y	–	–
142903	foliated porphyritic biotite monzogranite	–	538730	7195900	**2594**	**4**	Y	–	–
139463	pegmatite-banded gneiss	–	576316	7207105	**2523**	**7**	Y	–	–
Halfway Gneiss									
164309	foliated porphyritic biotite granodiorite	–	413480	7225160	**2555**	**4**	Y	Y	–
142988	biotite tonalite	–	401300	7223420	**2552**	**4**	Y	Y	–
168950	pegmatite-banded tonalite gneiss	–	360390	7165760	**2518**	**2**	–	Y	–
188973	metagranodiorite	–	491577	7251062	**2429**	**4**	–	Y	–
Dalgaringa Supersuite									
168952	biotite–hornblende tonalite	–	362230	7165800	**2002**	**5**	–	Y	–
159781[(a)]	mesocratic granodiorite	–	362235	7165795	**2002**	**–**	Y	–	–
142925	biotite monzogranite	–	440930	7200850	**2002**	**3**	Y	Y	–
142926	foliated biotite tonalite	–	443290	7199960	**2002**	**2**	Y	Y	–
159780[(a)]	biotite monzogranite	–	362235	7165795	**2000**	**–**	Y	–	–
144833[(a)]	leucocratic granodiorite	–	443400	7200000	**1999**	**–**	Y	–	–
142930	coarse leucocratic pegmatite	–	428660	7192580	**1994**	**2**	Y	–	–
142933	biotite–hypersthene–cpx mafic granulite	–	421290	7189830	**1989**	**3**	Y	Y	–
159782[(a)]	fine-grained foliated tonalite	–	362235	7165795	**1985**	**–**	Y	–	–
142932	porphyritic granodiorite	Nardoo Granite	425750	7187380	**1977**	**4**	Y	Y	–
142928	biotite tonalite	Nardoo Granite	444850	7186360	**1974**	**4**	Y	Y	–
144836	mesocratic tonalite	Nardoo Granite	439700	7195200	**1974**	**–**	Y	–	–

Table 1. continued

Sample	Sample description	Rock name	MGA Zone 50 grid coordinate		Igneous crystallization age (Ma)		Sm–Nd data	Lu–Hf data	Oxygen data
			Easting	Northing	age	±			
mafic rocks									
144854[a]	amphibolite	–	425100	7194900	**2000**	**–**	Y	–	–
159765[a]	mafic granulite	–	415520	7192420	**2000**	**–**	Y	–	–
Moorarie Supersuite									
southern plutons									
142931	biotite–muscovite granodiorite dyke	–	442540	7208100	**1817**	**11**	Y	–	–
142849	foliated coarse-grained monzogranite	–	560760	7186340	**1813**	**8**	Y	Y	–
142854	foliated granite dyke	–	588400	7191700	**1811**	**9**	Y	–	–
159995	biotite granodiorite	–	413700	7225400	**1811**	**6**	Y	–	–
159987	foliated porphyritic biotite granodiorite	Dumbie Granodiorite	453100	7235160	**1810**	**9**	Y	Y	–
169088	foliated biotite monzogranite		355440	7440020	**1806**	**7**	Y	–	–
188975	metatonalite	Dumbie Granodiorite	453174	7235217	**1804**	**5**	–	Y	Y
142900	muscovite–biotite monzogranite	–	529856	7197186	**1802**	**9**	Y	–	–
144814	biotite monzogranite	Scrubber Granite	460514	7128830	**1800**	**–**	Y	–	–
142852	recrystallized monzogranite dyke	–	591429	7187811	**1797**	**4**	Y	–	–
159996	biotite monzogranite	Scrubber Granite	413420	7224140	**1796**	**6**	Y	Y	Y
Minnie Creek batholith									
183205	foliated mesocratic tonalite	–	386327	7310931	**1807**	**3**	Y	–	–
180947	medium-grained mesocratic monzogranite	–	448344	7291435	**1807**	**5**	Y	–	–
88412	foliated porphyritic monzogranite	–	389940	7332230	**1801**	**5**	Y	Y	–
88411	biotite monzogranite	–	392360	7332260	**1795**	**10**	Y	–	–
191995	foliated monzogranite	–	405118	7196088	**1795**	**7**	Y	Y	Y
88407	porphyritic monzogranite	–	413885	7328156	**1794**	**8**	Y	–	–
178025	biotite monzogranite dyke	–	352200	7356340	**1794**	**4**	Y	–	–
88405	biotite granodiorite	–	417899	7321184	**1792**	**5**	Y	Y	–
88408	granodiorite dyke	–	413783	7328204	**1792**	**4**	Y	–	–
190660	metamonzogranite	Rubberoid Granite	465066	7280382	**1791**	**4**	–	Y	Y
190661	metatonalite	–	465066	7280382	**1801**	**4**	–	Y	Y
190662	gneissic metamonzogranite	Middle Spring Granite	504728	7267401	**1788**	**7**	–	Y	Y

Table 1. continued

Sample	Sample description	Rock name	MGA Zone 50 grid coordinate		Igneous crystallization age (Ma)		Sm–Nd data	Lu–Hf data	Oxygen data
			Easting	Northing	age	±			
88420	biotite granodiorite	–	380093	7318519	**1787**	**4**	Y	–	–
183269	leucocratic equigranular biotite monzogranite	–	395353	7321676	**1786**	**6**	Y	–	–
88414	porphyritic monzogranite	–	364335	7337800	**1783**	**5**	Y	–	–
178024	biotite granodiorite	–	349960	7350180	**1783**	**5**	Y	Y	Y
180933	porphyritic biotite monzogranite dyke	–	432693	7301516	**1782**	**6**	Y	–	–
180938	equigranular biotite monzogranite	–	456845	7296488	**1782**	**5**	Y	Y	Y
88419	porphyritic monzogranite	–	382401	7317220	**1781**	**6**	Y	Y	–
88415	porphyritic granodiorite dyke	–	364313	7337732	**1777**	**8**	Y	–	–
northern plutons									
169088	foliated biotite monzogranite	–	355440	7440020	**1806**	**7**	Y	Y	Y
169087	foliated biotite granodiorite	–	351550	7442960	**1794**	**9**	Y	Y	Y
88444	biotite granodiorite	–	371564	7464595	**1786**	**5**	Y	–	–
88452[(b)]	biotite granodiorite	Booaloo Granodiorite	397322	7517354	**1785**	**–**	Y	–	–
88466[(b)]	biotite granodiorite	–	377458	7516482	**1785**	**–**	Y	–	–
169086	biotite monzogranite	–	348780	7454740	**1784**	**5**	Y	–	–
169089	granophyric syenogranite	–	354260	7431450	**1778**	**11**	–	Y	Y
168780[(b)]	porphyritic biotite granodiorite	–	425540	7351240	**1776**	**–**	Y	–	–
169058	augen orthogneiss	Gooche Gneiss	426780	7357910	**1776**	**8**	–	Y	–
mafic rocks									
183203	metagabbro	–	429537	7310047	**1800**	**–**	Y	–	–
183268	metagabbro	–	441573	7301070	**1800**	**–**	Y	–	–
88446	fine-grained mafic rock	–	424419	7518183	**1800**	**–**	Y	–	–
88448	fine-grained mafic rock	–	423268	7519273	**1800**	**–**	Y	–	–
88449	fine-grained mafic rock	–	423277	7519257	**1800**	**–**	Y	–	–
Durlacher Supersuite									
northern Capricorn Orogen plutons									
169090	porphyritic biotite monzogranite	–	349780	7412530	**1696**	**20**	Y	–	–
88410	muscovite–biotite monzogranite	–	392170	7337210	**1688**	**7**	Y	–	–
169092	biotite–muscovite monzogranite	–	361420	7409000	**1681**	**10**	Y	–	–

Table 1. continued

Sample	*Sample description*	*Rock name*	*MGA Zone 50 grid coordinate*		*Igneous crystallization age (Ma)*		*Sm–Nd data*	*Lu–Hf data*	*Oxygen data*
			Easting	*Northing*	*age*	±			
178030	biotite granodiorite	–	355600	7395370	**1678**	**6**	Y	–	–
178027	biotite–muscovite granodiorite	–	363140	7357610	**1677**	**5**	Y	–	–
169053	biotite–muscovite monzogranite	–	423630	7350161	**1677**	**7**	–	Y	Y
178029	biotite monzogranite	Pimbyana Granite	385720	7367230	**1675**	**11**	Y	Y	Y
169062	porphyritic syenogranite	Dingo Creek Granite	414280	7367460	**1674**	**8**	–	Y	Y
178028	biotite–muscovite syenogranite dyke	Dingo Creek Granite	385760	7367230	**1674**	**8**	Y	–	–
168771	porphyritic syenogranite	Dingo Creek Granite	536530	7133729	**1674**	**–**	Y	–	–
169060	porphyritic syenogranite	Pimbyana Granite	419130	7355190	**1673**	**15**	Y	–	–
168764	porphyritic syenogranite	Pimbyana Granite	429490	7351520	**1673**	**–**	Y	–	–
169055	biotite–muscovite monzogranite	Yangibana Granite	430040	7349370	**1659**	**10**	–	Y	Y
southern Capricorn Orogen									
Davey Well batholith									
183215	coarse-grained porphyritic biotite monzogranite	Davey Well Granite	388798	7302568	**1667**	**4**	Y	Y	Y
191993	foliated porphyritic biotite–garnet monzogranite	–	409860	7294862	**1666**	**8**	Y	–	–
183208	foliated biotite–muscovite monzogranite dyke	–	395769	7296452	**1666**	**6**	Y	–	–
183212	granitic gneiss	–	369872	7298294	**1666**	**5**	Y	–	–
183207	metatonalite/quartz diorite	Tetlow Granite	392922	7297584	**1662**	**5**	Y	Y	Y
185944	porphyritic monzogranite	Davey Well Granite	406039	7246928	**1653**	**10**	–	Y	Y
Discretion Granite									
142855	porphyritic monzogranite	Discretion Granite	592500	7197900	**1619**	**15**	Y	Y	Y

NOTES: (a) Sample from Sheppard et al. (2004)
(b) Sample from Sheppard et al. (2010b)

Table 2. Whole-rock Sm–Nd analyses for felsic and mafic rocks in the western Capricorn Orogen

Sample	Age (Ma)	Sm (ppm)	Nd (ppm)	$^{143}Nd/^{144}Nd$	$^{147}Sm/^{144}Nd$	$^{143}Nd/^{144}Nd_{(i)}$	$\varepsilon_{Nd(i)}$	$T_{DM}2$ (Ga)
northern Yilgarn Craton								
139459	**2738**	2.8	23.2	0.510192	0.074125	0.508853	-4.5	3.3
168942	**2711**	5.2	30.4	0.510787	0.103635	0.508933	-3.7	3.2
139467	**2700**	5.9	41.5	0.510341	0.085987	0.508809	-6.4	3.4
142913	**2687**	3.8	21.1	0.510775	0.108362	0.508854	-5.8	3.3
142902	**2661**	11.2	78.9	0.510337	0.085401	0.508838	-6.8	3.4
142906	**2630**	12.4	83.7	0.510401	0.089115	0.508855	-7.3	3.4
142914	**2615**	21.3	136.9	0.510563	0.093886	0.508944	-5.9	3.3
142907	**2608**	8.9	57.3	0.510526	0.093597	0.508916	-6.6	3.3
142903	**2594**	10.8	80.5	0.510461	0.080823	0.509078	-3.8	3.1
139463	**2523**	6.0	32.7	0.510954	0.111523	0.509099	-5.2	3.1
Halfway Gneiss								
164309	**2555**	11.2	69.0	0.510962	0.098343	0.509312	-0.5	2.8
142988	**2552**	5.7	30.3	0.511162	0.112769	0.509266	-1.3	2.9
Dalgaringa Supersuite								
159781	**2002**	6.1	22.6	0.511933	0.163811	0.509774	-5.3	2.7
142925	**2002**	1.0	8.0	0.511277	0.111900	0.509802	-5.0	2.8
142926	**2002**	4.9	26.1	0.511351	0.111900	0.509876	-3.6	2.7
159780	**2000**	1.9	16.5	0.510706	0.070275	0.509781	-5.2	2.7
144833	**1999**	1.9	12.7	0.511061	0.089745	0.509880	-3.3	2.6
142930	**1994**	0.3	1.7	0.511280	0.113100	0.509795	-5.1	2.7
142933	**1989**	5.7	25.3	0.511775	0.135410	0.510002	-1.2	2.4
159782	**1985**	7.4	39.9	0.511229	0.111774	0.509768	-5.9	2.8
Nardoo Granite								
142932	**1977**	1.7	6.7	0.511814	0.152912	0.509824	-5.0	2.7
142928	**1974**	3.3	22.1	0.511026	0.091061	0.509843	-4.7	2.7
144836	**1977**	4.8	30.0	0.511138	0.097302	0.509872	-4.1	2.6
mafic rocks								
144854	**2000**	2.5	7.6	0.512650	0.197200	0.510054	0.1	2.3
159765	**2000**	2.5	7.8	0.512648	0.190800	0.510136	1.7	2.2
Moorarie Supersuite								
southern plutons								
142931	**1815**	1.9	12.0	0.511081	0.094414	0.509954	-6.6	2.7
142849	**1813**	0.2	1.1	0.510815	0.103441	0.509582	-13.9	3.3
142854	**1812**	3.3	28.2	0.510768	0.071221	0.509919	-7.3	2.8
159995	**1811**	10.8	103.4	0.510732	0.062885	0.509983	-6.1	2.7
159987	**1810**	15.5	90.7	0.511115	0.103124	0.509887	-8.0	2.8
169088	**1806**	6.5	37.1	0.511308	0.105889	0.510050	-4.9	2.6
142900	**1802**	4.4	26.8	0.511131	0.098997	0.509957	-6.8	2.7
144814	**1800**	4.5	24.9	0.511256	0.108540	0.509971	-6.6	2.7
142852	**1797**	4.4	37.5	0.510754	0.071549	0.509908	-7.9	2.8
159996	**1796**	5.0	30.9	0.511195	0.097667	0.510041	-5.4	2.6
Minnie Creek batholith								
183205	**1808**	6.3	30.0	0.511562	0.126131	0.510062	-4.6	2.5
180947	**1804**	6.6	28.9	0.511700	0.139019	0.510050	-5.0	2.6
88412	**1801**	6.7	38.4	0.511407	0.105954	0.510152	-3.1	2.4
88411	**1795**	7.6	46.1	0.511285	0.099878	0.510106	-4.1	2.5
191995	**1795**	4.8	28.7	0.511339	0.100977	0.510157	-3.5	2.4
88407	**1794**	7.5	42.8	0.511401	0.106433	0.510145	-3.4	2.4

Table 2. continued

Sample	Age (Ma)	Sm (ppm)	Nd (ppm)	$^{143}Nd/^{144}Nd$	$^{147}Sm/^{144}Nd$	$^{143}Nd/^{144}Nd_{(i)}$	$\varepsilon_{Nd(i)}$	T_{DM2} (Ga)
178025	**1794**	3.8	28.0	0.511209	0.082267	0.510238	-1.5	2.3
88405	**1792**	7.3	39.2	0.511447	0.112303	0.510123	-3.8	2.5
88408	**1792**	4.9	29.3	0.511354	0.100148	0.510173	-2.9	2.4
88420	**1787**	3.6	19.2	0.511507	0.114016	0.510167	-3.1	2.4
183269	**1786**	3.3	19.4	0.511351	0.103014	0.510137	-3.6	2.5
88414	**1783**	3.8	31.7	0.511003	0.072543	0.510153	-3.5	2.4
178024	**1783**	6.7	39.9	0.511381	0.102044	0.510184	-2.9	2.4
180933	**1782**	10.3	47.4	0.511597	0.131224	0.510059	-5.4	2.6
180938	**1782**	6.4	34.8	0.511384	0.110284	0.510090	-4.7	2.5
88419	**1781**	4.6	30.2	0.511249	0.092549	0.510165	-3.3	2.4
88415	**1777**	7.3	50.1	0.511211	0.088009	0.510182	-3.1	2.4
northern plutons								
169088	**1806**	6.5	37.1	0.511308	0.105889	0.510050	-4.9	2.6
169087	**1794**	7.7	38.4	0.511548	0.121450	0.510115	-4.0	2.5
88444	**1785**	6.6	34.5	0.511395	0.114964	0.510045	-5.6	2.6
88452	**1785**	5.9	30.6	0.511439	0.117044	0.510065	-5.2	2.6
88466	**1785**	6.8	35.4	0.511405	0.115285	0.510051	-5.4	2.6
169086	**1784**	9.9	64.7	0.511114	0.092625	0.510027	-5.9	2.6
168780	**1776**	7.6	51.5	0.511162	0.088987	0.510122	-4.3	2.5
mafic rocks								
183203	**1810**	3.1	14.6	0.511688	0.129344	0.510148	-2.9	2.4
183268	**1800**	1.3	6.6	0.511648	0.123091	0.510190	-2.3	2.4
88446	**1799**	6.9	28.3	0.512067	0.146802	0.510330	0.4	2.1
88448	**1799**	6.6	26.4	0.512140	0.151640	0.510345	0.7	2.1
88449	**1799**	1.6	6.5	0.512161	0.151820	0.510364	1.1	2.1
Durlacher Supersuite								
northern Capricorn Orogen plutons								
169090	**1696**	5.1	32.5	0.511287	0.094097	0.510237	-4.1	2.4
88410	**1688**	4.7	25.7	0.511412	0.111342	0.510189	-5.7	2.5
169092	**1681**	3.8	16.9	0.511661	0.134915	0.510225	-6.3	2.5
178030	**1678**	8.5	53.0	0.511274	0.096792	0.510206	-5.1	2.5
178027	**1677**	12.4	59.3	0.511529	0.126119	0.510138	-6.5	2.6
178029	**1675**	10.3	52.2	0.511465	0.118658	0.510158	-6.1	2.6
168771	**1674**	16.6	99.9	0.511290	0.100478	0.510184	-5.7	2.5
178028	**1674**	16.1	87.0	0.511411	0.112121	0.510177	-5.8	2.5
169060	**1673**	4.7	28.5	0.511346	0.099990	0.510246	-4.5	2.4
168764	**1673**	13.8	101.9	0.511072	0.081931	0.510171	-5.9	2.5
southern Capricorn Orogen								
Davey Well batholith								
183215	**1667**	10.7	56.6	0.511390	0.113918	0.510147	-6.8	2.6
191993	**1666**	8.0	40.3	0.511421	0.120069	0.510110	-7.5	2.7
183208	**1666**	25.3	124.3	0.511447	0.122806	0.510107	-7.5	2.7
183212	**1666**	4.2	20.6	0.511531	0.123410	0.510176	-5.9	2.5
183207	**1662**	16.6	90.9	0.511334	0.110632	0.510119	-7.0	2.6
Discretion Granite								
142855	**1619**	13.1	92.6	0.511052	0.085673	0.510140	-7.9	2.7

Sm–Nd analyses

Samples from 73 granitic rocks and gneisses, ranging in age from c. 2738 to 1619 Ma, were analysed from the Capricorn Orogen, and from the northern margin of the Yilgarn Craton (the Yarlarweelor Gneiss Complex; Fig. 1). The samples yielded evolved to highly evolved (unradiogenic) whole-rock Sm–Nd isotopic compositions with $\varepsilon_{Nd(i)}$ values from –13.9 to –0.5, and two-stage depleted-mantle model ages ($T_{DM}2$) between c. 3.4 and 2.3 Ga (Table 2). The seven associated mafic rocks, with ages of c. 2000 and 1800 Ma, have the least evolved (most radiogenic) compositions, with $\varepsilon_{Nd(i)}$ values between –2.9 and +1.7 and two-stage depleted-mantle model ages between c. 2.4 and 2.1 Ga (Table 2). There is no clear correlation between age and isotopic composition, and within each magmatic supersuite the Nd data form vertical arrays suggesting a mixed source for the magma including relatively juvenile material and highly evolved crust (Fig. 3a). Despite the mafic rocks having the least evolved isotopic compositions, none of them has a composition equivalent to that of the model depleted mantle.

Lu–Hf analyses

Four-hundred and forty-eight analyses of magmatic zircons from 35 granitic rocks, ranging in age from c. 2555 to 1619 Ma, yielded variably evolved Lu–Hf isotopic compositions with $\varepsilon_{Hf(i)}$ values spanning –18.6 to +7.5, corresponding with two-stage depleted-mantle model ages ($T_{DM}2$) between c. 3.4 and 2.1 Ga (Table 2). In common with the Nd data, there is no correlation between Hf isotopic composition and age. The ranges of Hf isotopic compositions of magmatic zircons obtained from individual samples, particularly from granites of the Dalgaringa and Moorarie Supersuites, are relatively large and form vertical arrays (Fig. 3b). This indicates that both relatively juvenile and highly evolved (unradiogenic) crust were involved in the formation of these granitic rocks. The Hf isotopic composition of 121 inherited zircons, which range in age from c. 3724 to 1706 Ma, show similar variably evolved Hf compositions to the magmatic zircons (Table 3; Fig. 3b).

Oxygen analyses

Two-hundred and thirteen $^{18}O/^{16}O$ analyses were conducted on magmatic and inherited zircons. Samples included 11 granitic rocks from the Moorarie Supersuite (six of which were from the Minnie Creek batholith), and eight granitic rocks from the Durlacher Supersuite (three of which were from the Davey Well batholith, and one from the Discretion Granite; Table 3). Analyses were made in both central and exterior portions of zircons where possible. Values for $\delta^{18}O$ ranged between 3.3 and 10.5‰ (± 0.06 – 0.30‰ 1σ).

Moorarie Supersuite

Eighty-nine oxygen analyses were made on magmatic and inherited zircons from the Moorarie Supersuite. The magmatic zircons (n = 63), for which analyses were taken from both central and exterior portions, yielded a range of $\delta^{18}O$ values between 5.9 and 10.5‰. Those from the Minnie Creek batholith (n = 34) show a slightly narrower range between 6.5 and 9.8‰ (Table 3). A large proportion of analyses shows small compositional variations between central and exterior parts of the zircons (between 0.0 and 1.7‰), but the change is not systematic and varies towards both light and heavy compositions (Table 3). Complementary Hf isotopic analyses show significant variations of up to 8.1 ε_{Hf} units (average = 2–3 ε_{Hf} units) between the central and exterior portions (Fig. 4a) but, again, the variation is not systematic, ranging to more- and less-evolved compositions.

Twenty-six analyses were made of 26 inherited zircons ranging in age from c. 2755 to 1840 Ma (most zircons have ages between c. 2280 and 2100 Ma). The zircons have a range of $\delta^{18}O$ values between 3.3 and 9.1‰, although three zircons with the lightest analyses, between 3.3 and 4.9‰, may have been hydrothermally altered. Complementary Hf isotope analyses indicate a range of evolved compositions, and the two datasets overlap (ε_{Hf} values recalculated to c. 1800 Ma) with the most evolved compositions of the magmatic zircons (Fig. 4a).

Durlacher Supersuite

One-hundred and twenty-four $^{18}O/^{16}O$ analyses were made on magmatic and inherited zircons from the Durlacher Supersuite. The magmatic zircons (n = 94), for which analyses were taken from both central and exterior portions, yielded a range of $\delta^{18}O$ values between 6.3 and 10.5‰ (Table 3). Those from the Davey Well batholith (n = 31) and the Discretion Granite (n = 14) yielded a range of values between 6.3 and 7.3‰. Compositional variations between central and exterior parts of the magmatic zircons are small (0.0 – 1.1‰) and generally trend towards lighter compositions, although the Hf isotope analyses show large variations of up to 5.7 ε_{Hf} units (average = 1–3 ε_{Hf} units), mostly towards more-evolved compositions (Fig. 4b).

Thirty analyses of 30 inherited zircons, ranging in age from c. 2683 to 1706 Ma (most zircons have ages of c. 2100 and 1800 Ma) have a wide range of $\delta^{18}O$ values between 4.5 and 10.3‰, although the zircon with the lightest analyses at 4.5‰ may have been hydrothermally altered. Complementary Hf isotope analyses indicate that the c. 1800 Ma zircons mostly have moderately evolved compositions, and plot within the same $\delta^{18}O$ vs $\varepsilon_{Hf(i)}$ space (ε_{Hf} values recalculated to c. 1650 Ma) as the magmatic zircons, whereas all the older inherited zircons have considerably more-evolved compositions (Fig. 4b).

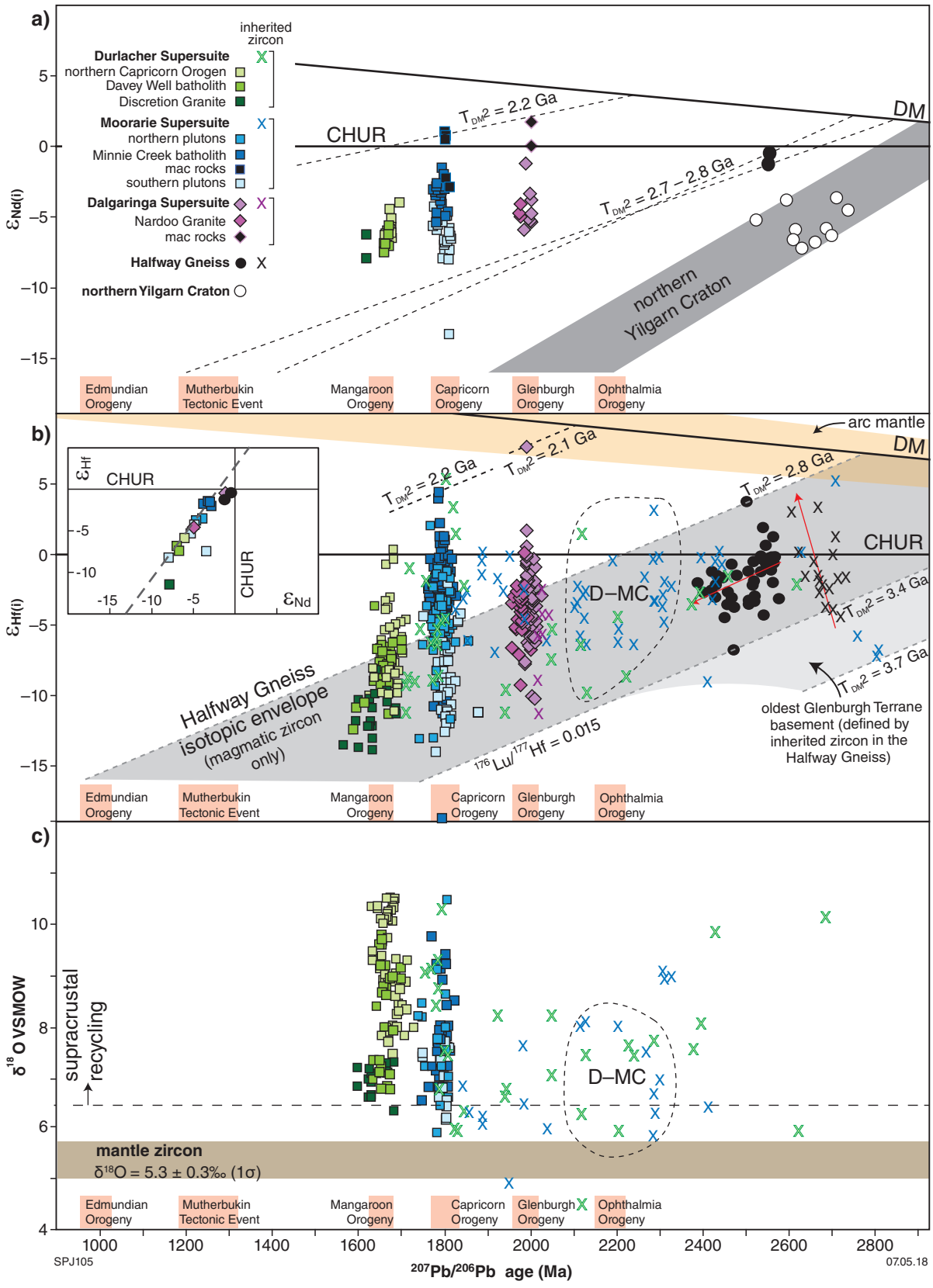
a)
inherited zircon
Durlacher Supersuite
northern Capricorn Orogen
Davey Well batholith
Discretion Granite
Moorarie Supersuite
northern plutons
Minnie Creek batholith
mac rocks
southern plutons
Dalgaringa Supersuite
Nardoo Granite
mac rocks
Halfway Gneiss
northern Yilgarn Craton
CHUR
DM
T DM2 = 2.2 Ga
T DM2 = 2.7 – 2.8 Ga
northern Yilgarn Craton
εNd(i)
Edmundian Orogeny
Mutherbukin Tectonic Event
Mangaroon Orogeny
Capricorn Orogeny
Glenburgh Orogeny
Ophthalmia Orogeny
b)
arc mantle
DM
T DM2 = 2.2 Ga
T DM2 = 2.1 Ga
T DM2 = 2.8 Ga
T DM2 = 3.4 Ga
T DM2 = 3.7 Ga
CHUR
D–MC
Halfway Gneiss isotopic envelope (magmatic zircon only)
176Lu/177Hf = 0.015
oldest Glenburgh Terrane basement (defined by inherited zircon in the Halfway Gneiss)
εHf
εNd
εHf(i)
c)
δ18O VSMOW
supracrustal recycling
D–MC
mantle zircon
δ18O = 5.3 ± 0.3‰ (1σ)
SPJ105
207Pb/206Pb age (Ma)
07.05.18

Figure 3. **(left) Plotted results of isotopic evolution paths for sampled lithological suites: a) whole-rock $\varepsilon_{Nd(i)}$ evolution diagram for both felsic and mafic magmatic rocks of the Capricorn Orogen and the northern Yilgarn Craton. Data are presented in Table 2; b) $\varepsilon_{Hf(i)}$ evolution diagram for magmatic and inherited zircons from felsic magmatic rocks comprising the four main magmatic events. Isotopic data are presented in Table 3. Field for arc mantle based on data of Dhuime et al. (2011). Inset shows a comparison between $\varepsilon_{Hf(i)}$ composition of magmatic zircons and whole-rock $\varepsilon_{Nd(i)}$ compositions for the same sample, which plot on the terrestrial array (dashed grey line) of Vervoort et al. (1999); c) δ^{18}O VSMOW evolution for magmatic and inherited zircons from the Moorarie and Durlacher Supersuites. Data are presented in Table 3. The compositional field for zircon in equilibrium with mantle-derived melts has a δ^{18}O VSMOW value of 5.3 ± 0.3‰ (1σ; Valley, 2003). Abbreviation: D–MC, deep to middle crustal component, see text for explanation**

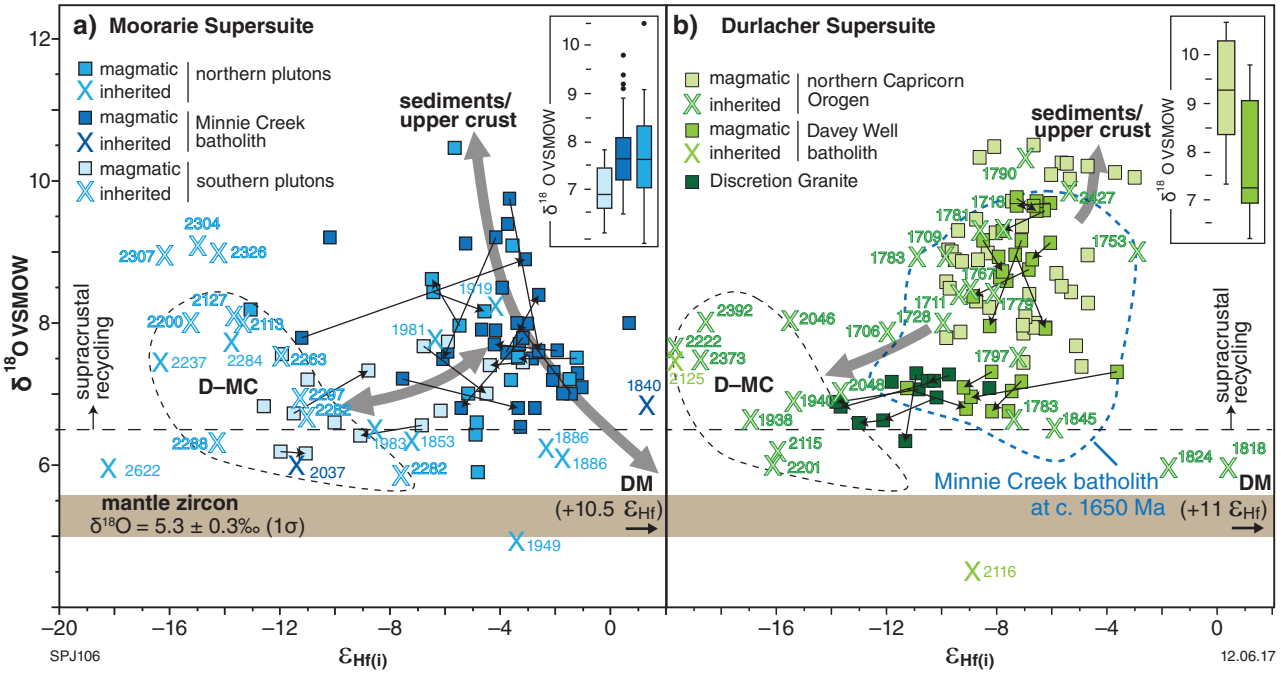

Figure 4. **δ^{18}O vs $\varepsilon_{Hf(i)}$ plot for magmatic zircons in granitic rocks formed during intracontinental reworking: a) Moorarie Supersuite; b) Durlacher Supersuite. Analyses were made in central and edge regions of magmatic zircons where possible to track the isotopic evolution of individual magma pulses and batches; thin arrows show centre–edge pairs. ε_{Hf} composition of the inherited zircons is shown at the time of emplacement of the magmatic event, i.e. $\varepsilon_{Hf(1800\ Ma)}$ and $\varepsilon_{Hf(1650\ Ma)}$, respectively (recalculated data presented in Table 3), assuming a $^{176}Lu/^{177}Hf$ composition of 0.015 for average continental crust (Griffin et al., 2004). The crystallization age (Ma [1σ]) of inherited zircons is given next to each analysis. Box-and-whisker plots (insets) show the range and median values of δ^{18}O VSMOW compositions for each magmatic event. Whiskers extend to 95th and 5th percentiles; outliers shown as closed dots. Compositional field for zircon in equilibrium with mantle-derived melts has δ^{18}O VSMOW value of 5.3 ± 0.3‰ (1σ; Valley, 2003). Abbreviation: D–MC, deep to mid-crustal component**

Isotopic constraints on magma genesis

Granitic and mafic rocks from each of the four magmatic events have a wide range of initial Nd isotopic compositions (Table 2), generally forming vertical $\varepsilon_{Nd(i)}$ arrays (Fig. 3a). The granitic rocks are all more evolved than Chondritic Uniform Reservoir (CHUR), but the associated mafic rocks extend to more radiogenic compositions (Fig. 3a). The range in isotopic composition is replicated by magmatic zircons in the Lu–Hf system (Fig. 3b; Table 3). The majority of magmatic zircons are more evolved than CHUR and, apart from magmatic zircons, from the Durlacher Supersuite, the vertical arrays extend to radiogenic compositions, and the least-evolved zircons have compositions comparable with the initial whole-rock Nd isotopic composition of the mafic rocks. Although none of the zircons has a composition equivalent to depleted mantle, the least evolved analyses from the Halfway Gneiss and Dalgaringa Supersuite are comparable in composition to magmatic zircon of new crust formed in magmatic arcs (Dhumie et al., 2011; orange band in Fig. 3b). Generally, these least-evolved analyses are only a very minor proportion of the data, although they are comparable to the whole-rock Nd isotopic composition of contemporaneous mafic rocks; (Fig. 3a). The vertical $\varepsilon_{Nd(i)}$ and $\varepsilon_{Hf(i)}$ arrays indicate that most of the granitic rocks were generated by mixing of radiogenic (juvenile) crust with highly evolved crust, either in a deep crustal setting

during magma generation, or by assimilation of evolved shallow crustal material during magma emplacement, or both.

Halfway Gneiss: oldest crustal basement

Inherited zircons within the Halfway Gneiss range from c. 2600 to as old as c. 3558 Ma. The oldest zircons (>2750 Ma) have the most juvenile Hf isotopic compositions, giving $T_{DM}2$ model ages of c. 3700 Ma (Table 3; Johnson et al., 2011b). These gneissic rocks lack any evidence for interaction with, or assimilation of, (meta)sedimentary material (Sheppard et al., 2010a; Johnson et al., 2011b), suggesting that these zircons may have been derived from the deep crust during melting. If this is the case, then the isotopic compositions of these zircons indicate that vestiges of the Glenburgh Terrane were formed from juvenile sources at c. 3700 Ma (Johnson et al., 2011b). Inherited zircons dated at 2730–2600 Ma define a steeply sloping $\varepsilon_{Hf(i)}$ array (subvertical arrow, Fig. 3b). The most evolved zircons in this component have isotopic compositions equivalent to the oldest crust in the Glenburgh Terrane (c. 3700 Ma) and show a progressive trend to more juvenile compositions through time (c. 130 Ma), indicating mixing between the oldest Glenburgh Terrane crust, and increasing components of a source similar to juvenile depleted mantle. Magmatic zircons that define the youngest component of the Halfway Gneiss at 2555–2430 Ma have compositions that lie within the isotopic envelope of the 2730–2600 Ma zircons and become more evolved through time (subhorizontal arrow, Fig. 3b), lying on a trend that corresponds to the $^{176}Lu/^{177}Hf$ composition of average continental crust (0.015; Griffin et al., 2004). This implies that the exposed granitic gneisses with ages between c. 2555 and 2430 Ma were formed by the remelting and redistribution of pre-existing crust without the addition of significant juvenile mantle-derived material.

Dalgaringa Supersuite: continental margin magmatism

Magmatic zircons from the Dalgaringa Supersuite show a wide range of $\varepsilon_{Hf(i)}$ compositions, equivalent to the whole-rock Nd isotopic composition for both mafic and felsic rocks (Fig. 3a,b). The most juvenile compositions observed in this study are associated with the Dalgaringa Supersuite rocks; however, the majority of magmatic zircons have evolved compositions that lie within the isotopic envelope of the Halfway Gneiss. The granitic rocks are mostly intermediate to felsic (i.e. tonalite, granodiorite and quartz diorite), and have whole-rock major, trace and rare earth element compositions similar to those in Phanerozoic Andean-type batholiths (Sheppard et al., 2004). The whole-rock major and trace element compositions also indicate that the magmatic rocks were generated from a chemically heterogeneous source in the middle to deep crust (Sheppard et al., 2004). The rocks lack any evidence for interaction with major metasedimentary components, and peak pressure–temperature estimates suggest that the currently exposed granitic rocks were emplaced in the middle crust (Johnson et al., 2011a). These features suggest that the highly evolved isotopic component of the Hf and Nd arrays (Fig. 3a,b) may characterize the deep crustal source. The range of isotopic compositions is consistent with mixing, melting, and assimilation of the isotopically and chemically heterogeneous Halfway Gneiss, and older vestiges, with juvenile basaltic melts in a suprasubduction zone setting. The formation of the Dalgaringa Supersuite within an active continental margin represents a significant period of crustal growth in the evolution of the orogen, with subsequent events dominated by intracontinental reworking.

Moorarie Supersuite: intraplate reworking, Stage 1

Granitic rocks of the Moorarie Supersuite are relatively silicic (61–77 wt% SiO_2, average = 70 wt% SiO_2) and peraluminous, and have calc-alkalic major and trace element compositions that are distinct from granitic rocks typically formed in Andean-type margins (Sheppard et al., 2010b). They show a very wide range of whole-rock Nd and magmatic zircon Hf isotopic compositions, although rocks from the Minnie Creek batholith and those in the northern part of the orogen are generally less evolved than those in the south (Fig. 3a,b). The mafic rocks, all of which form decametre-scale inclusions within the Minnie Creek batholith, have the least-evolved compositions, overlapping in part with the least-evolved granitic rocks from the batholith (Fig. 3a). The most-evolved rocks within the Minnie Creek batholith, and nearly all of the other granitic rocks in the Moorarie Supersuite, have isotope compositions that lie within the isotopic envelope of the Halfway Gneiss. The strong vertical $\varepsilon_{Nd(i)}$ and $\varepsilon_{Hf(i)}$ arrays, and presence of radiogenic mafic material (Fig. 3a), suggest that rocks of the Moorarie Supersuite were generated by the interaction and variable mixing between a source similar to depleted mantle and evolved crust, either in the deep crust during melt formation, or in the shallow crust during emplacement, or both.

Where multiple Hf isotope analyses have been made on single magmatic zircons, significant variations of up to 8.1 $\varepsilon_{Hf(i)}$ units (average = 2–3 ε_{Hf} units) are recorded between the central and exterior portions of zircons, although the sense of the variation is not systematic between centres and edges (Fig. 4a). Complementary $^{18}O/^{16}O$ analyses show a similar but smaller nonsystematic heterogeneity, with a range of $\delta^{18}O$ values recorded between 5.9 and 10.5‰ (Fig. 4a; Table 3). These intragrain isotopic variations are present within all the analysed samples irrespective of geographic location. The range of $\varepsilon_{Hf(i)}$ and $\delta^{18}O$ magmatic zircon compositions define at least three end-member isotopic components (Fig. 4a), with these characteristics:

- radiogenic $\varepsilon_{Hf(i)}$ compositions and light $\delta^{18}O$ values, similar to that of depleted mantle
- variably evolved $\varepsilon_{Hf(i)}$ compositions and heavy $\delta^{18}O$ values characteristic of sedimentary and upper-crustal rocks

- variably evolved $\varepsilon_{Hf(i)}$ compositions with relatively light to moderate $\delta^{18}O$ values which might represent a deep or mid-crustal component (D–MC in Fig. 4a; i.e. an old or evolved crustal component that has not interacted significantly with shallow-crustal material).

This third component is also defined by abundant inherited zircons within the Moorarie Supersuite granitic rocks, which have a restricted range of U–Pb dates mostly between c. 2280 and 2115 Ma (Fig. 4a; Table 3).

Most magmatic zircons from the Minnie Creek batholith and granitic rocks in the northern part of the orogen show a greater variation, both within and between zircons, in $\delta^{18}O$ values than $\varepsilon_{Hf(i)}$ compositions, plotting on a mixing trend between depleted mantle and sedimentary and upper crustal end members (Fig. 4a). Intragrain variations are not consistent. Centre–edge pairs show both increases and decreases in $\delta^{18}O$ values towards juvenile or more-evolved $\varepsilon_{Hf(i)}$ compositions (Fig. 4a). Some of the magmatic zircon cores have highly evolved $\varepsilon_{Hf(i)}$ compositions and moderate $\delta^{18}O$ values similar to the inferred deep or mid-crustal component. These relationships demonstrate that individual magmatic zircons crystallized in a dynamic magmatic setting, where individual magma batches were constantly changing composition due to crustal assimilation and wallrock interaction, as well as periods of magma recharge, producing more juvenile compositions. It is also highly likely that individual rocks contain magmatic zircons derived from multiple magma batches, which coalesced during magma ascent and emplacement. The presence of abundant, metre- to kilometre-scale, greenschist facies inclusions of metasedimentary material within the Minnie Creek batholith, and the emplacement of the northern plutons into similar low-grade metasedimentary rocks, indicate that these magmatic rocks represent the upper crustal portions of the magmatic system.

Magmatic zircons from the granitic rocks in the southern part of the orogen show a greater variation in $\varepsilon_{Hf(i)}$ composition than in $\delta^{18}O$ values (Fig. 4a). A significant proportion of the magmatic zircons have isotopic compositions similar to the inferred deep or mid-crustal end member, with a few analyses plotting close to a mixing trend between depleted-mantle and sedimentary and upper crustal components. Although there is no consistency in the direction in which isotopic composition changes between centre–edge pairs, there is a relatively strong orientation of trends towards or away from the inferred deep or mid-crustal component (Fig. 4a). The strong influence of the deep or mid-crustal component on the isotopic composition of the magmatic zircons suggests that these rocks could have been generated by the melting of cryptic c. 2280 and 2115 Ma material in the deep to middle crust. The cause of melting is not known, but may have been related to the intrusion of low-volume, juvenile, depleted-mantle melts. The relatively light $\delta^{18}O$ values of the magmatic zircon (Fig. 4a inset) suggest that these rocks did not interact significantly with the shallow crust, and therefore may represent the deeper portions of the magmatic system.

Despite these minor variations, all the granitic rocks from the Moorarie Supersuite appear to have common source components. This indicates mixing of the upper and middle–lower crust with some depleted-mantle input, which implies the Moorarie Supersuite was dominated by crustal reworking, with only minor amounts of new crustal growth.

Durlacher Supersuite: intraplate reworking, Stage 2

Granitic rocks associated with the Durlacher Supersuite are relatively silicic (59–76 wt% SiO_2, average = 70 wt% SiO_2) and peraluminous, and have calc-alkalic major and trace element compositions. They show a relatively narrow, but highly evolved range of whole-rock Nd and magmatic zircon Hf isotopic compositions that lie within the isotopic envelope of the Moorarie Supersuite (Fig. 3a,b). The distinct lack of any radiogenic whole-rock compositions, and absence of any associated mafic material, suggests that these granitic rocks may have been generated in a setting without the involvement of significant depleted-mantle melts. This is consistent with the range of magmatic zircon $\varepsilon_{Hf(i)}$ and $\delta^{18}O$ compositions, which are nearly identical to those of the Minnie Creek batholith (compositions recalculated at c. 1650 Ma; Fig. 4b). Additionally, the few inherited zircons present in these rocks (Table 3) also have ages and Hf and $\delta^{18}O$ isotopic compositions similar to magmatic zircons from the Minnie Creek batholith (Figs 3b and 4b).

In the northern part of the orogen (Fig. 1), the granitic rocks contain abundant enclaves and rafts of partially assimilated granitic gneisses from the Moorarie Supersuite, as well as low- to medium-grade metasedimentary rocks (i.e. Pooranoo Metamorphics; Sheppard et al., 2005, 2010a). Magmatic zircons from the granitic rocks have variable, but mostly heavy, $\delta^{18}O$ compositions from 7.4 to 12.9‰ (Table 3; Fig. 4b inset; mean = 9.3‰), consistent with the assimilation of shallow crustal rocks. The generation and emplacement of the granitic rocks were synchronous with low-pressure, moderate- to high-temperature metamorphism during the Mangaroon Orogeny (Sheppard et al., 2005). The isotopic composition of the magmatic zircons suggests that the magmas were generated by the melting of pre-existing crust, with similar compositions to the Minnie Creek batholith, and subsequent contamination by shallow crustal rocks during magma emplacement and crystallization.

In the southern and central parts of the orogen, the Discretion Granite and large parts of the Davey Well batholith (Fig. 1) show no evidence for interaction with shallow crustal rocks; magmatic zircons from these rocks have the lightest $\delta^{18}O$ compositions, from 6.3 – 9.8‰ (median = 7.3‰; Fig. 4b inset; Table 3). Within these zircons, variations of up to 5.3 ε_{Hf} units (average = 1.5 ε_{Hf} units) are recorded between centres and edges, with the exterior portions generally recording more-evolved compositions (Fig. 4b). Complementary $^{18}O/^{16}O$ analyses show similarly small heterogeneities ($\delta^{18}O$ values differ by up to 1.2‰; Table 3), with the exterior portions of zircons generally recording lighter $\delta^{18}O$ compositions (Fig. 4b). Most zircon centres have isotopic compositions

equivalent to those of magmatic zircons from the Minnie Creek batholith (compositions recalculated at c. 1650 Ma; Fig. 4b). With rare exceptions, centre–edge pairs, particularly those from the Discretion Granite, consistently show a change in composition towards the deep to mid-crustal component (D–MC; compositions recalculated at c. 1650 Ma; Fig. 4b). Granitic rocks of the Davey Well batholith and the Discretion Granite post-date deformation and metamorphic events associated with the Mangaroon Orogeny (Sheppard et al., 2010a). The isotopic composition of the magmatic zircons suggests that these melts were also generated by the melting of pre-existing crust, similar in composition to the Minnie Creek batholith. The lack of shallow crustal enclaves or material within the granitic rocks, and the low to moderate $\delta^{18}O$ compositions of the magmatic zircons, suggest that these magmas did not interact with shallow crustal material, and were probably emplaced in the middle crust. The relatively consistent intragrain variations show that during zircon crystallization, either during magma transport or emplacement, these magmas re-equilibrated with highly evolved crust similar in composition to the deep to mid-crustal component.

The primary source of the Durlacher Supersuite magmatic rocks was the melting and recycling of mid-crustal granitic rocks with compositions similar to those of the Moorarie Supersuite; in particular, those of the Minnie Creek batholith. Rocks from the northern part of the orogen also preserve a minor contribution from the upper crust, whereas the southern and central parts show minor mixing with a deep to mid-crustal component. A similar relationship was observed for granitic rocks from the Moorarie Supersuite, suggesting that the southern and central parts of the orogen likely preserve a deeper crustal section, compared to the northern part. However, in contrast to the Moorarie Supersuite, rocks of the Durlacher Supersuite appear to have formed exclusively by crustal reworking with no new crustal growth.

Differentiation and thermal history of Capricorn Orogen crust

The orogen-scale isotopic (whole-rock Nd and in situ magmatic zircon Hf) evolution of the four main ≥1600 Ma magmatic events in the western Capricorn Orogen reveals a near-complete record of crustal differentiation. Following generation of the Halfway Gneiss, the magmatic rocks record a progressive history of stabilization, from new crustal growth along a subduction margin (Dalgaringa Supersuite) to intraplate reworking (Moorarie and Durlacher Supersuites) that is closely followed by broad cooling of the crust.

Vertical isotopic arrays and contributing source components

Most of the magmatic rocks have isotopic compositions that form vertical Hf and Nd arrays (Fig. 3). The most-evolved components from each magmatic event have isotopic compositions that generally lie within the isotopic envelope of the Halfway Gneiss basement rocks and, at least for the Dalgaringa and Moorarie Supersuite rocks, extend to compositions that are more radiogenic than CHUR (Fig. 3). These data imply that the magmas could have been generated by simple two-component melting and mixing between the Halfway Gneiss and mantle-derived material. However, the complementary Hf and O isotope data from magmatic and inherited zircon, particularly from the Moorarie Supersuite, demonstrate that this model is far too simplistic (Fig. 4a). In fact, the scarcity of zircons inherited from the Halfway Gneiss within any of the younger magmatic rocks suggests that basement rocks may not have formed a major source component. Instead, the Halfway Gneiss isotope data record a range of sources that include components from a previously unrecognized crustal source with U–Pb dates between c. 2280 and 2115 Ma (D–MC, Figs 3 and 4), as well as a range of magmatic processes related to the transport and emplacement of these magmatic rocks at shallower crustal levels. Although zircon can be formed during deep crustal melting (e.g. Yakymchuk and Brown, 2014), most magmatic zircons form during the cooling and crystallization of melt in shallow to mid-crustal plutons, by which time the melt compositions may have been greatly modified by fractionation, crustal assimilation and wallrock interaction. Therefore, without additional isotopic information such as complementary zircon oxygen data, it is particularly difficult from zircon Hf data alone to resolve the contributions of various source components and magmatic processes to the isotopic complexity of the felsic magmatic rocks. Such complexity has also been noted in circum-Pacific, I-type granitic rocks (Lackey et al., 2005; Kemp et al., 2007) that formed in the absence of evolved continental crust (White and Chappell 1977), and which are considered to be major contributors to crustal growth.

The recognition of a 'cryptic' 2280–2115 Ma deep crustal reservoir has significant implications for the tectonic evolution of the Capricorn Orogen. The moderately evolved Hf and light to moderate oxygen isotopic composition of this crustal reservoir indicates that it was generated from significant mantle-derived components with minor amounts of evolved crust, and is similar in composition to the I-type granitic rocks from the Lachlan Fold Belt in eastern Australia (Kemp et al., 2007). Considering the age and isotopic composition of this 'cryptic' crust, it is possible that it may have formed in a suprasubduction setting leading up to the 2215–2145 Ma Ophthalmia Orogeny (Figs 2 and 5a) that sutured the Glenburgh Terrane and Pilbara Craton (Occhipinti et al., 2004; Johnson et al., 2011a). Exposed crust of this age and character is currently unknown within the orogen.

Crustal differentiation during intraplate reworking

Following the assembly of the West Australian Craton during the 2005–1950 Ma Glenburgh Orogeny (Fig. 5b), the Moorarie and Durlacher Supersuites were generated entirely in an intraplate setting (Fig. 5c,d; Sheppard et al., 2005, 2010b). Despite the different crustal levels

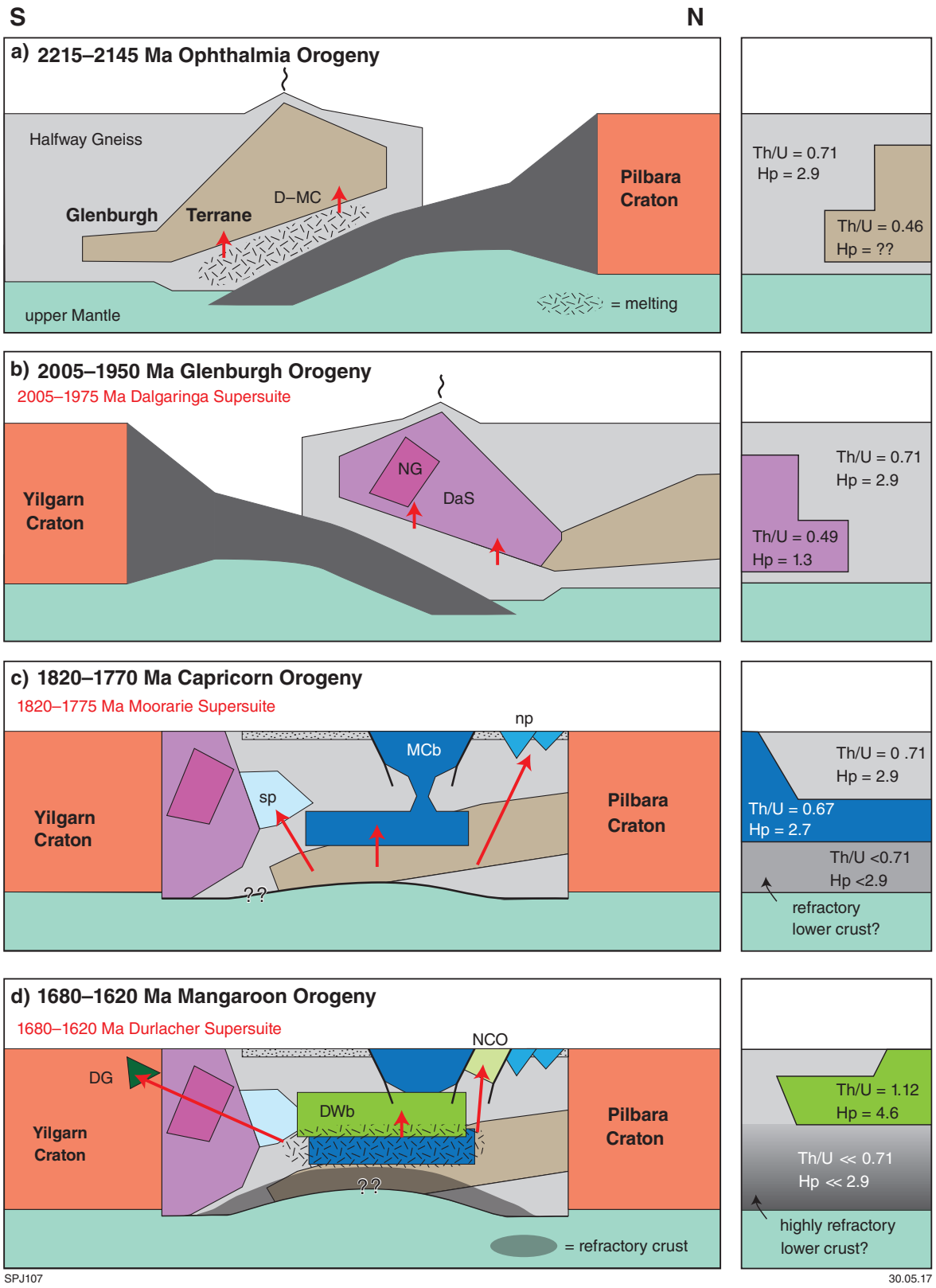

Figure 5. Series of cartoons illustrating the tectono-magmatic evolution of the Capricorn Orogen as derived from the isotopic data presented here: a) Ophthalmia Orogeny; b) Glenburgh Orogeny; c) Capricorn Orogeny; d) Mangaroon Orogeny. Panels on the right-hand side provide a summary of the median Th/U ratio of magmatic zircon (Table 3) and the present-day heat production (Hp [μWm^{-3}]; Korhonen and Johnson, 2015) for the major crustal components. Abbreviations: D–MC, deep to mid-crustal component; DG, Discretion Granite (Durlacher Supersuite); DaS, Dalgaringa Supersuite; DWb, Davey Well batholith (Durlacher Supersuite); MCb, Minnie Creek batholith (Moorarie Supersuite); NG, Nardoo Granite (Dalgaringa Supersuite); np, northern plutons (Moorarie Supersuite); NCO, northern Capricorn Orogen plutons (Durlacher Supersuite); sp, southern plutons (Moorarie Supersuite)

exposed, the Hf and O isotopic composition of magmatic and inherited zircons indicate that all granitic rocks of the Moorarie Supersuite were generated from three main source components including minor amounts of mantle-derived material, shallow crustal rock, as well as a significant contribution from the 2280–2115 Ma component (D–MC, Figs 3, 4 and 5c). Granitic rocks of the Durlacher Supersuite show no isotopic evidence for the involvement of mantle-derived source components, and appear to have been generated by the direct melting and recycling of rocks similar in isotopic composition to the Moorarie Supersuite (Fig. 5d), although the thermal and tectonic driver for melt generation is currently unknown. The deeper level granitic rocks, such as the Davey Well batholith and Discretion Granite, also interacted strongly with the 2280–2115 Ma component.

The progression from an active magmatic arc (Dalgaringa Supersuite) to reworking with minor amounts of new crustal growth (Moorarie Supersuite) to exclusive reworking (Durlacher Supersuite) was accompanied by a progressive decrease in the contribution from mantle-derived sources (Fig. 4a,b), and a complementary increase in radiogenic heat production (Fig. 5a–d; Korhonen and Johnson, 2015). This progression is reflected by an increase in the Th/U ratio of magmatic zircon with time (Fig. 6; Korhonen and Johnson, 2015). The greatest step in heat production and zircon Th/U ratio is recorded by the granitic rocks of the Durlacher Supersuite (Figs 5d and 6), following which the orogen did not experience any further major felsic magmatic events (Fig. 2). In magmatically active regions of crust, lower-crustal fertility is maintained principally due to the input of mantle-derived material (e.g. Petford and Gallgher, 2001). In the Capricorn Orogen, the change in tectonic setting from an active margin to intraplate orogen may have been the principal driver of differentiation of the crust, due to decreasing accessibility to fertile mantle sources following collision. The generation of voluminous felsic magmatic rocks during intraplate reworking would have led to a complementary and rapid depletion in the lower crust, eventually leading to completely refractory lower crust during the generation of the Durlacher Supersuite rocks (Fig. 5d).

A deep crustal seismic reflection line across the Capricorn Orogen has identified a region of lower crust, the MacAdam Seismic Province (Fig. 1b), that has a significantly different reflective character to shallower, overlying parts of the Glenburgh Terrane (Johnson et al., 2013). Inverse gravity modelling across this part of the seismic line indicates that this distinct portion of lower crust is extremely dense (3000–3300 kg/m^3; Aitken, et al., 2014), even for typical lower crustal rocks, and may therefore be the refractory portion of the orogenic crust.

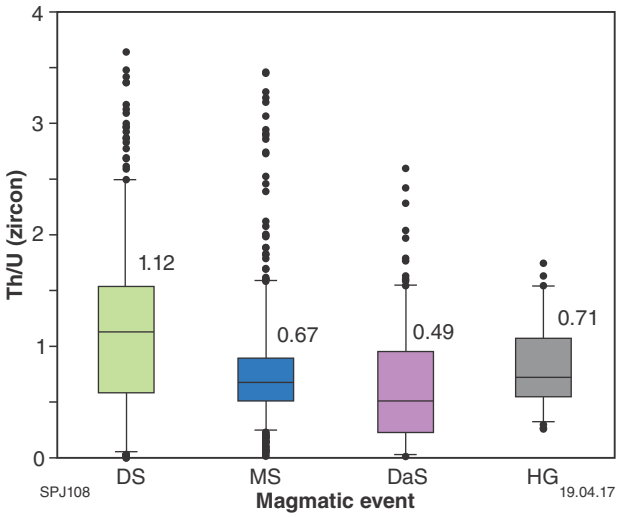

Figure 6. **Box-and-whisker plot (after Korhonen and Johnson, 2015) showing the median Th/U ratios of magmatic zircons from the four main magmatic events. Whiskers extend to 95th and 5th percentiles; outliers shown as closed dots. Abbreviations: DaS, Dalgaringa Supersuite; DS, Durlacher Supersuite; HG, Halfway Gneiss; MS, Moorarie Supersuite**

References

Afonso, JC and Ranalli, G 2004, Crustal and mantle strengths in continental lithosphere: is the jelly sandwich model absolute?: Tectonophysics, v. 394, p. 221–232.

Aitken, ARA, Joly, A, Dentith, MC, Johnson, SP, Thorne, AM and Tyler, IM 2014, 3D architecture, structural evolution, and mineral prospectivity of the Gascoyne Province: Geological Survey of Western Australia, Report 123, 94p.

Amelin, Y, Lee, D-C and Halliday, AN 2000, Early–middle Archaean crustal evolution deduced from Lu–Hf and U–Pb isotopic studies of single zircon grains: Geochimica et Cosmochimica Acta, v. 64, p. 4205–4225.

Blichert-Toft, J and Albarède, F 1997, The Lu–Hf isotope geochemistry of chondrites and the evolution of the mantle–crust system: Earth and Planetary Science Letters, v. 148, p. 243–258.

Brown, M and Rushmer, T (eds) 2006, Evolution and differentiation of continental crust: Cambridge University Press, Cambridge, 550p.

Cavosie, AJ, Valley, JW, Kita, NT, Spicuzza, MJ, Ushikubo, T and Wilde, SA 2011, The origin of high $\delta^{18}O$ zircons: marbles, megacrysts, and metamorphism: Contributions to Mineralogy and Petrology, v. 162, p. 961–974.

Cawood, PA and Tyler, IMT 2004, Assembling and reactivating the Proterozoic Capricorn Orogen: lithotectonic elements, orogenies, and significance: Precambrian Research, v. 128, p. 201–218.

Cawood, PA, Hawkesworth, CJ and Dhuime, B 2013, The continental record and the generation of continental crust: Geological Society of America Bulletin, v. 125, p. 33–47.

Cherniak, DJ and Watson, EB 2003, Diffusion in zircon, *in* Zircon *edited by* JM Hanchar and PWO Hoskin: Reviews in Mineralogy and Geochemistry, v. 53, p. 113–143.

Cutten, HN, Johnson, SP, Thorne, AM, Wingate, MTD, Kirkland, CL, Belousova, EA, Blay, OA and Zwingmann, H 2016, Deposition, provenance, inversion history and mineralization of the Proterozoic Edmund and Collier Basins, Capricorn Orogen: Geological Survey of Western Australia, Report 127, 74 p.

DeBievre, P and Taylor, P 1993, Table of the isotopic composition of the elements: International Journal of Mass Spectrometry and Ion Processes, v. 123, p. 149.

Dhumie, B, Hawksworth, C and Cawood, P 2011, When continents formed: Science, v. 331, p. 154–155.

Fisher, CM, Hanchar, JM, Miller, CF, Phillips, S, Vervoort, JD and Whitehouse, MJ 2017, Combining Nd isotopes in monazite and Hf isotopes in zircon to understand complex open-system processes in granitic magmas: Geology v. 45, p. 267–270.

Geological Survey of Western Australia 2016, Compilation of geochronology information, 2016, digital data package.

Goldstein, SL, O'Nions, RK and Hamilton, PJ 1984, A Sm–Nd isotopic study of atmospheric dusts and particulates from major river systems: Earth and Planetary Science Letters, v. 70, p. 221–236.

Griffin, WL, Belousova, EA, Shee, SR, Pearson, NJ and O'Reilly, SY 2004, Archean crustal evolution in the northern Yilgarn Craton: U–Pb and Hf-isotope evidence from detrital zircons: Precambrian Research, v. 127, p. 19–41.

Griffin, WL, Pearson, N, Belousova, EA and Saeed, A 2007, Reply to 'Comment to short communication: Hf-isotope heterogeneity in zircon 91500' *by* WL Griffin, NJ Pearson, EA Belousova and A Saeed (v. 233 [2006] p. 358–363) *by* F Corfu, Chemical Geology v. 244, p. 354–356.

Hawkesworth, CJ and Kemp, AIS 2006a, The differentiation and rates of generation of the continental crust: Chemical Geology, v. 226, p. 134–143.

Hawkesworth, CJ and Kemp, AIS 2006b, Using hafnium and oxygen isotopes in zircons to unravel the record of crustal evolution: Chemical Geology, v. 226, p. 144–162.

Hiess, A, Bennett, VC, Nutman, AP and Williams, IS 2011, Archaean fluid-assisted crustal cannibalism recorded by low $\delta^{18}O$ and negative $\varepsilon_{Hf(T)}$ isotopic signatures of west Greenland granite: Contributions to Mineralogy and Petrology, v. 161, p. 1027–1050.

Ickert, RB, Hiess, J, Williams, IS, Holden, P, Ireland, TR, Lanc, P, Schram, N, Foster, JJ and Clement, SW 2008, Determining high precision, in situ, oxygen isotope ratios with a SHRIMP II: Analyses of MPI-DING silicate-glass reference materials and zircon from contrasting granites: Chemical Geology, v. 257, p. 114–128.

Iizuka, T, Komiya, T, Rino, S, Maruyama, S and Hirata, T 2010, Detrital zircon evidence for Hf isotopic evolution of granitoid crust and continental growth: Geochimica et Cosmochimica Acta, v. 74, p. 2450–2472.

Johnson, SP, Korhonen, FJ, Kirkland, CL, Cliff, JB, Belousova, EA and Sheppard S 2017, An isotopic perspective on growth and differentiation of Proterozoic orogenic crust: from subduction magmatism to cratonization: Lithos, v. 268–271, p. 76–86.

Johnson, SP, Sheppard, S, Rasmussen, B, Wingate, MTD, Kirkland, CL, Muhling, JR, Fletcher, IR and Belousova, EA 2011a, Two collisions, two sutures: punctuated pre-1950 Ma assembly of the West Australian Craton during the Ophthalmian and Glenburgh Orogenies: Precambrian Research, v. 189, p. 239–262.

Johnson, SP, Sheppard, S, Wingate, MTD, Kirkland, CL and Belousova, EA, 2011b, Temporal and hafnium isotopic evolution of the Glenburgh Terrane basement: an exotic crustal fragment in the Capricorn Orogen: Geological Survey of Western Australia, Report 110, 27p.

Johnson, SP, Thorne, AM, Tyler, IM, Korsch, RJ, Kennett, BLN, Cutten, HN, Goodwin, J, Blay, OA, Blewett, RS, Joly, A, Dentith, MC, Aitken, ARA, Holzschuh, J, Salmon, M, Reading, A, Heinson, G, Boren, G, Ross, J, Costelloe, RD and Fomin, T 2013, Crustal architecture of the Capricorn Orogen, Western Australia and associated metallogeny: Australian Journal of Earth Sciences, v. 60, p. 681–705.

Joly, A, Porwal, A and McCuaig TC 2012, Exploration targeting for orogenic gold deposits in the Granites–Tanami Orogen: Mineral systems analysis, targeting model and prospectivity analysis: Ore Geology Reviews, v. 48, p. 349–383.

Kelsey, DE, Clark, C and Hand, H 2008, Thermobarometric modelling of zircon and monazite growth in melt-bearing systems: examples using model metapelitic and metapsammitic granulites: Journal of Metamorphic Geology, v. 26, p. 199–212.

Kemp, AIS, Hawkesworth, CJ, Foster, GL, Paterson, BA, Woodhead, JD, Hergt, JM, Gray, CM and Whitehouse, MJ 2007, Magmatic and crustal differentiation history of granitic rocks from Hf–O isotopes in zircon: Science, v. 315, p. 980–983.

Kirkland, CL, Johnson, SP, Smithies, RH, Hollis, JA, Wingate, MTD, Tyler, IM, Hickman, AH, Cliff, JB, Tessalina, S, Belousova, EA and Murphy, RC 2013, Not-so-suspect terrane: constraints on the crustal evolution of the Rudall Province: Precambrian Research, v. 235, p. 131–149.

Kirkland, CL, Whitehouse, M, Pease, V and Van Kranendonk, M 2010, Oxygen isotopes in detrital zircons: Insight into crustal recycling during the evolution of the Greenland Shield: Lithosphere, v. 2, p. 3–12.

Kita, N, Ushikubo, T, Fu, B and Valley, J 2009, High precision SIMS oxygen isotope analysis and the effect of sample topography: Chemical Geology, v. 264, p. 43–57.

Korhonen, FJ and Johnson, SP 2015, The role of radiogenic heat in prolonged intraplate reworking: The Capricorn Orogen explained?: Earth and Planetary Science Letters, v. 428, p. 22–32.

Korhonen, FJ, Johnson, SP, Fletcher, IR, Rasmussen, B, Sheppard, S, Muhling, JR, Dunkley, DJ, Wingate, MTD, Roberts, MP and Kirkland, CL 2015, Pressure–temperature–time evolution of the Mutherbukin Tectonic Event, Capricorn Orogen: Geological Survey of Western Australia, Report 146, 64p.

Lackey, JS, Valley, JW and Saleeby, JB 2005, Supracrustal input to magmas in the deep crust of Sierra Nevada batholith: Evidence from high-δ^{18}O zircon: Earth and Planetary Science Letters, v. 235, p. 315–330.

Li, X-H, Long, W-G, Li, Q-L, Liu, Y, Zheng, Y-F, Yang, Y-H, Chamberlain, KR, Wan, D-F, Guo, C-H, Wang, X-C and Tao, H 2010, Penglai zircon megacrysts: a potential new working reference material for microbeam determination of Hf–O isotopes and U–Pb age: Geostandards and Geoanalytical Research, v. 34, p. 117–134.

Martin, DMcB and Thorne, AM 2004, Tectonic setting and basin evolution of the Bangemall Supergroup in the northwestern Capricorn Orogen: Precambrian Research, v. 128, p. 385–409.

McCuaig, TC and Hronsky, JMA 2014, The mineral systems concept: the key to exploration targeting: Society of Economic Geologists Special Publication 18, p. 153–175.

McCuaig, TC, Beresford, S and Hronsky, JMA 2010, Translating the mineral systems approach into an effective exploration targeting system: Ore Geology Reviews, v. 38, p. 128–138.

McKenzie, DP and Priestley, KF 2008, The influence of lithospheric thickness variations on continental evolution: Lithos, v. 102, p. 1–11.

Morris, PA and Pirajno, F 2005, Mesoproterozoic sill complexes in the Bangemall Supergroup, Western Australia: geology, geochemistry, and mineralization potential: Geological Survey of Western Australia, Report 99, 75p.

Occhipinti, SA, Sheppard, S, Passchier, C, Tyler, IM and Nelson, DR 2004, Palaeoproterozoic crustal accretion and collision in the southern Capricorn Orogen: the Glenburgh Orogeny: Precambrian Research, v. 128, p. 237–255.

Page, FZ, Ushikubo, T, Kita, NT, Riciputi, LR and Valley, JW 2007, High-precision oxygen isotope analysis of picogram samples reveals 2 μm gradients and slow diffusion in zircon: American Mineralogist: v. 92, p. 1772–1775.

Payne, JL, McInerney, DJ, Barovich, KM, Kirkland, C, Pearson, NJ and Hand, M 2016, Strengths and limitations of zircon Lu–Hf and O isotopes in modelling crustal growth: Lithos, v. 248–251, p. 175–192.

Peck, WH, Valley, JW and Graham, CM 2003, Slow oxygen diffusion rates in igneous zircons from metamorphic rocks: American Mineralogist, v. 88, p. 1003–1014.

Petford, N and Gallagher, K 2001, Partial melting of mafic (amphibolite) lower crust by periodic influx of basaltic magma: Earth and Planetary Science Letters, v. 193, p. 483–499.

Richard, P, Shimizu, N and Allègre, CJ 1976, ^{143}Nd/^{146}Nd, a natural tracer: an application to oceanic basalts: Earth and Planetary Science Letters, v. 31, p. 269–273.

Rudnick, RL 1995, Making continental crust: Nature, v. 378, p. 571–578.

Rudnick, RL and Taylor, SR 1987, The composition and petrogenesis of the lower crust: a xenolith study: Journal of Geophysical Research: Solid Earth 92 (B13), p. 13981–14005.

Sandiford, M and McLaren, S 2002, Tectonic feedback and the ordering of heat producing elements within the continental lithosphere: Earth and Planetary Science Letters, v. 204, p. 133–150.

Scherer, E, Münker, C and Mezger, K 2001, Calibration of the lutetium–hafnium clock: Science, v. 293, p. 683–687.

Sheppard, S, Occhipinti, SA and Tyler, IM 2004, A 2005–1970 Ma Andean-type batholith in the southern Gascoyne Complex, Western Australia: Precambrian Research, v. 128, p. 257–277.

Sheppard, S, Occhipinti, SA and Nelson, DR 2005, Intracontinental reworking in the Capricorn Orogen, Western Australia: the 1680–1620 Ma Mangaroon Orogeny: Australian Journal of Earth Sciences, v. 52, p. 443–460.

Sheppard, S, Rasmussen, B, Muhling, JR, Farrell, TR and Fletcher, IR 2007, Grenvillian-aged orogenesis in the Palaeoproterozoic Gascoyne Complex, Western Australia: 1030–950 Ma reworking of the Proterozoic Capricorn Orogen: Journal of Metamorphic Geology, v. 25, p. 477–494.

Sheppard, S, Bodorkos, S, Johnson, SP, Wingate, MTD and Kirkland, CL 2010b, The Paleoproterozoic Capricorn Orogeny: intracontinental reworking not continent–continent collision: Geological Survey of Western Australia, Report 108, 33p.

Sheppard, S, Johnson, SP, Wingate, MTD, Kirkland, CL and Pirajno, F 2010a, Explanatory Notes for the Gascoyne Province: Geological Survey of Western Australia, 336p.

Valley, JW 2003, Oxygen isotopes in zircon, *in* Zircon *edited by* JM Hanchar and PWO Hoskin: Reviews in Mineralogy and Geochemistry, v. 53, p. 343–385.

Vervoort, JD, Patchett, PJ, Blichert-Toft, J and Albarède, F 1999, Relationships between Lu–Hf and Sm–Nd isotopic systems in the global sedimentary systems: Earth and Planetary Science Letters, v. 168, p. 79–99.

Wingate, MTD 2003, Age and palaeomagnetism of dolerite intrusions of the southeastern Collier Basin and the Earaheedy and Yerrida Basins, Western Australia: Geological Survey of Western Australia, Record 2003/3, 35p.

Wingate, MTD and Kirkland, CL 2015, Introduction to geochronology information released in 2015, *in* Compilation of geochronology information, 2015: Geological Survey of Western Australia, digital data package, 5p.

White, AJR and Chappell, BW 1977, Ultrametamorphism and granitoid genesis: Tectonophysics, v. 43, p. 7–22.

Woodhead, JD and Hergt, JM 2005, A preliminary appraisal of seven natural zircon reference materials for in situ Hf isotope determination: Geostandards and Geoanalytical Research, v. 29, p. 183–195.

Yakymchuk, C and Brown, M 2014, Behaviour of zircon and monazite during crustal melting: Journal of the Geological Society of London, v. 171, p. 465–479.

Appendix

Supplementary information: analytical techniques

Whole-rock Sm–Nd isotopes

Eighty samples (73 granitic and seven mafic rocks) were analysed for Sm–Nd isotope compositions. The isotope analyses were carried out at the Australian National University (ANU). About 100–200 mg of powdered sample was weighed into clean Teflon bombs, together with an appropriate amount of a mixed ^{149}Sm–^{150}Nd spike. The samples were dissolved in HF–HNO_3 in the bombs for 48 hours at a temperature of 190°C. The solutions were dried and the residue then redissolved in 4 N HCl on a hotplate for 24 hours to produce a clear solution. This solution was further dried and taken up in 2 M HNO_3 and the REE elements separated using TRU-Spec ion exchange resin in small Teflon columns. Sm and Nd were separated and collected by passing the solution through a further set of ion exchange columns loaded with HDEHP-coated Teflon powder (Richard et al., 1976).

Samarium and Nd were loaded with HNO_3 and H_3PO_4 reagents onto double Ta–Re filaments and analysed in a Finnigan MAT261 multicollector thermal ionization mass spectrometer. In each analytical session, the unknowns were analysed together with the La Jolla Nd standard or the in-house Ames nNd-1 Nd standard, or both. All analyses of the unknowns are reported already adjusted to the nominal $^{143}Nd/^{144}Nd$ value of 0.511860 for La Jolla. Mass fractionation was monitored and corrected for using the value $^{146}Nd/^{144}Nd = 0.7219$. Procedural blanks analysed during the period of this project were ~80 pg and are considered negligible compared to the total quantity of Nd in the samples.

Two-stage depleted-mantle model ages ($T_{DM}2$) were calculated for the Sm–Nd dataset following the method of Goldstein et al. (1984), based on the precise U–Pb zircon crystallization age of the rock as determined by SHRIMP U–Pb zircon dating. If no precise geochronology data were available for the sample, the age of the parent supersuite was used to calculate the model age.

Lu–Hf isotopes

Hafnium isotope analyses were conducted on previously dated zircons from 35 samples using a New Wave/Merchantek LUV213 laser-ablation microprobe, attached to a Nu Plasma multi-collector inductively coupled plasma mass spectrometer (LA-MC-ICP-MS) at Macquarie University, Sydney, New South Wales. The analyses employed a beam diameter of about 40 μm (with ablation pit typically 40–60 μm deep) placed, where possible, over the existing SIMS U–Pb or $^{18}O/^{16}O$ analysis pits, so as to sample the same zircon domain. The ablated sample material was transported from the laser cell to the ICP-MS torch by a helium carrier gas. The measurement of accurate $^{176}Hf/^{177}Hf$ ratios in zircon requires correction of the isobaric interferences of ^{176}Lu and ^{176}Yb on ^{176}Hf. Interference of ^{176}Lu on ^{176}Hf was corrected by measurement of interference-free ^{175}Lu, and using the invariant $^{176}Lu/^{175}Lu$ correction factor of 0.02669 (DeBievre and Taylor, 1993). The interference of ^{176}Yb on ^{176}Hf was corrected by measuring the interference-free ^{172}Yb isotope and using the $^{176}Yb/^{172}Yb$ ratio to calculate the intensity of ^{176}Yb. The appropriate value of $^{176}Yb/^{172}Yb$ (0.5865) was determined by successively doping a JMC475 Hf standard (100 ppb solution) with various amounts of Yb, and determining the value of $^{176}Yb/^{172}Yb$ required to yield the value of $^{176}Hf/^{177}Hf$ in the undoped solution.

Standard zircons (Mud Tank and Temora II) were analysed together with the samples. Samples were run over the course of several years, during which the mean Mud Tank $^{176}Hf/^{177}Hf$ value was 0.282528 ± 0.000026 (1σ) and the mean Temora $^{176}Hf/^{177}Hf$ value was 0.282686 ± 0.000034 (1σ). The mean Mud Tank values of each individual batch and the long-term average are within two standard deviations of the recommended value (0.282522 ± 0.000042 (2σ); Griffin et al., 2007). Temora II zircon has an average $^{176}Yb/^{177}Hf$ ratio of 0.037, which is similar to the average $^{176}Yb/^{177}Hf$ ratio of Gascoyne Province magmatic zircon of 0.042. The average $^{176}Hf/^{177}Hf$ ratio for Temora II during sample analyses is consistent with the published values of 0.282686 ± 8 (solution ICPMS; Woodhead and Hergt, 2005) and 0.282687 ± 24 (LA-ICP-MS, Hawkesworth and Kemp, 2006a).

Calculation of initial $^{176}Hf/^{177}Hf$ is based on the ^{176}Lu decay constant of Scherer et al. (2001) (1.865×10^{-11} yr^{-1}). Because $^{176}Hf/^{177}Hf$ departures from the Chondritic Uniform Reservoir (CHUR) evolution line are very small, epsilon (ε) notation is used (one epsilon unit represents a one part per 10 000 deviation from the CHUR composition). Calculation of ε_{Hf} values employs the decay constant of Scherer et al. (2001) and the CHUR values of Blichert-Toft and Albarède (1997).

Measured isotope compositions are referred to modelled bulk-Earth Hf reservoirs, including depleted mantle (Griffin et al., 2004) and CHUR (Blichert-Toft and Albarède, 1997). Model ages (T_{DM}), which are calculated using the measured $^{176}Lu/^{177}Hf$ of the zircon, provide only a minimum age for the source material of the magma from which the zircon crystallized because the $^{176}Lu/^{177}Hf$ ratio of zircon is much lower than the $^{176}Lu/^{177}Hf$ ratio of all reasonable reservoirs for Hf. Therefore, we have calculated two-stage model ages ($T_{DM}2$), which assumes the parental magma was produced from an average continental crust ($^{176}Lu/^{177}Hf = 0.015$) that originally was derived from a depleted-mantle source with $(^{176}Hf/^{177}Hf)_{(i)} = 0.279718$ at 4.56 Ga and $^{176}Lu/^{177}Hf = 0.0384$ (Griffin et al., 2004).

$^{18}O/^{16}O$ isotopes

Oxygen isotope ratios ($^{18}O/^{16}O$) were determined using a Cameca IMS 1280 multi-collector ion microprobe located at the Centre for Microscopy, Characterisation and Analysis (CMCA) at The University of Western Australia. Analytical conditions were similar to those outlined in detail by Kita et al. (2009). A static ~3 nA Cs^+ primary beam with an impact energy of 20 keV was focused to a 15 µm spot on the sample surface. Spot placement was guided by the location of SHRIMP U–Pb analyses, and cathodoluminescence (CL) images of the zircons in order to avoid mixtures between different zircon growth domains (i.e. core and rim structures). Where the magmatic zircons were large enough, analyses were made in the central and exterior portions of the zircons to explore compositional differences of the host magma during the crystallization and growth of the zircon.

Instrument parameters included a magnification of 130x between the sample and field aperture, 400 µm contrast aperture, 4000 µm field aperture, 120 µm entrance slit, 500 µm exit slits, and a 40 eV band pass for the energy slit with a 5 eV gap. Secondary O^- ions were accelerated to 10 keV and analysed with a mass resolving power of approximately 2400 using dual Faraday Cup detectors. A normal-incidence electron gun was used to provide charge compensation.

Each analysis spot was pre-sputtered for 10 seconds prior to automated peak-centering using secondary deflectors DTFA-X, DTFA-Y and DTCA-X. Each analysis consisted of 20 four-second cycles through the mass stations, which gave an average internal precision of 0.17‰ (1 SD_{mean}). Isotopes of ^{16}O and ^{18}O were collected with a mass resolving power of about 2200 using dual Faraday Cup detectors. Penglai zircon (Li et al., 2010) was used as an oxygen isotope standard and multiple grains of another well-characterized zircon (CZ3, Temora II) run as an unknown. Using Penglai as a primary standard, the CZ3 standard returned a mean $\delta^{18}O$ value for all sessions of 15.5 ± 0.2 (2 SD), in excellent agreement with the value reported by Cavosie et al. (2011; $\delta^{18}O$ of 15.4 ± 0.1). During one session, Temora II was run as an unknown and returned a $\delta^{18}O$ value of 8.2 ± 0.1, identical to the value reported by Ickert et al. (2008; $\delta^{18}O$ of 8.2 ± 0.2). Aberrant beam centering is of concern for accurate $\delta^{18}O$ measurements (Kirkland et al., 2010). All lens centering values are within the range of deflections previously shown for this instrument in this analytical configuration to have no significant effect on the results.

Table 3. Lu–Hf and oxygen isotopic composition of magmatic zircon grains from felsic intrusive rocks in the western Capricorn Orogen

Analysis No.	Spot location	$^{207}Pb/^{206}Pb$ date (Ma)	Th/U	$^{176}Hf/^{177}Hf$ measured	$^{176}Lu/^{177}Hf$ measured	$^{176}Yb/^{177}Hf$ measured	$^{176}Hf/^{177}Hf$ initial	$\varepsilon_{Hf(t)}$	$\varepsilon_{Hf(1800\ Ma)}$	$\varepsilon_{Hf(1650\ Ma)}$	$T_{DM}2$ (Ga)	$^{18}O/^{16}O$ [a][b]	$\delta^{18}O$ [c]
Halfway Gneiss													
GSWA 164309: foliated porphyritic biotite granodiorite													
magmatic													
1.1	–	**2560** ± 3	1.04	0.281246	0.002086	0.058487	0.281144 ± 0.000026	**-0.2** ± 0.9	–	–	**3.08**	–	–
2.1	–	**2563** ± 5	0.82	0.281243	0.001233	0.033703	0.281183 ± 0.000034	**1.3** ± 1.2	–	–	**2.99**	–	–
3.1	–	**2534** ± 5	0.85	0.281185	0.001103	0.037499	0.281132 ± 0.000028	**-1.2** ± 1.0	–	–	**3.13**	–	–
5.1	–	**2553** ± 9	0.38	0.281180	0.000687	0.023413	0.281146 ± 0.000013	**-0.2** ± 0.5	–	–	**3.08**	–	–
6.1	–	**2553** ± 6	0.94	0.281179	0.000867	0.031802	0.281137 ± 0.000022	**-0.6** ± 0.8	–	–	**3.10**	–	–
15.1	–	**2517** ± 8	0.58	0.281197	0.000704	0.024175	0.281163 ± 0.000016	**-0.5** ± 0.6	–	–	**3.07**	–	–
17.1	–	**2537** ± 4	0.56	0.281186	0.000628	0.021058	0.281156 ± 0.000013	**-0.3** ± 0.5	–	–	**3.07**	–	–
21.1	–	**2562** ± 9	0.69	0.281134	0.000862	0.027096	0.281092 ± 0.000018	**-2.0** ± 0.6	–	–	**3.20**	–	–
24.1	–	**2546** ± 7	0.86	0.281220	0.000896	0.028355	0.281176 ± 0.000012	**0.7** ± 0.4	–	–	**3.02**	–	–
26.1	–	**2576** ± 8	0.57	0.281088	0.000766	0.024275	0.281050 ± 0.000015	**-3.1** ± 0.5	–	–	**3.28**	–	–
28.1	–	**2546** ± 6	0.69	0.281205	0.001333	0.038111	0.281140 ± 0.000017	**-0.6** ± 0.6	–	–	**3.10**	–	–
29.1	–	**2539** ± 10	0.56	0.281248	0.000662	0.019819	0.281216 ± 0.000018	**1.9** ± 0.6	–	–	**2.93**	–	–
inherited													
13.1	–	**2566** ± 10	0.57	0.281194	0.001107	0.039080	0.281140 ± 0.000019	**-0.2** ± 0.7	–	–	**3.09**	–	–
19.1	–	**2605** ± 10	0.60	0.281236	0.000622	0.019315	0.281205 ± 0.000016	**3.1** ± 0.6	–	–	**2.91**	–	–
25.1	–	**2673** ± 6	0.56	0.281027	0.000232	0.007264	0.281015 ± 0.000022	**-2.1** ± 0.8	–	–	**3.30**	–	–
GSWA 142988: biotite tonalite													
magmatic													
3.1	–	**2558** ± 6	0.35	0.281176	0.001172	0.045702	0.281119 ± 0.000014	**-1.1** ± 0.5	–	–	**3.14**	–	–
7.1	–	**2666** ± 11	2.10	0.281206	0.000618	0.022574	0.281174 ± 0.000010	**3.4** ± 0.4	–	–	**2.94**	–	–
8.1	–	**2667** ± 5	0.49	0.281101	0.001318	0.056934	0.281034 ± 0.000014	**-1.6** ± 0.5	–	–	**3.26**	–	–
15.1	–	**2655** ± 5	1.03	0.281108	0.000716	0.030861	0.281072 ± 0.000008	**-0.5** ± 0.3	–	–	**3.18**	–	–
21.1	–	**2689** ± 6	0.49	0.281033	0.000743	0.031856	0.280995 ± 0.000010	**-2.5** ± 0.4	–	–	**3.33**	–	–
23.1	–	**2683** ± 5	0.73	0.280999	0.000734	0.031839	0.280961 ± 0.000007	**-3.8** ± 0.2	–	–	**3.41**	–	–
26.1	–	**2667** ± 5	0.59	0.281068	0.001270	0.060972	0.281003 ± 0.000013	**-2.7** ± 0.5	–	–	**3.33**	–	–
inherited													
1.1	–	**2806** ± 9	1.27	0.280852	0.001060	0.047229	0.280795 ± 0.000015	**-6.9** ± 0.5	–	–	**3.70**	–	–
5.1	–	**2701** ± 8	0.53	0.281122	0.001286	0.056760	0.281056 ± 0.000011	**0.0** ± 0.4	–	–	**3.18**	–	–
6.1	–	**3253** ± 5	0.74	0.280774	0.000902	0.037836	0.280718 ± 0.000013	**0.8** ± 0.5	–	–	**3.55**	–	–
9.1	–	**2704** ± 5	0.48	0.281142	0.001009	0.042690	0.281090 ± 0.000010	**1.2** ± 0.4	–	–	**3.10**	–	–
16.1	–	**2711** ± 4	0.35	0.281081	0.001551	0.065746	0.281001 ± 0.000011	**-1.8** ± 0.4	–	–	**3.30**	–	–
17.1	–	**2801** ± 5	0.78	0.280827	0.000729	0.030728	0.280788 ± 0.000009	**-7.2** ± 0.3	–	–	**3.72**	–	–
20.1	–	**3040** ± 5	0.66	0.280808	0.000899	0.036580	0.280756 ± 0.000009	**-2.8** ± 0.3	–	–	**3.62**	–	–
24.1	–	**3274** ± 4	0.38	0.280701	0.000915	0.036772	0.280643 ± 0.000007	**-1.4** ± 0.2	–	–	**3.71**	–	–
28.1	–	**2716** ± 6	1.21	0.280964	0.000795	0.037581	0.280923 ± 0.000011	**-4.4** ± 0.4	–	–	**3.47**	–	–

Analysis No.	Spot location	$^{207}Pb/^{206}Pb$ date (Ma)	Th/U	$^{176}Hf/^{177}Hf$ measured	$^{176}Lu/^{177}Hf$ measured	$^{176}Yb/^{177}Hf$ measured	$^{176}Hf/^{177}Hf$ initial	$\varepsilon_{Hf(t)}$	$\varepsilon_{Hf(1800\ Ma)}$	$\varepsilon_{Hf(1650\ Ma)}$	$T_{DM}2$ (Ga)	$^{18}O/^{16}O$ [(a)(b)]	$\delta^{18}O$ [(c)]
GSWA 168950: pegmatite-banded tonalite gneiss													
magmatic													
2.1	–	**2471** ± 2	0.00	0.281100	0.001780	0.088567	0.281016 ± 0.000008	**-6.8** ± 0.3	–	–	**3.43**	–	–
5.1	–	**2456** ± 6	0.29	0.281127	0.000227	0.013264	0.281116 ± 0.000012	**-3.5** ± 0.4	–	–	**3.22**	–	–
11.1	–	**2478** ± 2	0.02	0.281187	0.000560	0.032601	0.281161 ± 0.000011	**-1.5** ± 0.4	–	–	**3.10**	–	–
12.1	–	**2449** ± 4	0.14	0.281109	0.000303	0.018000	0.281095 ± 0.000012	**-4.5** ± 0.4	–	–	**3.27**	–	–
17.1	–	**2466** ± 11	0.45	0.281194	0.000075	0.004954	0.281190 ± 0.000012	**-0.7** ± 0.4	–	–	**3.04**	–	–
21.1	–	**2472** ± 2	0.01	0.281134	0.000708	0.042113	0.281101 ± 0.000708	**-3.7** ± 0.3	–	–	**3.24**	–	–
inherited													
1.1	–	**2506** ± 2	0.27	0.281121	0.000625	0.032041	0.281091 ± 0.000006	**-3.3** ± 0.2	–	–	**3.24**	–	–
3.1	–	**2518** ± 1	0.25	0.281152	0.000601	0.036244	0.281123 ± 0.000009	**-1.9** ± 0.3	–	–	**3.16**	–	–
6.1	–	**2635** ± 7	0.73	0.281092	0.000702	0.036276	0.281057 ± 0.000011	**-1.5** ± 0.4	–	–	**3.23**	–	–
8.1	–	**2519** ± 4	0.42	0.281105	0.000479	0.020540	0.281082 ± 0.000007	**-3.3** ± 0.3	–	–	**3.25**	–	–
9.1	–	**2507** ± 3	1.32	0.281117	0.000690	0.041587	0.281084 ± 0.000013	**-3.5** ± 0.5	–	–	**3.26**	–	–
10.1	–	**2564** ± 12	1.75	0.281152	0.000447	0.025597	0.281130 ± 0.000447	**-0.6** ± 0.3	–	–	**3.11**	–	–
13.1	–	**2701** ± 4	0.75	0.281010	0.001260	0.067265	0.280945 ± 0.000014	**-4.0** ± 0.5	–	–	**3.43**	–	–
14.1	–	**2730** ± 6	0.63	0.281073	0.001540	0.081686	0.280993 ± 0.000012	**-1.6** ± 0.4	–	–	**3.31**	–	–
15.1	–	**2619** ± 9	0.52	0.281154	0.000823	0.040745	0.281113 ± 0.000013	**0.1** ± 0.5	–	–	**3.11**	–	–
15.2	–	**2534** ± 2	0.01	0.281190	0.000565	0.031019	0.281163 ± 0.000013	**-0.1** ± 0.5	–	–	**3.06**	–	–
16.1	–	**2519** ± 3	0.35	0.281132	0.000842	0.043136	0.281092 ± 0.000842	**-3.0** ± 0.4	–	–	**3.23**	–	–
20.2	–	**2506** ± 8	0.40	0.281160	0.000197	0.010743	0.281151 ± 0.000012	**-1.2** ± 0.4	–	–	**3.11**	–	–
22.1	–	**2507** ± 2	0.01	0.281119	0.000565	0.033149	0.281092 ± 0.000009	**-3.2** ± 0.3	–	–	**3.24**	–	–
23.1	–	**2515** ± 5	0.27	0.281126	0.000189	0.010377	0.281117 ± 0.000011	**-2.2** ± 0.4	–	–	**3.18**	–	–
GSWA 188973: metagranodiorite													
magmatic													
2.1	–	**2419** ± 6	0.10	0.281214	0.000976	0.047891	0.281169 ± 0.000013	**-2.5** ± 0.5	–	–	**3.12**	–	–
7.1	–	**2457** ± 8	0.02	0.281196	0.001177	0.043967	0.281141 ± 0.000012	**-2.6** ± 0.4	–	–	**3.16**	–	–
10.1	–	**2421** ± 6	0.02	0.281234	0.000633	0.029098	0.281205 ± 0.000011	**-1.2** ± 0.4	–	–	**3.04**	–	–
11.1	–	**2387** ± 43	0.64	0.281240	0.000782	0.035950	0.281204 ± 0.000782	**-2.0** ± 0.5	–	–	**3.07**	–	–
12.1	–	**2466** ± 11	0.48	0.281167	0.000926	0.041717	0.281123 ± 0.000015	**-3.1** ± 0.5	–	–	**3.19**	–	–
13.1	–	**2432** ± 6	0.06	0.281229	0.000843	0.036155	0.281190 ± 0.000010	**-1.5** ± 0.4	–	–	**3.07**	–	–
14.1	–	**2401** ± 6	0.13	0.281241	0.001417	0.060308	0.281176 ± 0.000011	**-2.7** ± 0.4	–	–	**3.12**	–	–
16.1	–	**2445** ± 6	0.87	0.281229	0.001115	0.048109	0.281177 ± 0.000007	**-1.6** ± 0.2	–	–	**3.09**	–	–
22.1	–	**2429** ± 7	0.76	0.281202	0.000630	0.028830	0.281173 ± 0.000011	**-2.1** ± 0.4	–	–	**3.11**	–	–
24.1	–	**2428** ± 5	0.10	0.281205	0.001207	0.054466	0.281149 ± 0.000013	**-3.0** ± 0.5	–	–	**3.16**	–	–
inherited													
8.1	–	**2669** ± 5	0.56	0.281082	0.001117	0.050152	0.281025 ± 0.000016	**-1.9** ± 0.6	–	–	**3.28**	–	–
15.1	–	**2541** ± 4	0.22	0.281082	0.000846	0.033418	0.281041 ± 0.000009	**-4.3** ± 0.3	–	–	**3.33**	–	–
17.1	–	**2501** ± 10	0.23	0.281336	0.000898	0.035960	0.281293 ± 0.000007	**3.8** ± 0.3	–	–	**2.79**	–	–

Analysis No.	Spot location	$^{207}Pb/^{206}Pb$ date (Ma)	Th/U	$^{176}Hf/^{177}Hf$ measured	$^{176}Lu/^{177}Hf$ measured	$^{176}Yb/^{177}Hf$ measured	$^{176}Hf/^{177}Hf$ initial	$\varepsilon_{Hf(t)}$	$\varepsilon_{Hf(1800\ Ma)}$	$\varepsilon_{Hf(1650\ Ma)}$	T_{DM}^2 (Ga)	$^{18}O/^{16}O$ (a)(b)	$\delta^{18}O$ (c)
Dalgaringa Supersuite													
GSWA 168952: biotite–hornblende tonalite													
magmatic													
1.1	–	**2000** ± 10	1.48	0.281411	0.001138	0.055926	0.281368 ± 0.000013	**-5.1** ± 0.5	–	–	**2.96**	–	–
2.1	–	**1995** ± 10	1.36	0.281365	0.000802	0.030620	0.281335 ± 0.000011	**-6.4** ± 0.4	–	–	**3.04**	–	–
5.1	–	**2003** ± 9	1.20	0.281372	0.000687	0.035743	0.281346 ± 0.000012	**-5.8** ± 0.4	–	–	**3.01**	–	–
7.1	–	**1982** ± 12	1.45	0.281401	0.000677	0.032098	0.281375 ± 0.000010	**-5.2** ± 0.4	–	–	**2.96**	–	–
8.1	–	**2012** ± 10	0.82	0.281394	0.000911	0.039635	0.281359 ± 0.000015	**-5.1** ± 0.5	–	–	**2.97**	–	–
10.1	–	**1997** ± 11	0.88	0.281384	0.000927	0.041949	0.281349 ± 0.000010	**-5.8** ± 0.4	–	–	**3.01**	–	–
13.1	–	**2005** ± 8	1.26	0.281374	0.001049	0.047583	0.281334 ± 0.000011	**-6.1** ± 0.4	–	–	**3.04**	–	–
14.1	–	**1986** ± 8	1.40	0.281319	0.000440	0.019629	0.281302 ± 0.000010	**-7.7** ± 0.3	–	–	**3.12**	–	–
16.1	–	**1986** ± 8	1.07	0.281340	0.000890	0.039526	0.281306 ± 0.000011	**-7.6** ± 0.4	–	–	**3.11**	–	–
17.1	–	**2002** ± 8	2.42	0.281256	0.000722	0.032056	0.281229 ± 0.000009	**-10.0** ± 0.3	–	–	**3.27**	–	–
20.1	–	**2008** ± 6	0.89	0.281255	0.000925	0.043668	0.281220 ± 0.000012	**-10.1** ± 0.4	–	–	**3.29**	–	–
inherited													
4.1	–	**2014** ± 8	1.25	0.281387	0.001330	0.055124	0.281336 ± 0.000016	**-5.9** ± 0.6	–	–	**3.02**	–	–
11.1	–	**2023** ± 9	1.16	0.281368	0.000854	0.037465	0.281335 ± 0.000010	**-5.7** ± 0.3	–	–	**3.02**	–	–
19.1	–	**2013** ± 8	2.60	0.281274	0.000599	0.025807	0.281251 ± 0.000010	**-8.9** ± 0.3	–	–	**3.22**	–	–
21.1	–	**2016** ± 11	1.59	0.281202	0.000566	0.025563	0.281180 ± 0.000015	**-11.4** ± 0.5	–	–	**3.37**	–	–
GSWA 142925: biotite monzogranite													
magmatic													
2.1	–	**2000** ± 8	0.73	0.281467	0.001199	0.049017	0.281421 ± 0.000020	**-3.2** ± 0.7	–	–	**2.84**	–	–
3.1	–	**1981** ± 12	0.43	0.281415	0.000694	0.031617	0.281389 ± 0.000021	**-4.7** ± 0.7	–	–	**2.93**	–	–
4.1	–	**2002** ± 8	0.60	0.281418	0.000800	0.036650	0.281388 ± 0.000018	**-4.3** ± 0.6	–	–	**2.92**	–	–
5.1	–	**1993** ± 10	0.53	0.281486	0.000610	0.022389	0.281463 ± 0.000020	**-1.8** ± 0.7	–	–	**2.75**	–	–
6.1	–	**1995** ± 8	0.58	0.281474	0.000680	0.031599	0.281448 ± 0.000018	**-2.3** ± 0.6	–	–	**2.78**	–	–
7.1	–	**1990** ± 8	0.61	0.281451	0.001126	0.037746	0.281408 ± 0.000015	**-3.8** ± 0.5	–	–	**2.88**	–	–
13.1	–	**2011** ± 10	0.45	0.281459	0.000515	0.024000	0.281439 ± 0.000024	**-2.3** ± 0.8	–	–	**2.79**	–	–
14.1	–	**2001** ± 7	0.61	0.281452	0.000711	0.033514	0.281425 ± 0.000017	**-3.0** ± 0.6	–	–	**2.83**	–	–
15.1	–	**2024** ± 13	0.44	0.281436	0.000555	0.025213	0.281415 ± 0.000021	**-2.8** ± 0.7	–	–	**2.84**	–	–
16.1	–	**1998** ± 13	0.29	0.281354	0.000360	0.015640	0.281340 ± 0.000015	**-6.1** ± 0.5	–	–	**3.03**	–	–
17.1	–	**2008** ± 9	0.60	0.281426	0.000658	0.029441	0.281401 ± 0.000015	**-3.7** ± 0.5	–	–	**2.88**	–	–
18.1	–	**2006** ± 8	0.59	0.281440	0.000645	0.029568	0.281415 ± 0.000023	**-3.2** ± 0.8	–	–	**2.85**	–	–
19.1	–	**2012** ± 8	0.55	0.281422	0.000575	0.026089	0.281400 ± 0.000017	**-3.6** ± 0.6	–	–	**2.88**	–	–
20.1	–	**2004** ± 7	0.60	0.281441	0.000702	0.031566	0.281414 ± 0.000016	**-3.3** ± 0.6	–	–	**2.86**	–	–
21.1	–	**2008** ± 10	0.50	0.281470	0.000453	0.019845	0.281453 ± 0.000016	**-1.9** ± 0.6	–	–	**2.77**	–	–
22.1	–	**2001** ± 8	0.58	0.281437	0.000644	0.025985	0.281413 ± 0.000019	**-3.4** ± 0.7	–	–	**2.86**	–	–

Analysis No.	Spot location	$^{207}Pb/^{206}Pb$ date (Ma)	Th/U	$^{176}Hf/^{177}Hf$ measured	$^{176}Lu/^{177}Hf$ measured	$^{176}Yb/^{177}Hf$ measured	$^{176}Hf/^{177}Hf$ initial	$\varepsilon_{Hf(t)}$	$\varepsilon_{Hf(1800\ Ma)}$	$\varepsilon_{Hf(1650\ Ma)}$	$T_{DM}2$ (Ga)	$^{18}O/^{16}O$ [(a)(b)]	$\delta^{18}O$ [(c)]
GSWA 142926: foliated biotite tonalite													
magmatic													
1.1	–	**2009** ± 3	0.04	0.281512	0.000833	0.025598	0.281480 ± 0.000037	**-0.9** ± 1.3	–	–	**2.70**	–	–
2.1	–	**2006** ± 3	0.03	0.281476	0.000644	0.023064	0.281451 ± 0.000022	**-2.0** ± 0.8	–	–	**2.77**	–	–
3.1	–	**1979** ± 4	0.03	0.281428	0.000985	0.035840	0.281391 ± 0.000014	**-4.7** ± 0.5	–	–	**2.92**	–	–
4.1	–	**2010** ± 11	0.04	0.281396	0.000639	0.027461	0.281372 ± 0.000019	**-4.7** ± 0.7	–	–	**2.95**	–	–
5.1	–	**1999** ± 3	0.04	0.281431	0.001248	0.040596	0.281384 ± 0.000022	**-4.5** ± 0.8	–	–	**2.93**	–	–
7.1	–	**2007** ± 4	0.15	0.281470	0.000787	0.033070	0.281440 ± 0.000022	**-2.3** ± 0.8	–	–	**2.80**	–	–
8.1	–	**1990** ± 3	0.04	0.281411	0.000756	0.029728	0.281382 ± 0.000018	**-4.8** ± 0.6	–	–	**2.94**	–	–
10.1	–	**2002** ± 2	0.04	0.281453	0.001004	0.036004	0.281415 ± 0.000014	**-3.3** ± 0.5	–	–	**2.86**	–	–
11.1	–	**2001** ± 3	0.04	0.281453	0.001028	0.035521	0.281414 ± 0.000013	**-3.4** ± 0.5	–	–	**2.86**	–	–
13.1	–	**2000** ± 5	0.07	0.281471	0.001259	0.053768	0.281423 ± 0.000018	**-3.1** ± 0.6	–	–	**2.84**	–	–
14.1	–	**1992** ± 4	0.03	0.281372	0.000847	0.032607	0.281340 ± 0.000016	**-6.2** ± 0.6	–	–	**3.03**	–	–
15.1	–	**2005** ± 7	0.69	0.281545	0.001187	0.052465	0.281500 ± 0.000021	**-0.3** ± 0.7	–	–	**2.66**	–	–
19.1	–	**2002** ± 3	0.04	0.281457	0.000870	0.033766	0.281424 ± 0.000022	**-3.0** ± 0.8	–	–	**2.83**	–	–
20.1	–	**2006** ± 3	0.03	0.281376	0.000889	0.035588	0.281342 ± 0.000013	**-5.8** ± 0.5	–	–	**3.02**	–	–
inherited													
12.1	–	**2039** ± 3	0.04	0.281396	0.000876	0.034916	0.281362 ± 0.000015	**-4.4** ± 0.5	–	–	**2.95**	–	–
GSWA 142933: biotite–hypersthene–clinopyroxene mafic granulite													
magmatic													
1.1	–	**1981** ± 8	0.91	0.281797	0.001674	0.062209	0.281734 ± 0.000048	**7.5** ± 1.7	–	–	**2.15**	–	–
2.1	–	**1986** ± 9	0.28	0.281517	0.000422	0.012576	0.281501 ± 0.000021	**-0.6** ± 0.7	–	–	**2.67**	–	–
3.1	–	**1997** ± 6	1.53	0.281519	0.001079	0.043744	0.281478 ± 0.000021	**-1.2** ± 0.7	–	–	**2.72**	–	–
4.1	–	**2004** ± 4	1.84	0.281455	0.000865	0.031283	0.281422 ± 0.000016	**-3.0** ± 0.6	–	–	**2.84**	–	–
5.1	–	**1977** ± 5	1.20	0.281514	0.001135	0.042475	0.281471 ± 0.000017	**-1.9** ± 0.6	–	–	**2.74**	–	–
6.1	–	**1972** ± 12	0.75	0.281523	0.000700	0.024642	0.281497 ± 0.000019	**-1.1** ± 0.7	–	–	**2.69**	–	–
7.1	–	**1975** ± 16	0.53	0.281528	0.000347	0.012779	0.281515 ± 0.000020	**-0.4** ± 0.7	–	–	**2.65**	–	–
8.1	–	**1975** ± 19	0.74	0.281583	0.000422	0.012241	0.281567 ± 0.000035	**1.5** ± 1.2	–	–	**2.53**	–	–
9.1	–	**2002** ± 6	0.35	0.281528	0.001047	0.035807	0.281488 ± 0.000022	**-0.7** ± 0.8	–	–	**2.69**	–	–
10.1	–	**1985** ± 9	1.01	0.281494	0.000787	0.029854	0.281464 ± 0.000024	**-2.0** ± 0.8	–	–	**2.75**	–	–
13.1	–	**1986** ± 9	0.44	0.281602	0.001756	0.074352	0.281536 ± 0.000013	**0.6** ± 0.5	–	–	**2.59**	–	–
14.1	–	**1981** ± 4	2.28	0.281519	0.000365	0.011449	0.281505 ± 0.000021	**-0.6** ± 0.7	–	–	**2.67**	–	–
17.1	–	**1986** ± 7	1.43	0.281508	0.000870	0.033555	0.281475 ± 0.000012	**-1.6** ± 0.4	–	–	**2.73**	–	–
22.1	–	**1985** ± 7	1.39	0.281568	0.001336	0.051700	0.281518 ± 0.000020	**-0.1** ± 0.7	–	–	**2.63**	–	–
23.1	–	**1989** ± 6	1.27	0.281452	0.000611	0.025529	0.281429 ± 0.000023	**-3.1** ± 0.8	–	–	**2.83**	–	–
GSWA 142932: Nardoo Granite, porphyritic granodiorite													
magmatic													
1.1	–	**1978** ± 9	0.37	0.281403	0.000734	0.023684	0.281375 ± 0.000021	**-5.3** ± 0.7	–	–	**2.96**	–	–
2.1	–	**1972** ± 6	0.20	0.281351	0.000603	0.018878	0.281328 ± 0.000028	**-7.1** ± 1.0	–	–	**3.07**	–	–
3.1	–	**1999** ± 9	0.44	0.281351	0.000783	0.024848	0.281321 ± 0.000026	**-6.7** ± 0.9	–	–	**3.07**	–	–
5.1	–	**1965** ± 8	0.59	0.281421	0.000974	0.030150	0.281385 ± 0.000025	**-5.3** ± 0.9	–	–	**2.95**	–	–
6.1	–	**1975** ± 7	0.07	0.281284	0.000495	0.017553	0.281265 ± 0.000031	**-9.3** ± 1.1	–	–	**3.21**	–	–
7.1	–	**1991** ± 7	0.30	0.281414	0.000615	0.023221	0.281391 ± 0.000020	**-4.5** ± 0.7	–	–	**2.92**	–	–

Analysis No.	Spot location	$^{207}Pb/^{206}Pb$ date (Ma)	Th/U	$^{176}Hf/^{177}Hf$ measured	$^{176}Lu/^{177}Hf$ measured	$^{176}Yb/^{177}Hf$ measured	$^{176}Hf/^{177}Hf$ initial	$\varepsilon_{Hf(t)}$	$\varepsilon_{Hf(1800\ Ma)}$	$\varepsilon_{Hf(1650\ Ma)}$	$T_{DM}2$ (Ga)	$^{18}O/^{16}O$ [a][b]	$\delta^{18}O$ [c]
8.1	–	**1966** ± 9	0.44	0.281510	0.001061	0.039033	0.281470 ± 0.000023	**-2.2** ± 0.8	–	–	**2.75**	–	–
11.1	–	**1979** ± 19	1.10	0.281500	0.001728	0.065560	0.281435 ± 0.000032	**-3.2** ± 1.1	–	–	**2.83**	–	–
12.1	–	**1974** ± 9	0.20	0.281460	0.000715	0.023423	0.281433 ± 0.000022	**-3.3** ± 0.8	–	–	**2.83**	–	–
13.1	–	**1973** ± 7	0.64	0.281472	0.000808	0.029155	0.281442 ± 0.000013	**-3.1** ± 0.5	–	–	**2.81**	–	–
17.1	–	**1985** ± 7	0.40	0.281488	0.000794	0.024936	0.281458 ± 0.000023	**-2.2** ± 0.8	–	–	**2.77**	–	–
22.1	–	**1977** ± 8	0.19	0.281474	0.000864	0.029107	0.281442 ± 0.000017	**-3.0** ± 0.6	–	–	**2.81**	–	–
23.1	–	**1978** ± 7	0.52	0.281437	0.001222	0.039320	0.281391 ± 0.000019	**-4.7** ± 0.7	–	–	**2.92**	–	–
inherited													
4.1	–	**2024** ± 16	0.24	0.281452	0.000753	0.023779	0.281423 ± 0.000020	**-2.6** ± 0.7	–	–	**2.82**	–	–
16.1	–	**2026** ± 16	0.17	0.281390	0.000481	0.014119	0.281371 ± 0.000021	**-4.3** ± 0.7	–	–	**2.94**	–	–
GSWA 142928: Nardoo Granite, biotite tonalite													
magmatic													
1.1	–	**1975** ± 9	0.31	0.281444	0.000850	0.036242	0.281412 ± 0.000025	**-4.1** ± 0.9	–	–	**2.88**	–	–
2.1	–	**1977** ± 14	0.96	0.281440	0.000714	0.030371	0.281413 ± 0.000017	**-4.0** ± 0.6	–	–	**2.88**	–	–
3.1	–	**1955** ± 27	0.21	0.281474	0.000853	0.029275	0.281442 ± 0.000017	**-3.4** ± 0.6	–	–	**2.82**	–	–
4.1	–	**1968** ± 8	0.29	0.281481	0.000637	0.018172	0.281457 ± 0.000031	**-2.6** ± 1.1	–	–	**2.78**	–	–
5.1	–	**1962** ± 12	0.52	0.281422	0.000873	0.031028	0.281389 ± 0.000023	**-5.2** ± 0.8	–	–	**2.94**	–	–
6.1	–	**1956** ± 11	0.37	0.281378	0.000713	0.027123	0.281352 ± 0.000022	**-6.6** ± 0.8	–	–	**3.03**	–	–
9.1	–	**1979** ± 11	0.75	0.281428	0.001086	0.042271	0.281387 ± 0.000016	**-4.9** ± 0.6	–	–	**2.93**	–	–
13.1	–	**1959** ± 7	0.17	0.281491	0.001011	0.033066	0.281453 ± 0.000016	**-3.0** ± 0.6	–	–	**2.80**	–	–
14.1	–	**1968** ± 8	0.62	0.281440	0.000992	0.040495	0.281403 ± 0.000022	**-4.5** ± 0.8	–	–	**2.90**	–	–
16.1	–	**1976** ± 5	0.47	0.281449	0.000766	0.028071	0.281420 ± 0.000016	**-3.7** ± 0.6	–	–	**2.86**	–	–
17.1	–	**1967** ± 13	0.57	0.281470	0.000982	0.036103	0.281433 ± 0.000015	**-3.5** ± 0.5	–	–	**2.84**	–	–
18.1	–	**1984** ± 17	0.49	0.281556	0.000810	0.028790	0.281525 ± 0.000015	**0.2** ± 0.5	–	–	**2.62**	–	–
20.1	–	**1982** ± 20	0.34	0.281416	0.000444	0.015876	0.281399 ± 0.000016	**-4.4** ± 0.6	–	–	**2.90**	–	–
21.1	–	**1972** ± 11	0.59	0.281484	0.001346	0.048587	0.281434 ± 0.000022	**-3.4** ± 0.8	–	–	**2.83**	–	–
22.1	–	**1981** ± 10	0.76	0.281455	0.000263	0.010104	0.281445 ± 0.000013	**-2.7** ± 0.5	–	–	**2.80**	–	–
Moorarie Supersuite													
southern plutons													
GSWA 142849: foliated coarse-grained monzogranite													
magmatic													
4.1	centre	**1829** ± 16	0.38	0.281554	0.001885	0.087914	0.281489 ± 0.000023	**-4.7** ± 0.8	–	–	**2.81**	–	–
	edge			0.281500	0.000428	0.017301	0.281485 ± 0.000021	**-4.8** ± 0.7	–	–	**2.81**	–	–
5.1	centre	**1835** ± 12	0.44	0.281520	0.000619	0.025722	0.281498 ± 0.000016	**-4.2** ± 0.6	–	–	**2.78**	–	–
18.1	centre	**1797** ± 11	0.25	0.281388	0.000476	0.019413	0.281372 ± 0.000012	**-9.5** ± 0.4	–	–	**3.09**	–	–
	edge			0.281450	0.000660	0.025424	0.281428 ± 0.000015	**-7.6** ± 0.5	–	–	**2.96**	–	–
22.1	centre	**1783** ± 17	0.24	0.281455	0.000613	0.026226	0.281434 ± 0.000018	**-7.6** ± 0.6	–	–	**2.96**	–	–
	edge			0.281387	0.000643	0.018631	0.281365 ± 0.000014	**-10.1** ± 0.5	–	–	**3.11**	–	–
25.1	edge	**1823** ± 17	0.31	0.281398	0.000778	0.020889	0.281371 ± 0.000013	**-9.0** ± 0.5	–	–	**3.07**	–	–

Analysis No.	Spot location	$^{207}Pb/^{206}Pb$ date (Ma)	Th/U	$^{176}Hf/^{177}Hf$ measured	$^{176}Lu/^{177}Hf$ measured	$^{176}Yb/^{177}Hf$ measured	$^{176}Hf/^{177}Hf$ initial	$\varepsilon_{Hf(t)}$	$\varepsilon_{Hf(1800\ Ma)}$	$\varepsilon_{Hf(1650\ Ma)}$	$T_{DM}2$ (Ga)	$^{18}O/^{16}O$ [(a)(b)]	$\delta^{18}O$ [(c)]
GSWA 159987: Dumbie Granodiorite, foliated porphyritic biotite granodiorite													
magmatic													
1.1	–	**1816** ± 18	1.76	0.281554	0.000264	0.011033	0.281545 ± 0.000023	**-3.0** ± 0.8	–	–	**2.69**	–	–
9.1	centre	**1793** ± 19	0.93	0.281404	0.000431	0.019959	0.281389 ± 0.000012	**-9.0** ± 0.4	–	–	**3.05**	–	–
	edge			0.281432	0.000590	0.025474	0.281412 ± 0.000014	**-8.2** ± 0.5	–	–	**3.00**	–	–
13.1	–	**1812** ± 7	0.07	0.281389	0.000313	0.014486	0.281378 ± 0.000015	**-9.0** ± 0.5	–	–	**3.06**	–	–
14.1	centre	**1813** ± 6	0.08	0.281352	0.000555	0.025523	0.281333 ± 0.000011	**-10.6** ± 0.4	–	–	**3.16**	–	–
	edge			0.281404	0.000807	0.040398	0.281376 ± 0.000016	**-9.0** ± 0.6	–	–	**3.07**	–	–
16.1	centre	**1806** ± 9	0.05	0.281434	0.000290	0.012142	0.281424 ± 0.000012	**-7.5** ± 0.4	–	–	**2.97**	–	–
	edge			0.281378	0.000475	0.021962	0.281362 ± 0.000012	**-9.7** ± 0.4	–	–	**3.11**	–	–
inherited													
4.1	–	**2107** ± 16	0.07	0.281397	0.000445	0.021538	0.281379 ± 0.000012	**-2.2** ± 0.4	–	–	**2.86**	–	–
5.1	–	**2125** ± 10	0.92	0.281381	0.000577	0.026301	0.281358 ± 0.000012	**-2.6** ± 0.4	–	–	**2.90**	–	–
6.1	–	**2390** ± 27	0.17	0.281279	0.000646	0.026304	0.281250 ± 0.000012	**-0.3** ± 0.4	–	–	**2.96**	–	–
8.1	–	**2120** ± 12	1.42	0.281391	0.000943	0.035174	0.281353 ± 0.000016	**-2.8** ± 0.6	–	–	**2.91**	–	–
10.1	–	**2105** ± 10	1.04	0.281387	0.001018	0.038127	0.281346 ± 0.000011	**-3.4** ± 0.4	–	–	**2.94**	–	–
12.1	–	**2419** ± 9	0.26	0.281196	0.000978	0.047829	0.281151 ± 0.000014	**-3.2** ± 0.5	–	–	**3.17**	–	–
15.1	–	**2112** ± 10	1.25	0.281335	0.001465	0.071180	0.281276 ± 0.000012	**-5.8** ± 0.4	–	–	**3.09**	–	–
17.1	–	**2100** ± 8	1.20	0.281372	0.000775	0.034389	0.281341 ± 0.000010	**-3.7** ± 0.3	–	–	**2.96**	–	–
18.1	–	**2427** ± 7	0.30	0.281252	0.000653	0.030317	0.281222 ± 0.000013	**-0.5** ± 0.5	–	–	**3.00**	–	–
19.1	–	**2442** ± 8	0.50	0.281232	0.000546	0.023337	0.281207 ± 0.000013	**-0.7** ± 0.5	–	–	**3.02**	–	–
22.1	–	**2308** ± 6	0.25	0.281286	0.000636	0.033596	0.281258 ± 0.000009	**-1.9** ± 0.3	–	–	**3.00**	–	–
23.1	–	**2304** ± 5	0.14	0.281242	0.000166	0.007681	0.281235 ± 0.000013	**-2.8** ± 0.5	–	–	**3.06**	–	–
26.1	–	**2435** ± 6	0.45	0.281247	0.000291	0.011957	0.281233 ± 0.000008	**0.1** ± 0.3	–	–	**2.97**	–	–
27.1	–	**2424** ± 9	0.56	0.281226	0.001012	0.046061	0.281179 ± 0.000012	**-2.0** ± 0.4	–	–	**3.10**	–	–
GSWA 188975: Dumbie Granodiorite, metatonalite													
magmatic													
1.1	–	**1803** ± 6	0.07	0.281361	0.001092	0.032081	0.281324 ± 0.000012	**-11.1** ± 0.4	–	–	**3.19**	–	–
2.1	–	**1792** ± 6	0.05	0.281500	0.000876	0.039489	0.281470 ± 0.000013	**-6.2** ± 0.5	–	-9.3	**2.87**	0.0020135 ± 0.0076	**6.8** ± 0.08
3.1	–	**1789** ± 8	0.22	0.281375	0.000340	0.014568	0.281363 ± 0.000008	**-10.0** ± 0.3	–	-13.1	**3.11**	0.0020132 ± 0.0084	**6.6** ± 0.09
7.1	–	**1791** ± 9	0.13	0.281335	0.000014	0.000694	0.281335 ± 0.000007	**-11.0** ± 0.2	–	-14.2	**3.18**	0.0020144 ± 0.0064	**7.2** ± 0.07
	edge			0.281414	0.000665	0.030313	0.281391 ± 0.000011	**-8.8** ± 0.4	–	-12.1	**3.04**	0.0020146 ± 0.0092	**7.3** ± 0.09
11.1	–	**1807** ± 6	0.07	0.281321	0.000672	0.023893	0.281298 ± 0.000009	**-11.9** ± 0.3	–	-15.4	**3.25**	0.0020151 ± 0.0123	**7.6** ± 0.13
16.1	–	**1813** ± 8	0.15	0.281342	0.000999	0.038351	0.281308 ± 0.000007	**-11.5** ± 0.2	–	–	**3.22**	–	–
19.1	–	**1812** ± 7	0.15	0.281393	0.000876	0.030319	0.281363 ± 0.000010	**-9.5** ± 0.3	–	–	**3.10**	–	–
21.1	centre	**1803** ± 6	0.15	0.281332	0.000954	0.037148	0.281299 ± 0.000010	**-12.0** ± 0.4	–	-15.3	**3.25**	0.0020123 ± 0.0097	**6.2** ± 0.10
	edge			0.281340	0.000409	0.016353	0.281326 ± 0.000007	**-11.0** ± 0.2	–	-14.5	**3.19**	0.0020123 ± 0.0082	**6.2** ± 0.08
22.1	–	**1812** ± 9	0.19	0.281396	0.000298	0.012007	0.281386 ± 0.000006	**-8.7** ± 0.2	–	–	**3.05**	–	–

Analysis No.	Spot location	$^{207}Pb/^{206}Pb$ date (Ma)	Th/U	$^{176}Hf/^{177}Hf$ measured	$^{176}Lu/^{177}Hf$ measured	$^{176}Yb/^{177}Hf$ measured	$^{176}Hf/^{177}Hf$ initial	$\varepsilon_{Hf(t)}$	$\varepsilon_{Hf(1800\ Ma)}$	$\varepsilon_{Hf(1650\ Ma)}$	$T_{DM}2$ (Ga)	$^{18}O/^{16}O$ [a][b]	$\delta^{18}O$ [c]
inherited													
5.1	–	**2307** ± 5	0.18	0.281197	0.000441	0.016556	0.281178 ± 0.000011	**-4.8** ± 0.4	-16.2	-19.6	**3.18**	0.0020178 ± 0.0136	**8.9** ± 0.14
6.1	–	**2113** ± 9	1.07	0.281286	0.000718	0.029987	0.281257 ± 0.000009	**-6.4** ± 0.3	-13.4	-16.7	**3.14**	0.0020159 ± 0.0076	**8.0** ± 0.08
8.1	–	**2202** ± 119	0.42	0.281243	0.000276	0.009638	0.281231 ± 0.000007	**-5.3** ± 0.2	–	–	**3.13**	–	–
12.1	–	**2288** ± 8	0.25	0.281250	0.000427	0.017717	0.281231 ± 0.000012	**-3.3** ± 0.4	-14.3	-17.7	**3.07**	0.0020125 ± 0.0101	**6.3** ± 0.10
14.1	–	**2326** ± 6	0.16	0.281243	0.000135	0.005472	0.281237 ± 0.000010	**-2.2** ± 0.4	-14.2	-17.6	**3.04**	0.0020179 ± 0.0072	**9.0** ± 0.08
15.2	–	**2304** ± 41	0.28	0.281235	0.000565	0.021789	0.281210 ± 0.000005	**-3.7** ± 0.2	-15.0	-18.4	**3.11**	0.0020181 ± 0.0058	**9.1** ± 0.06
18.1	–	**1914** ± 6	0.01	0.281390	0.000537	0.014758	0.281370 ± 0.000009	**-6.9** ± 0.3	–	–	**3.01**	–	–
20.1	–	**2200** ± 10	0.27	0.281218	0.000276	0.011130	0.281206 ± 0.000008	**-6.2** ± 0.3	-15.3	-18.6	**3.19**	0.0020159 ± 0.0071	**8.0** ± 0.07
23.1	–	**2122** ± 8	0.81	0.281324	0.000494	0.018354	0.281304 ± 0.000010	-4.53 ± 0.3	–	–	**3.02**	–	–
GSWA 159996: Scrubber Granite, biotite monzogranite													
magmatic													
1.1	–	**1811** ± 14	0.53	0.281458	0.000401	0.014407	0.281444 ± 0.000027	**-6.7** ± 0.9	–	–	**2.92**	–	–
5.1	centre	**1749** ± 27	0.63	0.281606	0.000733	0.025950	0.281582 ± 0.000020	**-3.2** ± 0.7	–	-5.4	**2.65**	0.0020181 ± 0.0094	**7.5** ± 0.10
	edge			0.281575	0.000811	0.022975	0.281548 ± 0.000015	**-4.4** ± 0.5	–	-6.6	**2.72**	0.0020180 ± 0.0094	**7.4** ± 0.10
8.1	centre	**1805** ± 13	0.61	0.281462	0.000576	0.020170	0.281442 ± 0.000015	**-6.9** ± 0.5	–	-10.3	**2.93**	0.0020163 ± 0.0064	**6.6** ± 0.07
	edge			0.281412	0.000956	0.031246	0.281379 ± 0.000020	**-9.1** ± 0.7	–	-12.5	**3.07**	0.0020160 ± 0.0067	**6.4** ± 0.07
9.1	centre	**1798** ± 9	0.75	0.281467	0.000519	0.017984	0.281449 ± 0.000018	**-6.8** ± 0.6	–	-10.1	**2.91**	0.0020186 ± 0.0149	**7.7** ± 0.15
	edge			0.281537	0.000680	0.019456	0.281514 ± 0.000018	**-4.5** ± 0.6	–	-7.8	**2.77**	0.0020172 ± 0.0094	**7.0** ± 0.10
21.1	–	**1792** ± 8	0.22	0.281514	0.000586	0.020616	0.281494 ± 0.000014	**-5.3** ± 0.5	–	–	**2.82**	–	–
22.1	–	**1805** ± 10	0.62	0.281604	0.000743	0.024528	0.281579 ± 0.000015	**-2.0** ± 0.5	–	–	**2.62**	–	–
25.1	–	**1788** ± 8	0.52	0.281510	0.000731	0.024090	0.281485 ± 0.000023	**-5.7** ± 0.8	–	–	**2.84**	–	–
inherited													
10.1	–	**2127** ± 18	0.64	0.281279	0.000755	0.027891	0.281248 ± 0.000012	**-6.4** ± 0.4	-13.7	-17.0	**3.15**	0.0020193 ± 0.0059	**8.1** ± 0.06
13.1	centre	**2282** ± 8	0.46	0.281360	0.000972	0.036369	0.281318 ± 0.000010	**-0.4** ± 0.3	-11.1	-14.4	**2.88**	0.0020165 ± 0.0076	**6.6** ± 0.08
13.1	edge			0.281451	0.000815	0.027242	0.281416 ± 0.000014	**3.1** ± 0.5	-7.6	-11.0	**2.66**	0.0020149 ± 0.0089	**5.8** ± 0.09
19.1	–	**2263** ± 8	0.53	0.281325	0.000706	0.023638	0.281295 ± 0.000016	**-1.6** ± 0.6	-12.0	-15.3	**2.95**	0.0020182 ± 0.0069	**7.5** ± 0.07
20.1	–	**2297** ± 8	0.72	0.281343	0.000668	0.021058	0.281314 ± 0.000016	**-0.2** ± 0.6	-11.3	-14.6	**2.88**	0.0020170 ± 0.0096	**6.9** ± 0.10
Minnie Creek batholith													
GSWA 191995: foliated monzogranite													
magmatic													
1.1	–	**1799** ± 8	0.50	0.281608	0.000842	0.034424	0.281579 ± 0.000032	**-2.1** ± 1.1	–	–	**2.62**	–	–
5.1	–	**1790** ± 18	0.75	0.281698	0.000985	0.045937	0.281665 ± 0.000044	**0.7** ± 1.5	–	-2.4	**2.43**	0.0020213 ± 0.0139	**8.0** ± 0.14
7.1	–	**1778** ± 8	0.71	0.281295	0.001103	0.040932	0.281258 ± 0.000030	**-14.0** ± 1.1	–	–	**3.36**	–	–
15.1	–	**1792** ± 8	0.53	0.281141	0.000639	0.028734	0.281119 ± 0.000026	**-18.6** ± 0.9	–	–	**3.65**	–	–
18.1	–	**1788** ± 7	0.37	0.281553	0.000704	0.026126	0.281529 ± 0.000014	**-4.2** ± 0.5	–	-7.2	**2.74**	0.0020190 ± 0.0115	**7.9** ± 0.12
19.1	–	**1808** ± 12	0.38	0.281645	0.001040	0.042244	0.281609 ± 0.000019	**-0.9** ± 0.7	–	–	**2.55**	–	–
22.1	–	**1803** ± 16	1.89	0.281363	0.000385	0.018436	0.281350 ± 0.000024	**-10.2** ± 0.8	–	-13.6	**3.13**	0.0020238 ± 0.0085	**9.2** ± 0.09
24.1	–	**1797** ± 7	0.41	0.281370	0.000703	0.030045	0.281346 ± 0.000068	**-10.5** ± 2.4	–	–	**3.15**	–	–

Analysis No.	Spot location	$^{207}Pb/^{206}Pb$ date (Ma)	Th/U	$^{176}Hf/^{177}Hf$ measured	$^{176}Lu/^{177}Hf$ measured	$^{176}Yb/^{177}Hf$ measured	$^{176}Hf/^{177}Hf$ initial	$\varepsilon_{Hf(t)}$	$\varepsilon_{Hf(1800\ Ma)}$	$\varepsilon_{Hf(1650\ Ma)}$	T_{DM}^2 (Ga)	$^{18}O/^{16}O$ [a][b]	$\delta^{18}O$ [c]
inherited													
4.1	–	**1825** ± 10	0.18	0.281593	0.001496	0.060581	0.281541 ± 0.000024	**-2.9** ± 0.8	-3.4	-6.7	**2.69**	–	–
21.1	–	**1884** ± 7	0.19	0.281569	0.000704	0.028496	0.281544 ± 0.000018	**-1.5** ± 0.6	-3.3	-6.7	**2.64**	–	–
23.1	–	**1840** ± 11	0.67	0.281718	0.001321	0.058784	0.281672 ± 0.000011	**2.1** ± 0.4	1.2	-2.1	**2.38**	0.0020190 ± 0.0115	**6.8** ± 0.12
25.1	–	**2409** ± 6	0.46	0.281048	0.001203	0.047716	0.280993 ± 0.000012	**-9.0** ± 0.4	-22.4	-25.7	**3.53**	0.0020182 ± 0.0097	**6.4** ± 0.10
GSWA 88412: foliated porphyritic monzogranite													
magmatic													
4.1	centre	**1792** ± 12	0.78	0.281669	0.001359	0.057430	0.281623 ± 0.000016	**-0.7** ± 0.6	–	–	**2.53**	–	–
	edge			0.281611	0.000886	0.025725	0.281581 ± 0.000017	**-2.2** ± 0.6	–	–	**2.62**	–	–
5.1	centre	**1781** ± 12	0.69	0.281627	0.001221	0.056695	0.281586 ± 0.000013	**-2.3** ± 0.5	–	–	**2.62**	–	–
	edge			0.281661	0.000824	0.033651	0.281633 ± 0.000011	**-0.6** ± 0.4	–	–	**2.51**	–	–
7.1	centre	**1787** ± 12	0.94	0.281644	0.001325	0.058780	0.281599 ± 0.000018	**-1.7** ± 0.6	–	–	**2.58**	–	–
	edge			0.281601	0.000953	0.028479	0.281569 ± 0.000021	**-2.8** ± 0.7	–	–	**2.65**	–	–
9.1	centre	**1806** ± 10	0.82	0.281656	0.001392	0.057692	0.281608 ± 0.000018	**-0.9** ± 0.6	–	–	**2.55**	–	–
	edge			0.281674	0.001170	0.036208	0.281634 ± 0.000016	**0.0** ± 0.6	–	–	**2.49**	–	–
10.1	centre	**1781** ± 17	0.67	0.281614	0.000831	0.035342	0.281586 ± 0.000015	**-2.3** ± 0.5	–	–	**2.62**	–	–
	edge			0.281618	0.000738	0.022726	0.281593 ± 0.000018	**-2.0** ± 0.6	–	–	**2.60**	–	–
19.1	centre	**1786** ± 13	0.72	0.281601	0.001286	0.057640	0.281557 ± 0.000015	**-3.2** ± 0.5	–	–	**2.68**	–	–
	edge			0.281664	0.000699	0.029764	0.281640 ± 0.000014	**-0.3** ± 0.5	–	–	**2.49**	–	–
22.1	centre	**1799** ± 10	0.73	0.281668	0.001218	0.056469	0.281626 ± 0.000011	**-0.5** ± 0.4	–	–	**2.51**	–	–
	edge			0.281669	0.000933	0.032311	0.281637 ± 0.000013	**-0.1** ± 0.5	–	–	**2.49**	–	–
23.1	centre	**1794** ± 10	0.76	0.281597	0.000702	0.031921	0.281573 ± 0.000014	**-2.5** ± 0.5	–	–	**2.64**	–	–
	edge			0.281608	0.000908	0.031836	0.281577 ± 0.000010	**-2.3** ± 0.4	–	–	**2.63**	–	–
GSWA 88405: biotite granodiorite													
magmatic													
3.1	centre	**1803** ± 17	0.61	0.281642	0.000779	0.034881	0.281615 ± 0.000019	**-0.7** ± 0.7	–	–	**2.54**	–	–
	edge			0.281544	0.000978	0.027399	0.281511 ± 0.000027	**-4.5** ± 0.9	–	–	**2.77**	–	–
9.1	–	**1785** ± 14	0.60	0.281610	0.001640	0.072339	0.281554 ± 0.000032	**-3.3** ± 1.1	–	–	**2.69**	–	–
14.1	centre	**1814** ± 16	0.64	0.281654	0.000955	0.043694	0.281621 ± 0.000017	**-0.3** ± 0.6	–	–	**2.52**	–	–
	edge			0.281613	0.000504	0.022943	0.281596 ± 0.000028	**-1.2** ± 1.0	–	–	**2.57**	–	–
15.1	–	**1781** ± 18	0.47	0.281550	0.000673	0.023296	0.281527 ± 0.000023	**-4.4** ± 0.8	–	–	**2.75**	–	–
19.1	centre	**1785** ± 13	0.60	0.281722	0.001089	0.049292	0.281685 ± 0.000026	**1.3** ± 0.9	–	–	**2.39**	–	–
	edge			0.281734	0.000698	0.028652	0.281710 ± 0.000023	**2.2** ± 0.8	–	–	**2.33**	–	–
23.1	centre	**1794** ± 16	0.35	0.281582	0.001139	0.046635	0.281543 ± 0.000013	**-3.5** ± 0.5	–	–	**2.71**	–	–
	edge			0.281635	0.000667	0.020399	0.281612 ± 0.000018	**-1.1** ± 0.6	–	–	**2.55**	–	–
29.1	centre	**1794** ± 14	0.59	0.281576	0.000719	0.029815	0.281552 ± 0.000011	**-3.2** ± 0.4	–	–	**2.69**	–	–
	edge			0.281595	0.000699	0.031875	0.281571 ± 0.000010	**-2.5** ± 0.3	–	–	**2.64**	–	–
37.1	centre	**1796** ± 10	0.56	0.281632	0.000812	0.033936	0.281604 ± 0.000007	**-1.3** ± 0.3	–	–	**2.57**	–	–
	edge			0.281626	0.000942	0.040946	0.281594 ± 0.000009	**-2.0** ± 0.3	–	–	**2.60**	–	–

Analysis No.	Spot location	$^{207}Pb/^{206}Pb$ date (Ma)	Th/U	$^{176}Hf/^{177}Hf$ measured	$^{176}Lu/^{177}Hf$ measured	$^{176}Yb/^{177}Hf$ measured	$^{176}Hf/^{177}Hf$ initial	$\varepsilon_{Hf(t)}$	$\varepsilon_{Hf(1800\ Ma)}$	$\varepsilon_{Hf(1650\ Ma)}$	T_{DM}^2 (Ga)	$^{18}O/^{16}O$ [(a)(b)]	$\delta^{18}O$ [(c)]
GSWA 190660: metamonzogranite													
magmatic													
1.1	centre	**1787** ± 10	0.13	0.281573	0.000563	0.020453	0.281554 ± 0.000016	**-3.3** ± 0.6	–	-6.4	**2.69**	0.0020220 ± 0.0166	**7.7** ± 0.19
	edge			0.281533	0.001135	0.043740	0.281495 ± 0.000018	**-5.4** ± 0.6	–	-8.4	**2.82**	0.0020202 ± 0.0173	**6.8** ± 0.19
3.1	centre	**1806** ± 9	0.27	0.281443	0.000613	0.022423	0.281422 ± 0.000021	**-7.5** ± 0.7	–	-11.0	**2.97**	0.0020213 ± 0.0117	**7.2** ± 0.15
	edge			0.281583	0.001239	0.037957	0.281541 ± 0.000016	**-3.3** ± 0.6	–	-6.8	**2.70**	0.0020204 ± 0.0067	**6.8** ± 0.11
4.1	–	**1796** ± 5	0.11	0.281583	0.001406	0.046908	0.281535 ± 0.000012	**-3.8** ± 0.4	–	–	**2.72**	–	–
5.1	–	**1791** ± 4	0.15	0.281567	0.001608	0.058240	0.281512 ± 0.000013	**-4.7** ± 0.5	–	–	**2.78**	–	–
6.1	centre	**1792** ± 5	0.17	0.281620	0.000893	0.031164	0.281590 ± 0.000015	**-1.9** ± 0.5	–	-5.1	**2.60**	0.0020222 ± 0.0073	**7.6** ± 0.13
	edge			0.281563	0.001115	0.032713	0.281525 ± 0.000013	**-4.2** ± 0.5	–	-7.3	**2.75**	0.0020224 ± 0.0118	**7.7** ± 0.16
7.1	–	**1787** ± 6	0.14	0.281551	0.001039	0.039342	0.281516 ± 0.000009	**-4.7** ± 0.3	–	-7.7	**2.77**	0.0020227 ± 0.0115	**7.9** ± 0.15
8.1	–	**1796** ± 4	0.28	0.281582	0.001283	0.045827	0.281538 ± 0.000009	**-3.7** ± 0.3	–	–	**2.72**	–	–
9.1	–	**1794** ± 14	0.71	0.281568	0.001110	0.038556	0.281530 ± 0.000009	**-4.0** ± 0.3	–	–	**2.73**	–	–
10.1	–	**1792** ± 6	0.25	0.281571	0.001508	0.054549	0.281520 ± 0.000013	**-4.4** ± 0.5	–	–	**2.76**	–	–
11.1	–	**1786** ± 8	0.21	0.281554	0.000816	0.026048	0.281526 ± 0.000011	**-4.3** ± 0.4	–	–	**2.75**	–	–
12.1	–	**1794** ± 7	0.13	0.281548	0.001489	0.057237	0.281497 ± 0.000014	**-5.1** ± 0.5	–	–	**2.81**	–	–
13.1	–	**1802** ± 10	0.85	0.281541	0.001424	0.041926	0.281492 ± 0.000023	**-5.1** ± 0.8	–	–	**2.81**	–	–
14.1	centre	**1781** ± 5	0.13	0.281572	0.001122	0.039477	0.281534 ± 0.000013	**-4.1** ± 0.5	–	-7.0	**2.73**	0.0020257 ± 0.0088	**9.2** ± 0.15
	edge			0.281517	0.001115	0.030606	0.281479 ± 0.000035	**-6.1** ± 1.2	–	-9.0	**2.86**	0.0020221 ± 0.0144	**7.5** ± 0.19
15.1	–	**1776** ± 9	0.19	0.281618	0.002537	0.086659	0.281533 ± 0.000012	**-4.3** ± 0.4	–	–	**2.74**	–	–
16.1	–	**1789** ± 10	0.13	0.281559	0.001768	0.059768	0.281499 ± 0.000015	**-5.2** ± 0.5	–	–	**2.81**	–	–
17.1	–	**1784** ± 7	0.10	0.281568	0.001855	0.055791	0.281505 ± 0.000012	**-5.1** ± 0.4	–	–	**2.80**	–	–
inherited													
2.1	–	**1933** ± 9	0.49	0.281531	0.001386	0.058868	0.281480 ± 0.000017	**-2.6** ± 0.6	-5.5	-8.8	**2.75**	–	–
GSWA 190661: metatonalite													
magmatic													
1.1	centre	**1794** ± 10	0.25	0.281356	0.000882	0.035771	0.281326 ± 0.000020	**-11.2** ± 0.7	–	-14.4	**3.19**	0.0020206 ± 0.0120	**7.8** ± 0.22
	edge			0.281589	0.000987	0.032360	0.281555 ± 0.000015	**-3.1** ± 0.5	–	-6.3	**2.68**	0.0020226 ± 0.0120	**8.9** ± 0.21
2.1	centre	**1804** ± 8	0.26	0.281592	0.001206	0.044968	0.281551 ± 0.000011	**-3.0** ± 0.4	–	-6.4	**2.68**	0.0020210 ± 0.0098	**8.0** ± 0.22
	edge			0.281586	0.001169	0.040458	0.281546 ± 0.000010	**-3.2** ± 0.4	–	-6.6	**2.69**	0.0020206 ± 0.0175	**7.8** ± 0.26
3.1	–	**1810** ± 10	0.23	0.281591	0.001137	0.043512	0.281552 ± 0.000009	**-2.8** ± 0.3	–	-6.4	**2.68**	0.0020200 ± 0.0105	**7.5** ± 0.23
4.1	–	**1795** ± 9	0.26	0.281581	0.001431	0.059084	0.281532 ± 0.000010	**-3.9** ± 0.4	–	–	**2.73**	–	–
5.1	–	**1789** ± 5	0.01	0.281633	0.000527	0.019338	0.281615 ± 0.000011	**-1.1** ± 0.4	–	–	**2.55**	–	–
7.1	–	**1803** ± 7	0.39	0.281568	0.001180	0.038610	0.281528 ± 0.000011	**-3.9** ± 0.4	–	–	**2.73**	–	–
9.1	centre	**1805** ± 7	0.62	0.281598	0.002016	0.068636	0.281529 ± 0.000010	**-3.8** ± 0.4	–	-7.1	**2.73**	0.0020204 ± 0.0098	**7.6** ± 0.24
	edge			0.281590	0.000793	0.029534	0.281563 ± 0.000014	**-2.6** ± 0.5	–	-6.0	**2.65**	0.0020219 ± 0.0079	**8.4** ± 0.23
10.1	–	**1802** ± 8	0.41	0.281601	0.001241	0.048822	0.281559 ± 0.000008	**-2.8** ± 0.3	–	–	**2.67**	–	–
12.1	centre	**1807** ± 7	0.19	0.281628	0.000971	0.035553	0.281595 ± 0.000016	**-1.4** ± 0.6	–	-4.9	**2.58**	0.0020304 ± 0.0180	**7.0** ± 0.30
	edge			0.281581	0.001237	0.038877	0.281539 ± 0.000019	**-3.4** ± 0.7	–	-6.8	**2.71**	0.0020214 ± 0.0148	**8.0** ± 0.27

Analysis No.	Spot location	$^{207}Pb/^{206}Pb$ date (Ma)	Th/U	$^{176}Hf/^{177}Hf$ measured	$^{176}Lu/^{177}Hf$ measured	$^{176}Yb/^{177}Hf$ measured	$^{176}Hf/^{177}Hf$ initial	$\varepsilon_{Hf(t)}$	$\varepsilon_{Hf(1800\ Ma)}$	$\varepsilon_{Hf(1650\ Ma)}$	T_{DM}^2 (Ga)	$^{18}O/^{16}O$ [(a)(b)]	$\delta^{18}O$ [(c)]
GSWA 190662: Middle Spring Granite, gneissic metamonzogranite													
magmatic													
1.1	centre	**1797** ± 21	1.40	0.281606	0.000642	0.023993	0.281584 ± 0.000024	**-2.0** ± 0.8	–	–	**2.61**	–	–
	edge	**1797** ± 21		0.281550	0.000538	0.021085	0.281532 ± 0.000030	**-3.9** ± 1.1	–	–	**2.73**	–	–
2.1	–	**1762** ± 22	0.58	0.281616	0.000845	0.023373	0.281588 ± 0.000030	**-2.7** ± 1.1	–	–	**2.63**	–	–
3.1	–	**1773** ± 21	2.10	0.281375	0.000668	0.024868	0.281353 ± 0.000024	**-10.8** ± 0.8	–	–	**3.15**	–	–
6.1	centre	**1784** ± 18	0.84	0.281768	0.000232	0.010157	0.281760 ± 0.000044	**4.0** ± 1.5	–	–	**2.22**	–	–
	edge	**1784** ± 18		0.281621	0.000440	0.016772	0.281606 ± 0.000043	**-1.5** ± 1.5	–	–	**2.57**	–	–
14.1	centre	**1795** ± 13	0.81	0.281694	0.000816	0.028890	0.281666 ± 0.000028	**0.9** ± 1.0	–	–	**2.43**	–	–
	edge	**1795** ± 13		0.281687	0.000968	0.035064	0.281654 ± 0.000032	**0.4** ± 1.1	–	–	**2.45**	–	–
19.1	–	**1770** ± 16	1.09	0.281566	0.000336	0.014567	0.281555 ± 0.000016	**-3.7** ± 0.6	–	-6.4	**2.70**	0.0020171 ± 0.0096	**9.8** ± 0.10
22.1	–	**1789** ± 26	2.15	0.281573	0.000549	0.016969	0.281554 ± 0.000025	**-3.2** ± 0.9	–	–	**2.68**	–	–
25.1	–	**1788** ± 26	0.67	0.281499	0.000576	0.020303	0.281479 ± 0.000012	**-5.9** ± 0.4	–	–	**2.85**	–	–
inherited													
4.1	–	**1848** ± 10	0.27	0.281589	0.001622	0.059680	0.281532 ± 0.000048	**-2.7** ± 1.7	-3.7	-7.0	**2.69**	–	–
7.1	–	**1841** ± 66	1.50	0.281541	0.000513	0.018838	0.281523 ± 0.000029	**-3.2** ± 1.0	-4.1	-7.4	**2.72**	–	–
10.1	–	**2703** ± 6	0.17	0.281252	0.000981	0.035289	0.281201 ± 0.000061	**5.2** ± 2.1	-14.9	-18.2	**2.85**	–	–
11.1	–	**1819** ± 35	1.45	0.281622	0.001775	0.051287	0.281561 ± 0.000049	**-2.3** ± 1.7	-2.7	-6.0	**2.65**	–	–
GSWA 178024: biotite granodiorite													
magmatic													
1.1	–	**1784** ± 14	1.84	0.281831	0.001687	0.041817	0.281774 ± 0.000083	**4.4** ± 2.9	–	–	**2.19**	–	–
2.1	–	**1770** ± 10	1.15	0.281645	0.001372	0.048062	0.281599 ± 0.000037	**-2.1** ± 1.3	–	-4.7	**2.60**	0.0020174 ± 0.0119	**7.2** ± 0.12
3.1	–	**1787** ± 12	0.85	0.281666	0.002011	0.061158	0.281598 ± 0.000063	**-1.7** ± 2.2	–	-4.7	**2.59**	0.0020169 ± 0.0096	**7.0** ± 0.10
4.1	–	**1779** ± 10	1.25	0.281665	0.001234	0.042637	0.281623 ± 0.000024	**-1.0** ± 0.8	–	-3.8	**2.53**	0.0020172 ± 0.0091	**7.1** ± 0.09
5.1	–	**1763** ± 12	0.90	0.281625	0.001173	0.050380	0.281586 ± 0.000035	**-2.7** ± 1.2	–	-5.2	**2.63**	0.0020165 ± 0.0088	**6.8** ± 0.09
20.1	centre	**1800** ± 12	0.70	0.281582	0.002642	0.077277	0.281492 ± 0.000037	**-5.2** ± 1.3	–	–	**2.82**	–	–
	edge			0.281563	0.000751	0.028764	0.281537 ± 0.000016	**-3.6** ± 0.6	–	–	**2.71**	–	–
21.1	centre	**1802** ± 21	0.84	0.281547	0.000418	0.014322	0.281533 ± 0.000011	**-3.7** ± 0.4	–	-7.1	**2.72**	0.0020217 ± 0.0159	**9.4** ± 0.16
	edge			0.281584	0.000541	0.020019	0.281566 ± 0.000015	**-2.5** ± 0.5	–	-5.9	**2.65**	0.0020182 ± 0.0119	**7.6** ± 0.12
22.1	centre	**1794** ± 14	0.87	0.281602	0.001092	0.041762	0.281565 ± 0.000017	**-2.8** ± 0.6	–	–	**2.66**	–	–
	edge			0.281590	0.000985	0.026126	0.281556 ± 0.000032	**-3.1** ± 1.1	–	–	**2.68**	–	–
24.1	–	**1792** ± 14	0.71	0.281688	0.000951	0.036268	0.281656 ± 0.000023	**0.4** ± 0.8	–	–	**2.45**	–	–
25.1	centre	**1789** ± 15	0.83	0.281608	0.000577	0.021884	0.281588 ± 0.000016	**-2.0** ± 0.6	–	-5.1	**2.61**	0.0020175 ± 0.0106	**7.3** ± 0.11
	edge			0.281639	0.000783	0.028417	0.281612 ± 0.000012	**-1.2** ± 0.4	–	-4.3	**2.55**	0.0020175 ± 0.0089	**7.3** ± 0.09
26.1	–	**1766** ± 21	0.87	0.281591	0.000808	0.028878	0.281564 ± 0.000013	**-3.4** ± 0.5	–	–	**2.68**	–	–
27.1	–	**1761** ± 22	0.54	0.281627	0.000885	0.034781	0.281597 ± 0.000034	**-2.3** ± 1.2	–	–	**2.61**	–	–

Analysis No.	Spot location	$^{207}Pb/^{206}Pb$ date (Ma)	Th/U	$^{176}Hf/^{177}Hf$ measured	$^{176}Lu/^{177}Hf$ measured	$^{176}Yb/^{177}Hf$ measured	$^{176}Hf/^{177}Hf$ initial	$\varepsilon_{Hf(t)}$	$\varepsilon_{Hf(1800\ Ma)}$	$\varepsilon_{Hf(1650\ Ma)}$	$T_{DM}2$ (Ga)	$^{18}O/^{16}O$ (a)(b)	$\delta^{18}O$ (c)
GSWA 180938: equigranular biotite monzogranite													
magmatic													
4.1	–	**1774** ± 8	1.58	0.281686	0.001670	0.065476	0.281630 ± 0.000017	**-0.9** ± 0.6	–	–	**2.52**	–	–
10.1	–	**1823** ± 30	0.61	0.281535	0.000619	0.026267	0.281514 ± 0.000016	**-3.9** ± 0.6	–	-7.8	**2.75**	0.0020146 ± 0.0125	**8.5** ± 0.13
13.1	–	**1785** ± 7	0.77	0.281567	0.002510	0.082501	0.281482 ± 0.000019	**-5.9** ± 0.7	–	-8.7	**2.85**	0.0020128 ± 0.0093	**7.6** ± 0.10
14.1	–	**1767** ± 7	0.52	0.281648	0.001590	0.060128	0.281595 ± 0.000230	**-2.3** ± 8.1	–	–	**2.61**	–	–
16.1	–	**1788** ± 14	1.65	0.281506	0.000223	0.009793	0.281498 ± 0.000010	**-5.2** ± 0.3	–	-8.4	**2.81**	0.0020158 ± 0.0096	**9.1** ± 0.10
17.1	–	**1747** ± 36	1.18	0.281624	0.001293	0.046924	0.281581 ± 0.000013	**-3.2** ± 0.5	–	-5.4	**2.65**	0.0020106 ± 0.0081	**6.5** ± 0.09
19.1	–	**1800** ± 6	0.47	0.281600	0.001774	0.069553	0.281539 ± 0.000013	**-3.5** ± 0.5	–	–	**2.71**	–	–
26.1	–	**1778** ± 19	1.12	0.281583	0.002151	0.071666	0.281510 ± 0.000013	**-5.0** ± 0.5	–	–	**2.79**	–	–
inherited													
5.1	–	**2037** ± 7	0.92	0.281338	0.000622	0.024189	0.281314 ± 0.000008	**-6.1** ± 0.3	-11.4	-14.8	**3.06**	0.0020095 ± 0.0088	**6.0** ± 0.10
9.1	–	**2187** ± 4	0.52	0.281416	0.001000	0.040246	0.281374 ± 0.000016	**-0.6** ± 0.6	-9.1	-12.4	**2.82**	0.0020042 ± 0.0114	**3.3** ± 0.12
GSWA 88419: porphyritic monzogranite													
magmatic													
1.1	centre	**1764** ± 13	0.90	0.281612	0.001123	0.042077	0.281574 ± 0.000009	**-3.1** ± 0.3	–	–	**2.66**	–	–
	edge			0.281600	0.000940	0.025571	0.281569 ± 0.000013	**-3.3** ± 0.5	–	–	**2.67**	–	–
3.1	–	**1796** ± 13	0.87	0.281720	0.001254	0.057002	0.281677 ± 0.000031	**1.3** ± 1.1	–	–	**2.40**	–	–
5.1	centre	**1798** ± 17	0.77	0.281481	0.000587	0.024940	0.281461 ± 0.000009	**-6.4** ± 0.3	–	–	**2.89**	–	–
	edge			0.281700	0.000881	0.027824	0.281670 ± 0.000017	**1.1** ± 0.6	–	–	**2.42**	–	–
8.1	–	**1777** ± 17	0.32	0.281653	0.000843	0.023640	0.281625 ± 0.000014	**-1.0** ± 0.5	–	–	**2.53**	–	–
12.1	–	**1774** ± 11	0.92	0.281635	0.001429	0.057489	0.281587 ± 0.000027	**-2.4** ± 0.9	–	–	**2.62**	–	–
19.1	centre	**1790** ± 11	0.90	0.281656	0.000941	0.040871	0.281624 ± 0.000015	**-0.7** ± 0.5	–	–	**2.53**	–	–
	edge			0.281665	0.000808	0.024653	0.281638 ± 0.000016	**-0.3** ± 0.6	–	–	**2.50**	–	–
22.1	centre	**1783** ± 12	0.87	0.281641	0.001191	0.049983	0.281601 ± 0.000010	**-1.7** ± 0.4	–	–	**2.58**	–	–
	edge			0.281642	0.000972	0.027769	0.281609 ± 0.000013	**-1.4** ± 0.5	–	–	**2.56**	–	–
36.2	centre	**1785** ± 17	0.78	0.281651	0.000432	0.015004	0.281636 ± 0.000014	**-0.4** ± 0.5	–	–	**2.50**	–	–
	edge			0.281661	0.000284	0.009407	0.281651 ± 0.000010	**-0.3** ± 0.4	–	–	**2.48**	–	–
northern plutons													
GSWA 169088: foliated biotite monzogranite													
magmatic													
4.1	–	**1794** ± 11	0.72	0.281560	0.000313	0.013031	0.281549 ± 0.000011	**-3.3** ± 0.4	–	–	**2.69**	–	–
5.1	–	**1796** ± 9	0.93	0.281533	0.000867	0.033762	0.281503 ± 0.000009	**-4.9** ± 0.3	–	–	**2.79**	–	–
7.1	centre	**1810** ± 11	0.78	0.281620	0.001042	0.044395	0.281584 ± 0.000009	**-1.7** ± 0.3	–	–	**2.60**	–	–
	edge			0.281586	0.000779	0.032865	0.281559 ± 0.000019	**-2.6** ± 0.7	–	–	**2.66**	–	–
10.1	centre	**1803** ± 30	1.40	0.281630	0.000801	0.032322	0.281603 ± 0.000017	**-1.2** ± 0.6	–	–	**2.57**	0.0020141 ± 0.0066	**7.5** ± 0.07
	edge			0.281571	0.000827	0.035244	0.281543 ± 0.000019	**-3.3** ± 0.7	–	–	**2.70**	0.0020141 ± 0.0065	**7.5** ± 0.07
14.1	centre	**1801** ± 40	1.03	0.281519	0.001039	0.045700	0.281484 ± 0.000017	**-5.5** ± 0.6	–	–	**2.84**	0.0020150 ± 0.0080	**8.0** ± 0.08
	edge			0.281487	0.000925	0.039469	0.281455 ± 0.000015	**-6.5** ± 0.5	–	–	**2.90**	0.0020163 ± 0.0104	**8.6** ± 0.11

Analysis No.	Spot location	$^{207}Pb/^{206}Pb$ date (Ma)	Th/U	$^{176}Hf/^{177}Hf$ measured	$^{176}Lu/^{177}Hf$ measured	$^{176}Yb/^{177}Hf$ measured	$^{176}Hf/^{177}Hf$ initial	$\varepsilon_{Hf(t)}$	$\varepsilon_{Hf(1800\ Ma)}$	$\varepsilon_{Hf(1650\ Ma)}$	$T_{DM}2$ (Ga)	$^{18}O/^{16}O$ [a][b]	$\delta^{18}O$ [c]
16.1	centre	**1747** ± 42	1.09	0.281532	0.001223	0.052396	0.281492 ± 0.000017	**-6.4** ± 0.6	–	–	**2.85**	0.0020159 ± 0.0064	**8.4** ± 0.07
	edge			0.281538	0.000791	0.034148	0.281511 ± 0.000014	**-4.6** ± 0.5	–	–	**2.78**	0.0020154 ± 0.0080	**8.2** ± 0.08
22.1	–	**1815** ± 21	0.88	0.281515	0.000792	0.031862	0.281488 ± 0.000014	**-5.0** ± 0.5	–	–	**2.82**	–	–
23.1	–	**1824** ± 19	1.13	0.281501	0.001549	0.060776	0.281447 ± 0.000015	**-6.2** ± 0.5	–	–	**2.90**	–	–
inherited													
3.1	centre	**2622** ± 6	0.68	0.281152	0.000787	0.027604	0.281113 ± 0.000010	**0.2** ± 0.3	-18.2	-21.5	**3.11**	0.0020109 ± 0.0092	**5.9** ± 0.10
	edge	**2237** ± 8		0.281189	0.000328	0.012591	0.281175 ± 0.000013	**-6.5** ± 0.5	-16.4	-19.7	**3.24**	0.0020139 ± 0.0070	**7.4** ± 0.07
9.1	centre	**1886** ± 16	0.36	0.281582	0.000337	0.014703	0.281570 ± 0.000013	**-0.5** ± 0.5	-2.4	-5.8	**2.58**	0.0020115 ± 0.0100	**6.2** ± 0.10
	edge			0.281598	0.000310	0.013909	0.281587 ± 0.000017	**0.1** ± 0.6	-1.8	-5.2	**2.54**	0.0020184 ± 0.0068	**6.1** ± 0.07
17.1	–	**1949** ± 14	0.80	0.281559	0.000538	0.021805	0.281539 ± 0.000012	**-0.1** ± 0.4	-3.5	-6.8	**2.61**	0.0020089 ± 0.0071	**4.9** ± 0.08
GSWA 169087: foliated biotite granodiorite													
magmatic													
3.1	–	**1754** ± 20	0.90	0.281588	0.000641	0.023614	0.281567 ± 0.000012	**-3.6** ± 0.4	–	–	**2.68**	0.0020156 ± 0.0109	**7.2** ± 0.12
5.1	–	**1808** ± 9	0.24	0.281529	0.001199	0.049622	0.281488 ± 0.000012	**-5.2** ± 0.4	–	–	**2.82**	0.0020153 ± 0.0079	**7.0** ± 0.09
7.1	–	**1787** ± 24	0.50	0.281612	0.001490	0.051722	0.281562 ± 0.000022	**-3.0** ± 0.8	–	–	**2.67**	–	–
8.1	–	**1792** ± 27	0.52	0.281660	0.001707	0.059492	0.281602 ± 0.000018	**-1.5** ± 0.6	–	–	**2.57**	0.0020156 ± 0.0068	**7.2** ± 0.08
9.1	–	**1808** ± 22	0.74	0.281518	0.000621	0.024383	0.281497 ± 0.000012	**-4.9** ± 0.4	–	–	**2.80**	0.0020144 ± 0.0101	**6.6** ± 0.11
12.1	–	**1802** ± 15	0.88	0.281668	0.001988	0.074797	0.281600 ± 0.000017	**-1.3** ± 0.6	–	–	**2.57**	–	–
15.1	–	**1783** ± 12	0.34	0.281577	0.000819	0.035060	0.281549 ± 0.000024	**-3.6** ± 0.8	–	–	**2.70**	0.0020196 ± 0.0073	**9.1** ± 0.09
18.1	–	**1811** ± 9	0.19	0.281354	0.001424	0.064324	0.281305 ± 0.000014	**-11.6** ± 0.5	–	–	**3.23**	–	–
20.1	–	**1803** ± 16	0.53	0.281645	0.001284	0.046984	0.281601 ± 0.000017	**-1.3** ± 0.6	–	–	**2.57**	–	–
21.1	–	**1768** ± 15	1.31	0.281551	0.000989	0.037057	0.281518 ± 0.000016	**-5.0** ± 0.6	–	–	**2.78**	–	–
24.1	–	**1763** ± 5	0.02	0.281791	0.002087	0.086717	0.281721 ± 0.000045	**2.1** ± 1.6	–	–	**2.32**	–	–
inherited													
1.1	–	**1981** ± 20	0.74	0.281474	0.000478	0.017059	0.281456 ± 0.000010	**-2.4** ± 0.3	-6.4	-9.8	**2.78**	0.0020164 ± 0.0124	**7.6** ± 0.13
10.1	–	**1853** ± 19	0.72	0.281454	0.000587	0.023698	0.281433 ± 0.000009	**-6.1** ± 0.3	-7.3	-10.6	**2.91**	0.0020139 ± 0.0084	**6.3** ± 0.09
13.1	–	**2284** ± 8	0.33	0.281303	0.001545	0.064802	0.281236 ± 0.000011	**-3.3** ± 0.4	-13.8	-17.0	**3.07**	0.0020168 ± 0.0082	**7.7** ± 0.09
16.1	–	**1919** ± 9	0.21	0.281582	0.001829	0.065367	0.281515 ± 0.000026	**-1.7** ± 0.9	-4.2	-7.4	**2.68**	0.0020178 ± 0.0104	**8.2** ± 0.11
GSWA 169089: granophyric syenogranite													
magmatic													
2.1	–	**1739** ± 48	2.46	0.281389	0.002407	0.070594	0.281310 ± 0.000045	**-13.1** ± 1.6	–	–	**3.26**	0.0020157 ± 0.0087	**8.2** ± 0.09
3.2	–	**1776** ± 27	0.30	0.281578	0.002351	0.078067	0.281499 ± 0.000031	**-5.5** ± 1.1	–	–	**2.82**	–	–
4.1	–	**1790** ± 19	0.54	0.281536	0.000847	0.035048	0.281507 ± 0.000036	**-4.9** ± 1.3	–	–	**2.79**	0.0020122 ± 0.0089	**6.4** ± 0.09
4.3	–	**1797** ± 18	0.29	0.281530	0.000743	0.023971	0.281505 ± 0.000022	**-4.8** ± 0.8	–	–	**2.79**	–	–
5.1	–	**1805** ± 35	0.32	0.281521	0.001306	0.044182	0.281476 ± 0.000020	**-5.6** ± 0.7	–	–	**2.85**	0.0020203 ± 0.0089	**10.5** ± 0.09
5.2	–	**1774** ± 48	0.89	0.281537	0.000932	0.036791	0.281506 ± 0.000018	**-5.3** ± 0.6	–	–	**2.80**	–	–
8.1	–	**1784** ± 19	0.83	0.281533	0.001485	0.048779	0.281483 ± 0.000032	**-5.9** ± 1.1	–	–	**2.85**	0.0020148 ± 0.0087	**7.7** ± 0.09
8.2	–	**1772** ± 16	0.88	0.281503	0.001122	0.050778	0.281465 ± 0.000020	**-6.8** ± 0.7	–	–	**2.90**	–	–
10.1	–	**1782** ± 14	0.29	0.281540	0.000762	0.024760	0.281514 ± 0.000016	**-4.8** ± 0.6	–	–	**2.78**	0.0020112 ± 0.0076	**5.9** ± 0.08
10.2	–	**1766** ± 16	0.67	0.281588	0.001667	0.050291	0.281532 ± 0.000040	**-4.5** ± 1.4	–	–	**2.75**	–	–

Analysis No.	Spot location	$^{207}Pb/^{206}Pb$ date (Ma)	Th/U	$^{176}Hf/^{177}Hf$ measured	$^{176}Lu/^{177}Hf$ measured	$^{176}Yb/^{177}Hf$ measured	$^{176}Hf/^{177}Hf$ initial	$\varepsilon_{Hf(t)}$	$\varepsilon_{Hf(1800\ Ma)}$	$\varepsilon_{Hf(1650\ Ma)}$	T_{DM}^2 (Ga)	$^{18}O/^{16}O$ [a][b]	$\delta^{18}O$ [c]
inherited													
6.1	–	**1983** ± 10	0.73	0.281439	0.001253	0.040513	0.281392 ± 0.000012	**-4.6** ± 0.4	-8.6	-11.9	**2.92**	0.0020123 ± 0.0084	**6.5** ± 0.09
7.1	–	**2755** ± 10	0.45	0.280950	0.001736	0.059065	0.280858 ± 0.000019	**-5.8** ± 0.7	-26.6	-29.8	**3.59**	0.0020060 ± 0.0055	**3.3** ± 0.06
GSWA 169058: Gooche Gneiss, augen orthogneiss													
magmatic													
3.1	centre	**1771** ± 10	0.71	0.281653	0.001397	0.061344	0.281606 ± 0.000024	**-1.8** ± 0.8	–	–	**2.58**	–	–
	edge			0.281418	0.003785	0.111851	0.281291 ± 0.000035	**-13.0** ± 1.2	–	–	**3.29**	–	–
4.1	centre	**1777** ± 20	0.76	0.281571	0.000875	0.035105	0.281542 ± 0.000026	**-4.0** ± 0.9	–	–	**2.72**	–	–
	edge			0.281453	0.001842	0.050723	0.281391 ± 0.000030	**-9.3** ± 1.1	–	–	**3.06**	–	–
6.1	centre	**1771** ± 21	0.45	0.281642	0.001506	0.067601	0.281591 ± 0.000029	**-2.3** ± 1.0	–	–	**2.61**	–	–
	edge			0.281548	0.001904	0.055753	0.281484 ± 0.000043	**-6.1** ± 1.5	–	–	**2.85**	–	–
17.1	centre	**1778** ± 10	0.24	0.281654	0.001222	0.050825	0.281613 ± 0.000012	**-1.4** ± 0.4	–	–	**2.56**	–	–
	edge			0.281489	0.002038	0.059532	0.281420 ± 0.000020	**-8.2** ± 0.7	–	–	**2.99**	–	–
19.1	centre	**1793** ± 11	0.77	0.281563	0.000927	0.037795	0.281531 ± 0.000020	**-4.0** ± 0.7	–	–	**2.73**	–	–
	edge			0.281530	0.001535	0.045468	0.281478 ± 0.000016	**-5.9** ± 0.6	–	–	**2.85**	–	–
Durlacher Supersuite													
northern Capricorn Orogen plutons													
GSWA 169053, biotite–muscovite monzogranite													
magmatic													
9.1	–	**1682** ± 9	0.01	0.281618	0.001546	0.06642	0.281569 ± 0.000012	**-5.2** ± 0.4	–	–	**2.72**	0.0020236 ± 0.0098	**10.5** ± 0.11
15.2	–	**1683** ± 8	0.05	0.281588	0.001643	0.06950	0.281536 ± 0.000011	**-6.3** ± 0.4	–	–	**2.80**	0.0020260 ± 0.0082	**10.5** ± 0.10
18.1	–	**1679** ± 9	0.01	0.281474	0.002259	0.07741	0.281402 ± 0.000029	**-11.1** ± 1.0	–	–	**3.10**	0.0020234 ± 0.0106	**10.4** ± 0.12
19.1	–	**1667** ± 9	0.08	0.281537	0.002857	0.10174	0.281447 ± 0.000028	**-9.8** ± 1.0	–	–	**3.01**	0.0020231 ± 0.0099	**10.2** ± 0.11
20.1	–	**1676** ± 9	0.02	0.281580	0.001686	0.07137	0.281526 ± 0.000011	**-6.8** ± 0.4	–	–	**2.82**	0.0020236 ± 0.0108	**10.5** ± 0.12
21.1	–	**1682** ± 8	0.02	0.281556	0.001916	0.07104	0.281495 ± 0.000025	**-7.8** ± 0.9	–	–	**2.89**	0.0020259 ± 0.0068	**10.4** ± 0.09
22.1	–	**1680** ± 9	0.08	0.281523	0.001396	0.06008	0.281479 ± 0.000012	**-8.4** ± 0.4	–	–	**2.93**	0.0020255 ± 0.0059	**10.3** ± 0.09
23.1	–	**1669** ± 8	0.03	0.281559	0.001466	0.05906	0.281513 ± 0.000010	**-7.4** ± 0.3	–	–	**2.86**	0.0020255 ± 0.0077	**10.2** ± 0.10
24.1	–	**1621** ± 9	0.02	0.281534	0.002193	0.07869	0.281467 ± 0.000035	**-10.2** ± 1.2	–	–	**2.99**	–	–
25.1	–	**1630** ± 9	0.02	0.281482	0.001270	0.05542	0.281443 ± 0.000016	**-10.8** ± 0.6	–	–	**3.04**	0.0020257 ± 0.0089	**10.3** ± 0.11
26.1	–	**1645** ± 8	0.02	0.281556	0.001668	0.06752	0.281504 ± 0.000012	**-8.3** ± 0.4	–	–	**2.89**	0.0020256 ± 0.0074	**10.3** ± 0.10
27.1	–	**1645** ± 8	0.02	0.281612	0.001800	0.08118	0.281556 ± 0.000012	**-6.5** ± 0.4	–	–	**2.78**	0.0020257 ± 0.0088	**10.3** ± 0.11
28.2	–	**1673** ± 13	0.02	0.281565	0.001430	0.05978	0.281520 ± 0.000011	**-7.1** ± 0.4	–	–	**2.84**	0.0020260 ± 0.0097	**10.5** ± 0.12
inherited													
2.1	–	**1728** ± 9	1.12	0.281473	0.001284	0.06776	0.281431 ± 0.000011	**-9.0** ± 0.4	–	-10.1	**3.00**	0.0020186 ± 0.0098	**8.0** ± 0.11
3.1	–	**2222** ± 7	0.32	0.281130	0.000146	0.00743	0.281124 ± 0.000008	**-8.7** ± 0.3	–	-20.9	**3.36**	0.0020179 ± 0.0097	**7.6** ± 0.11
4.1	–	**1938** ± 17	0.70	0.281284	0.001403	0.04933	0.281232 ± 0.000012	**-11.3** ± 0.4	–	-16.9	**3.31**	0.0020159 ± 0.0098	**6.6** ± 0.11
5.1	–	**1940** ± 9	0.67	0.281295	0.000467	0.02306	0.281278 ± 0.000006	**-9.6** ± 0.2	–	-15.4	**3.20**	0.0020162 ± 0.0109	**6.8** ± 0.12
6.1	–	**1706** ± 9	0.17	0.281476	0.003026	0.09873	0.281378 ± 0.000022	**-11.4** ± 0.8	–	-11.9	**3.13**	0.0020183 ± 0.0115	**7.8** ± 0.13
7.1	–	**1790** ± 6	0.15	0.281576	0.001903	0.09198	0.281511 ± 0.000018	**-4.7** ± 0.6	–	-7.1	**2.78**	0.0020233 ± 0.0121	**10.3** ± 0.13
8.1	–	**2115** ± 12	0.47	0.281297	0.001019	0.05217	0.281256 ± 0.000013	**-6.4** ± 0.5	–	-16.0	**3.14**	0.0020152 ± 0.0126	**6.2** ± 0.14

Analysis No.	Spot location	$^{207}Pb/^{206}Pb$ date (Ma)	Th/U	$^{176}Hf/^{177}Hf$ measured	$^{176}Lu/^{177}Hf$ measured	$^{176}Yb/^{177}Hf$ measured	$^{176}Hf/^{177}Hf$ initial	$\varepsilon_{Hf(t)}$	$\varepsilon_{Hf(1800\ Ma)}$	$\varepsilon_{Hf(1650\ Ma)}$	$T_{DM}2$ (Ga)	$^{18}O/^{16}O$ [a][b]	$\delta^{18}O$ [c]
10.1	–	**1783** ± 30	1.25	0.281532	0.000962	0.03593	0.281499 ± 0.000014	**-5.3** ± 0.5	–	-7.6	**2.81**	0.0020162 ± 0.0093	**6.7** ± 0.11
11.1	–	**2048** ± 19	1.17	0.281343	0.000391	0.01629	0.281328 ± 0.000006	**-5.4** ± 0.2	–	-13.7	**3.02**	0.0020167 ± 0.0119	**7.0** ± 0.13
12.1	–	**1801** ± 6	0.19	0.281848	0.001734	0.07010	0.281789 ± 0.000011	**5.4** ± 0.4	–	2.8	**2.14**	0.0020175 ± 0.0155	**7.4** ± 0.16
13.1	–	**1713** ± 9	0.03	0.281538	0.001321	0.05597	0.281495 ± 0.000011	**-7.1** ± 0.4	–	-7.8	**2.87**	0.0020213 ± 0.0088	**9.3** ± 0.10
14.1	–	**1824** ± 9	0.59	0.281714	0.001490	0.06606	0.281662 ± 0.000018	**1.4** ± 0.6	–	-1.7	**2.42**	0.0020145 ± 0.0114	**5.9** ± 0.12
15.1	–	**2046** ± 7	0.62	0.281295	0.000629	0.03047	0.281271 ± 0.000010	**-7.5** ± 0.3	–	-15.6	**3.15**	0.0020214 ± 0.0082	**8.2** ± 0.10
16.1	–	**1770** ± 10	0.35	0.281495	0.002705	0.09545	0.281404 ± 0.000026	**-9.0** ± 0.9	–	-11.5	**3.03**	–	–
17.1	–	**1797** ± 9	0.21	0.281540	0.000888	0.04354	0.281510 ± 0.000015	**-4.6** ± 0.5	–	-7.2	**2.78**	0.0020199 ± 0.0099	**7.5** ± 0.12
20.2	–	**2201** ± 11	0.55	0.281278	0.000513	0.02512	0.281256 ± 0.000011	**-4.4** ± 0.4	–	-16.1	**3.08**	0.0020145 ± 0.0094	**5.9** ± 0.11
23.2	–	**2392** ± 7	0.22	0.281242	0.001359	0.06045	0.281180 ± 0.000010	**-2.8** ± 0.3	–	-18.3	**3.12**	0.0020210 ± 0.0091	**8.0** ± 0.11
26.2	–	**1818** ± 16	0.70	0.281774	0.001514	0.06716	0.281722 ± 0.000008	**3.4** ± 0.3	–	0.4	**2.29**	0.0020169 ± 0.0100	**6.0** ± 0.12
28.1	–	**2373** ± 10	1.17	0.281220	0.001095	0.05070	0.281170 ± 0.000012	**-3.5** ± 0.4	–	-18.8	**3.15**	0.0020201 ± 0.0091	**7.5** ± 0.11
GSWA 178029: Pimbyana Granite, biotite monzogranite													
magmatic													
1.1	centre	**1689** ± 27	1.07	0.281558	0.001108	0.05184	0.281523 ± 0.000010	**-6.6** ± 0.3	–	–	**2.82**	0.0020210 ± 0.0124	**8.0** ± 0.16
	edge			0.281535	0.001827	0.07056	0.281477 ± 0.000012	**-8.3** ± 0.4	–	–	**2.92**	0.0020215 ± 0.0072	**8.2** ± 0.12
3.1	–	**1664** ± 17	0.51	0.281560	0.001055	0.04820	0.281527 ± 0.000010	**-7.1** ± 0.3	–	–	**2.83**	0.0020210 ± 0.0089	**8.0** ± 0.13
4.1	–	**1653** ± 28	1.85	0.281498	0.001348	0.04415	0.281456 ± 0.000016	**-9.8** ± 0.6	–	–	**2.99**	0.0020206 ± 0.0077	**7.8** ± 0.12
7.1	–	**1704** ± 28	1.91	0.281606	0.001123	0.03925	0.281570 ± 0.000010	**-4.6** ± 0.3	–	–	**2.71**	–	–
8.1	–	**1701** ± 27	1.26	0.281559	0.001653	0.06136	0.281506 ± 0.000014	**-7.0** ± 0.5	–	–	**2.85**	0.0020218 ± 0.0069	**8.4** ± 0.12
9.1	–	**1694** ± 21	0.48	0.281599	0.000967	0.05184	0.281568 ± 0.000010	**-4.9** ± 0.3	–	–	**2.72**	–	–
11.1	–	**1696** ± 16	0.44	0.281585	0.001379	0.06753	0.281541 ± 0.000010	**-5.8** ± 0.4	–	–	**2.78**	0.0020225 ± 0.0086	**8.7** ± 0.13
12.1	–	**1674** ± 20	0.61	0.281573	0.000992	0.04848	0.281542 ± 0.000010	**-6.3** ± 0.3	–	–	**2.79**	–	–
13.1	–	**1696** ± 18	0.08	0.281524	0.000438	0.01454	0.281510 ± 0.000012	**-6.9** ± 0.4	–	–	**2.85**	–	–
15.1	–	**1650** ± 20	0.48	0.281516	0.001752	0.06794	0.281461 ± 0.000019	**-9.7** ± 0.7	–	–	**2.98**	0.0020232 ± 0.0087	**9.1** ± 0.13
16.1	–	**1667** ± 21	0.40	0.281633	0.001325	0.05144	0.281591 ± 0.000017	**-4.7** ± 0.6	–	–	**2.68**	0.0020229 ± 0.0097	**9.0** ± 0.14
20.1	–	**1677** ± 25	2.00	0.281769	0.001280	0.06623	0.281728 ± 0.000012	**0.4** ± 0.4	–	–	**2.37**	–	–
21.1	–	**1661** ± 19	0.49	0.281734	0.000798	0.03985	0.281709 ± 0.000024	**-0.7** ± 0.8	–	–	**2.42**	–	–
23.1	–	**1684** ± 52	1.12	0.281596	0.000813	0.03864	0.281570 ± 0.000009	**-5.1** ± 0.3	–	–	**2.72**	–	–
24.1	–	**1653** ± 17	0.36	0.281570	0.001163	0.05730	0.281534 ± 0.000008	**-7.1** ± 0.3	–	–	**2.82**	0.0020238 ± 0.0086	**9.4** ± 0.13
inherited													
25.1	–	**1742** ± 45	0.25	0.281595	0.002143	0.09633	0.281524 ± 0.000012	**-5.4** ± 0.4	–	**-6.7**	**2.78**	–	–
5.1	–	**1709** ± 32	1.60	0.281501	0.002066	0.08058	0.281434 ± 0.000022	**-9.3** ± 0.8	–	**-9.9**	**3.01**	0.0020228 ± 0.0082	**8.9** ± 0.13
14.1	–	**1711** ± 33	1.90	0.281497	0.001468	0.05406	0.281449 ± 0.000018	**-8.7** ± 0.6	–	**-9.4**	**2.97**	0.0020217 ± 0.0097	**8.3** ± 0.14
17.1	–	**1717** ± 47	2.08	0.281687	0.000709	0.03214	0.281664 ± 0.000005	**-1.0** ± 0.2	–	**-1.8**	**2.48**	–	–
19.1	–	**1753** ± 17	0.36	0.281662	0.001392	0.06542	0.281616 ± 0.000009	**-1.9** ± 0.3	–	**-3.5**	**2.57**	0.0020231 ± 0.0083	**9.0** ± 0.13

Analysis No.	Spot location	$^{207}Pb/^{206}Pb$ date (Ma)	Th/U	$^{176}Hf/^{177}Hf$ measured	$^{176}Lu/^{177}Hf$ measured	$^{176}Yb/^{177}Hf$ measured	$^{176}Hf/^{177}Hf$ initial	$\varepsilon_{Hf(t)}$	$\varepsilon_{Hf(1800\ Ma)}$	$\varepsilon_{Hf(1650\ Ma)}$	$T_{DM}2$ (Ga)	$^{18}O/^{16}O$ [(a)(b)]	$\delta^{18}O$ [(c)]
GSWA 169062: Dingo Creek Granite, porphyritic syenogranite													
magmatic													
2.1	–	**1660** ± 17	0.45	0.281650	0.000404	0.01763	0.281637 ± 0.000035	**-3.2** ± 1.2	–	–	**2.58**	–	–
3.1	centre	**1632** ± 30	1.61	0.281500	0.000018	0.00101	0.281499 ± 0.000011	**-8.8** ± 0.4	–	–	**2.91**	0.0020265 ± 0.0134	**9.5** ± 0.14
	edge			0.281520	0.000020	0.00117	0.281519 ± 0.000012	**-8.0** ± 0.4	–	–	**2.87**	0.0020262 ± 0.0173	**9.3** ± 0.18
4.1	–	**1687** ± 7	0.23	0.281596	0.000712	0.03358	0.281573 ± 0.000029	**-4.9** ± 1.0	–	–	**2.71**	–	–
14.1	centre	**1693** ± 11	0.22	0.281581	0.000728	0.02768	0.281558 ± 0.000013	**-5.3** ± 0.5	–	–	**2.74**	0.0020245 ± 0.0130	**8.4** ± 0.14
	edge			0.281596	0.000667	0.02839	0.281575 ± 0.000013	**-4.7** ± 0.5	–	–	**2.70**	0.0020242 ± 0.0162	**8.3** ± 0.17
15.1	–	**1659** ± 14	0.67	0.281623	0.000071	0.00270	0.281621 ± 0.000009	**-3.8** ± 0.3	–	–	**2.62**	–	–
16.1	centre	**1660** ± 42	1.77	0.281484	0.000021	0.00120	0.281483 ± 0.000012	**-8.7** ± 0.4	–	–	**2.93**	0.0020254 ± 0.0135	**8.9** ± 0.14
	edge			0.281457	0.000020	0.00121	0.281456 ± 0.000011	**-9.6** ± 0.4	–	–	**2.99**	0.0020256 ± 0.0099	**9.0** ± 0.11
18.1	centre	**1680** ± 11	1.55	0.281558	0.000582	0.02604	0.281539 ± 0.000010	**-6.2** ± 0.3	–	–	**2.79**	0.0020235 ± 0.0072	**7.9** ± 0.08
	edge			0.281550	0.000654	0.02905	0.281529 ± 0.000013	**-6.6** ± 0.5	–	–	**2.81**	0.0020236 ± 0.0163	**8.0** ± 0.17
19.1	centre	**1669** ± 12	0.90	0.281594	0.000505	0.02318	0.281578 ± 0.000013	**-5.1** ± 0.5	–	–	**2.71**	0.0020230 ± 0.0099	**7.7** ± 0.11
	edge			0.281543	0.000597	0.02780	0.281524 ± 0.000023	**-7.0** ± 0.8	–	–	**2.83**	0.0020233 ± 0.0099	**7.9** ± 0.11
21.1	–	**1656** ± 24	1.65	0.281462	0.000010	0.00103	0.281462 ± 0.000008	**-9.5** ± 0.3	–	–	**2.98**	0.0020254 ± 0.0161	**8.9** ± 0.17
22.1	centre	**1686** ± 14	2.27	0.281447	0.000015	0.00098	0.281447 ± 0.000006	**-9.4** ± 0.2	–	–	**2.99**	0.0020262 ± 0.0082	**9.3** ± 0.09
	edge			0.281435	0.000020	0.00111	0.281434 ± 0.000007	**-9.8** ± 0.2	–	–	**3.02**	0.0020248 ± 0.0104	**8.6** ± 0.11
23.1	centre	**1686** ± 22	1.67	0.281436	0.000023	0.00120	0.281435 ± 0.000014	**-9.8** ± 0.5	–	–	**3.02**	0.0020257 ± 0.0081	**9.0** ± 0.09
	edge			0.281451	0.000019	0.00112	0.281450 ± 0.000010	**-9.3** ± 0.4	–	–	**2.99**	0.0020253 ± 0.0144	**8.9** ± 0.15
25.1	centre	**1679** ± 5	0.15	0.281547	0.000927	0.04029	0.281518 ± 0.000011	**-7.0** ± 0.4	–	–	**2.84**	0.0020225 ± 0.0133	**7.4** ± 0.14
	edge			0.281610	0.001028	0.04570	0.281577 ± 0.000009	**-4.9** ± 0.3	–	–	**2.71**	0.0020224 ± 0.0107	**7.4** ± 0.11
26.1	–	**1679** ± 8	1.14	0.281561	0.000119	0.00613	0.281557 ± 0.000006	**-5.6** ± 0.2	–	–	**2.75**	0.0020281 ± 0.0170	**10.3** ± 0.18
inherited													
11.1	–	**1779** ± 22	0.30	0.281528	0.001396	0.06150	0.281481 ± 0.000023	**-6.1** ± 0.8	–	**-8.2**	**2.86**	0.0020244 ± 0.0123	**8.4** ± 0.13
13.1	–	**1767** ± 24	0.94	0.281520	0.001147	0.05259	0.281482 ± 0.000006	**-6.3** ± 0.2	–	**-8.2**	**2.86**	0.0020258 ± 0.0110	**9.1** ± 0.12
17.1	–	**1783** ± 19	0.59	0.281451	0.001336	0.06034	0.281406 ± 0.000015	**-8.7** ± 0.5	–	**-10.9**	**3.02**	0.0020250 ± 0.0105	**8.7** ± 0.11
27.1	–	**1781** ± 16	0.60	0.281500	0.000949	0.04338	0.281468 ± 0.000013	**-6.5** ± 0.5	–	**-8.7**	**2.88**	0.0020262 ± 0.0091	**9.3** ± 0.10
GSWA 169055: Yangibana Granite, biotite–muscovite monzogranite													
magmatic													
3.1	–	**1665** ± 20	0.97	0.281632	0.000364	0.01471	0.281621 ± 0.000008	**-3.7** ± 0.3	–	–	**2.62**	0.0020251 ± 0.0091	**10.1** ± 0.21
4.1	–	**1678** ± 21	0.2	0.281739	0.000980	0.04689	0.281708 ± 0.000014	**-0.3** ± 0.5	–	–	**2.41**	0.0020249 ± 0.0096	**10.0** ± 0.21
8.1	–	**1657** ± 15	0.79	0.281588	0.000276	0.01139	0.281579 ± 0.000013	**-5.3** ± 0.5	–	–	**2.72**	0.0020248 ± 0.0080	**10.0** ± 0.20
9.1	–	**1650** ± 12	0.41	0.281572	0.000235	0.01254	0.281565 ± 0.000010	**-6.0** ± 0.3	–	–	**2.75**	0.0020250 ± 0.0075	**10.1** ± 0.20
10.1	centre	**1667** ± 18	0.59	0.281535	0.001239	0.04777	0.281496 ± 0.000015	**-8.1** ± 0.5	–	–	**2.90**	0.0020258 ± 0.0067	**10.5** ± 0.20
	edge			0.281544	0.000954	0.04702	0.281514 ± 0.000017	**-7.4** ± 0.6	–	–	**2.86**	0.0020243 ± 0.0081	**9.7** ± 0.20
11.1	–	**1677** ± 13	0.16	0.281587	0.000753	0.03124	0.281563 ± 0.000025	**-5.5** ± 0.9	–	–	**2.74**	0.0020253 ± 0.0104	**10.2** ± 0.21
13.1	–	**1669** ± 18	0.97	0.281643	0.000154	0.00689	0.281638 ± 0.000011	**-3.0** ± 0.4	–	–	**2.58**	0.0020249 ± 0.0077	**10.1** ± 0.20
17.1	centre	**1673** ± 29	2.18	0.281551	0.000597	0.02308	0.281532 ± 0.000018	**-6.7** ± 0.6	–	–	**2.81**	0.0020258 ± 0.0098	**10.5** ± 0.21
	edge			0.281599	0.000359	0.01859	0.281588 ± 0.000011	**-4.7** ± 0.4	–	–	**2.69**	0.0020253 ± 0.0088	**10.2** ± 0.20

Analysis No.	Spot location	$^{207}Pb/^{206}Pb$ date (Ma)	Th/U	$^{176}Hf/^{177}Hf$ measured	$^{176}Lu/^{177}Hf$ measured	$^{176}Yb/^{177}Hf$ measured	$^{176}Hf/^{177}Hf$ initial	$\varepsilon_{Hf(t)}$	$\varepsilon_{Hf(1800\ Ma)}$	$\varepsilon_{Hf(1650\ Ma)}$	$T_{DM}2$ (Ga)	$^{18}O/^{16}O$ [(a)(b)]	$\delta^{18}O$ [(c)]
inherited													
2.1	–	**2616** ± 8	0.27	0.281083	0.000626	0.02332	0.281052 ± 0.000010	**-2.1** ± 0.3	–	**-23.2**	**3.25**	–	–
5.1	–	**1845** ± 25	0.93	0.281584	0.001089	0.04385	0.281546 ± 0.000011	**-2.3** ± 0.4	–	**-5.9**	**2.67**	0.0020174 ± 0.0071	**6.3** ± 0.20
14.1	–	**2683** ± 11	0.69	0.281657	0.000199	0.01066	0.281647 ± 0.000010	**20.6** ± 0.3	–	**-2.3**	**1.84**	0.0020251 ± 0.0071	**10.1** ± 0.20
18.1	–	**2427** ± 6	0.17	0.281568	0.000170	0.00918	0.281560 ± 0.000008	**11.6** ± 0.3	–	**-5.4**	**2.23**	0.0020245 ± 0.0097	**9.8** ± 0.21
southern Capricorn Orogen													
Davey Well batholith													
GSWA 183215: Davey Well Granite, coarse grained porphyritic biotite monzogranite													
magmatic													
1.1	–	**1671** ± 5	0.28	0.281526	0.000705	0.022900	0.281504 ± 0.000013	**-7.7** ± 0.5	–	–	**2.88**	–	–
4.1	centre	**1655** ± 41	1.69	0.281506	0.000462	0.017290	0.281492 ± 0.000016	**-8.5** ± 0.6	–	–	**2.91**	0.0020187 ± 0.0105	**9.2** ± 0.11
	edge			0.281530	0.000690	0.026534	0.281508 ± 0.000016	**-7.9** ± 0.6	–	–	**2.88**	0.0020176 ± 0.0067	**8.7** ± 0.07
6.1	–	**1674** ± 7	0.82	0.281523	0.000719	0.026862	0.281500 ± 0.000019	**-7.8** ± 0.7	–	–	**2.88**	–	–
8.1	centre	**1661** ± 23	1.47	0.281542	0.000495	0.019105	0.281526 ± 0.000012	**-7.1** ± 0.4	–	–	**2.83**	0.0020187 ± 0.0093	**9.2** ± 0.10
	edge			0.281516	0.000697	0.027257	0.281494 ± 0.000014	**-8.3** ± 0.5	–	–	**2.90**	0.0020162 ± 0.0067	**8.0** ± 0.07
11.1	–	**1641** ± 43	1.03	0.281565	0.000454	0.018174	0.281551 ± 0.000013	**-6.7** ± 0.5	–	–	**2.79**	–	–
13.1	–	**1673** ± 16	1.60	0.281536	0.000552	0.021061	0.281519 ± 0.000022	**-7.1** ± 0.8	–	–	**2.84**	–	–
16.1	centre	**1698** ± 14	1.27	0.281551	0.000569	0.021834	0.281533 ± 0.000019	**-6.1** ± 0.7	–	–	**2.79**	0.0020186 ± 0.0083	**9.1** ± 0.09
	edge			0.281535	0.000659	0.026197	0.281514 ± 0.000013	**-6.7** ± 0.5	–	–	**2.84**	0.0020181 ± 0.0067	**8.9** ± 0.07
18.2	–	**1670** ± 5	0.87	0.281560	0.000726	0.029913	0.281537 ± 0.000018	**-6.6** ± 0.6	–	–	**2.80**	–	–
23.1	–	**1642** ± 14	1.38	0.281515	0.000817	0.033271	0.281490 ± 0.000024	**-8.9** ± 0.8	–	–	**2.93**	0.0020171 ± 0.0078	**8.4** ± 0.08
23.2	–	**1658** ± 9	1.13	0.281559	0.000726	0.029516	0.281536 ± 0.000017	**-6.9** ± 0.6	–	–	**2.81**	0.0020179 ± 0.0089	**8.8** ± 0.09
25.1	–	**1668** ± 16	1.12	0.281516	0.000536	0.021006	0.281499 ± 0.000009	**-7.9** ± 0.3	–	–	**2.89**	0.0020182 ± 0.0118	**8.9** ± 0.12
26.1	centre	**1663** ± 7	0.83	0.281528	0.000696	0.026351	0.281506 ± 0.000007	**-7.8** ± 0.2	–	–	**2.88**	0.0020178 ± 0.0100	**8.7** ± 0.10
	edge			0.281534	0.000749	0.028663	0.281510 ± 0.000008	**-7.7** ± 0.3	–	–	**2.87**	0.0020175 ± 0.0075	**8.6** ± 0.08
27.1	–	**1649** ± 12	1.26	0.281548	0.000608	0.023200	0.281529 ± 0.000010	**-7.3** ± 0.3	–	–	**2.83**	–	–
28.1	centre	**1677** ± 13	0.96	0.281530	0.000613	0.020439	0.281511 ± 0.000007	**-7.3** ± 0.2	–	–	**2.86**	0.0020182 ± 0.0085	**9.0** ± 0.09
	edge			0.281555	0.000443	0.014765	0.281541 ± 0.000007	**-6.3** ± 0.2	–	–	**2.79**	0.0020162 ± 0.0128	**7.9** ± 0.13
30.1	–	**1647** ± 14	1.22	0.281543	0.000718	0.024128	0.281521 ± 0.000007	**-7.7** ± 0.2	–	–	**2.85**	–	–
GSWA 183207: Tetlow Granite, metatonalite/quartz diorite													
magmatic													
4.1	–	**1659** ± 26	1.15	0.281535	0.000597	0.020787	0.281516 ± 0.000008	**-7.5** ± 0.3	–	–	**2.86**	–	–
7.1	–	**1707** ± 20	1.06	0.281546	0.000540	0.019497	0.281529 ± 0.000009	**-6.0** ± 0.3	–	–	**2.80**	–	–
9.1	–	**1687** ± 18	1.37	0.281526	0.000554	0.020035	0.281508 ± 0.000008	**-7.2** ± 0.3	–	–	**2.86**	–	–
10.1	–	**1698** ± 21	1.21	0.281540	0.000711	0.021247	0.281517 ± 0.000007	**-6.6** ± 0.2	–	–	**2.83**	–	–
12.1	–	**1665** ± 12	1.26	0.281544	0.000692	0.022252	0.281522 ± 0.000007	**-7.2** ± 0.2	–	–	**2.84**	–	–
15.1	centre	**1649** ± 17	0.92	0.281575	0.000550	0.020270	0.281558 ± 0.000010	**-6.3** ± 0.4	–	–	**2.77**	0.0020184 ± 0.0104	**9.6** ± 0.11
	edge			0.281539	0.000793	0.026534	0.281514 ± 0.000009	**-7.8** ± 0.3	–	–	**2.87**	0.0020179 ± 0.0093	**9.3** ± 0.10
16.1	centre	**1656** ± 7	1.00	0.281562	0.000500	0.017996	0.281546 ± 0.000012	**-6.5** ± 0.4	–	–	**2.79**	0.0020187 ± 0.0094	**9.7** ± 0.10
	edge			0.281542	0.000559	0.020272	0.281524 ± 0.000007	**-7.3** ± 0.2	–	–	**2.84**	0.0020186 ± 0.0105	**9.7** ± 0.11

Analysis No.	Spot location	$^{207}Pb/^{206}Pb$ date (Ma)	Th/U	$^{176}Hf/^{177}Hf$ measured	$^{176}Lu/^{177}Hf$ measured	$^{176}Yb/^{177}Hf$ measured	$^{176}Hf/^{177}Hf$ initial	$\varepsilon_{Hf(t)}$	$\varepsilon_{Hf(1800\ Ma)}$	$\varepsilon_{Hf(1650\ Ma)}$	$T_{DM}2$ (Ga)	$^{18}O/^{16}O$ [a][b]	$\delta^{18}O$ [c]
17.1	–	**1664** ± 12	1.37	0.281565	0.000452	0.017467	0.281551 ± 0.000013	**-6.2** ± 0.5	–	–	**2.77**	–	–
20.1	–	**1659** ± 12	1.44	0.281552	0.000802	0.025936	0.281527 ± 0.000009	**-7.2** ± 0.3	–	–	**2.83**	–	–
21.1	centre	**1653** ± 19	0.95	0.281557	0.000410	0.016139	0.281544 ± 0.000009	**-6.7** ± 0.3	–	–	**2.80**	0.0020186 ± 0.0090	**9.7** ± 0.09
	edge			0.281579	0.000561	0.014941	0.281561 ± 0.000010	**-6.1** ± 0.3	–	–	**2.76**	0.0020187 ± 0.0109	**9.7** ± 0.11
22.1	centre	**1654** ± 11	1.23	0.281544	0.000580	0.023676	0.281526 ± 0.000010	**-7.3** ± 0.3	–	–	**2.84**	0.0020188 ± 0.0104	**9.8** ± 0.11
	edge			0.281566	0.000619	0.021289	0.281547 ± 0.000007	**-6.6** ± 0.2	–	–	**2.79**	0.0020191 ± 0.0091	**9.6** ± 0.10
25.1	–	**1662** ± 4	0.45	0.281564	0.000930	0.032569	0.281535 ± 0.000007	**-6.8** ± 0.3	–	–	**2.81**	–	–
inherited													
8.1	–	**2453** 6	0.33	0.281213	0.000878	0.031816	0.281172 0.000009	**-1.6** ± 0.3	–	-19.5	**3.09**	–	–
GSWA 185944: Davey Well Granite, porphyritic monzogranite													
magmatic													
2.1	–	**1591** ± 33	1.77	0.281480	0.000506	0.018040	0.281465 ± 0.000014	**-10.9** ± 0.5	–	–	**3.01**	–	–
12.1	–	**1681** ± 22	2.45	0.281519	0.000660	0.018882	0.281498 ± 0.000012	**-7.7** ± 0.4	–	–	**2.88**	–	–
18.1	–	**1610** ± 32	1.56	0.281494	0.000952	0.026806	0.281465 ± 0.000009	**-10.5** ± 0.3	–	–	**3.00**	–	–
21.1	centre	**1652** ± 24	1.64	0.281530	0.000651	0.021579	0.281510 ± 0.000041	**-7.9** ± 1.4	–	–	**2.87**	–	–
	edge			0.281554	0.000494	0.015276	0.281539 ± 0.000026	**-6.9** ± 0.9	–	–	**2.81**	–	–
22.1	centre	**1653** ± 61	2.97	0.281553	0.000692	0.023427	0.281531 ± 0.000026	**-7.1** ± 0.9	–	–	**2.83**	0.0020155 ± 0.0086	**7.2** ± 0.09
	edge			0.281518	0.000530	0.016059	0.281501 ± 0.000024	**-8.2** ± 0.8	–	–	**2.89**	0.0020146 ± 0.0068	**6.8** ± 0.07
24.1	centre	**1633** ± 18	1.30	0.281669	0.000865	0.029687	0.281642 ± 0.000039	**-3.7** ± 1.4	–	–	**2.59**	0.0020157 ± 0.0085	**7.3** ± 0.09
	edge			0.281514	0.000687	0.022640	0.281493 ± 0.000038	**-9.0** ± 1.3	–	–	**2.93**	0.0020150 ± 0.0077	**7.0** ± 0.08
27.1	centre	**1667** ± 17	1.81	0.281458	0.001654	0.054282	0.281406 ± 0.000025	**-11.3** ± 0.9	–	–	**3.10**	0.0020152 ± 0.0088	**7.1** ± 0.09
	edge			0.281485	0.000590	0.018749	0.281466 ± 0.000028	**-9.1** ± 1.0	–	–	**2.96**	0.0020147 ± 0.0085	**6.8** ± 0.09
28.1	centre	**1673** ± 17	1.36	0.281520	0.000343	0.010977	0.281509 ± 0.000014	**-7.5** ± 0.5	–	–	**2.86**	0.0020152 ± 0.0092	**7.0** ± 0.10
	edge			0.281525	0.000579	0.018337	0.281507 ± 0.000019	**-7.6** ± 0.7	–	–	**2.87**	0.0020146 ± 0.0098	**6.8** ± 0.10
29.1	centre	**1649** ± 46	2.07	0.281525	0.000663	0.022561	0.281504 ± 0.000013	**-8.2** ± 0.5	–	–	**2.89**	0.0020157 ± 0.0103	**7.3** ± 0.11
	edge			0.281500	0.000796	0.027377	0.281475 ± 0.000013	**-9.2** ± 0.5	–	–	**2.95**	0.0020153 ± 0.0096	**7.1** ± 0.10
32.1		**1586** ± 29	1.59	0.281440	0.000507	0.017385	0.281425 ± 0.000015	**-12.4** ± 0.5	–	–	**3.11**	–	–
inherited													
5.1	–	**2116** ± 10	0.55	0.281503	0.000680	0.024626	0.281476 ± 0.000020	**1.4** ± 0.7	–	-9.0	**2.64**	0.0020100 ± 0.0080	4.5 ± 0.08
9.1	–	**2125** ± 15	0.30	0.281155	0.000075	0.002723	0.281152 ± 0.000008	**-9.9** ± 0.3	–	-20.7	**3.36**	0.0020159 ± 0.0066	7.4 ± 0.07
Discretion Granite													
GSWA 142855: porphyritic monzogranite													
magmatic													
2.1	–	**1619** ± 42	1.62	0.281434	0.000734	0.028678	0.281412 ± 0.000013	**-12.2** ± 0.5	–	–	**3.12**	–	–
3.1	–	**1591** ± 36	2.92	0.281484	0.001490	0.052390	0.281439 ± 0.000010	**-11.8** ± 0.4	–	–	**3.07**	–	–
4.1	–	**1634** ± 31	3.64	0.281515	0.001635	0.068110	0.281464 ± 0.000021	**-9.9** ± 0.7	–	–	**2.99**	–	–
5.1	–	**1561** ± 45	1.78	0.281433	0.000823	0.031433	0.281409 ± 0.000017	**-13.6** ± 0.6	–	–	**3.16**	–	–
7.1	–	**1625** ± 172	2.62	0.281437	0.000639	0.024201	0.281417 ± 0.000015	**-11.8** ± 0.5	–	–	**3.10**	0.0020144 ± 0.0067	**7.1** ± 0.07
8.1	–	**1639** ± 31	2.97	0.281553	0.001456	0.057383	0.281508 ± 0.000019	**-8.3** ± 0.7	–	–	**2.89**	0.0020143 ± 0.0073	**7.1** ± 0.08

Analysis No.	Spot location	$^{207}Pb/^{206}Pb$ date (Ma)	Th/U	$^{176}Hf/^{177}Hf$ measured	$^{176}Lu/^{177}Hf$ measured	$^{176}Yb/^{177}Hf$ measured	$^{176}Hf/^{177}Hf$ initial	$\varepsilon_{Hf(t)}$	$\varepsilon_{Hf(1800\ Ma)}$	$\varepsilon_{Hf(1650\ Ma)}$	T_{DM}^2 (Ga)	$^{18}O/^{16}O$ (a)(b)	$\delta^{18}O$ (c)
10.1	centre	**1682** ± 63	2.32	0.281429	0.000735	0.027279	0.281406 ± 0.000018	**-10.9** ± 0.6	–	–	**3.09**	0.0020147 ± 0.0082	**7.3** ± 0.09
	edge			0.281412	0.000565	0.016494	0.281394 ± 0.000016	**-11.4** ± 0.6	–	–	**3.11**	0.0020128 ± 0.0077	**6.3** ± 0.08
14.1	centre	**1597** ± 42	1.91	0.281508	0.000994	0.038911	0.281478 ± 0.000016	**-10.3** ± 0.6	–	–	**2.98**	0.0020140 ± 0.0099	**7.2** ± 0.09
	edge			0.281400	0.000578	0.018457	0.281383 ± 0.000017	**-13.7** ± 0.6	–	–	**3.19**	0.0020137 ± 0.0085	**6.8** ± 0.09
17.1	centre	**1623** ± 43	2.00	0.281485	0.000689	0.027376	0.281464 ± 0.000025	**-10.2** ± 0.9	–	–	**3.00**	0.0020140 ± 0.0099	**7.0** ± 0.10
	edge			0.281435	0.000818	0.030479	0.281410 ± 0.000014	**-12.1** ± 0.5	–	–	**3.12**	0.0020134 ± 0.0085	**6.6** ± 0.09
20.1	centre	**1629** ± 25	1.85	0.281400	0.001366	0.052132	0.281358 ± 0.000016	**-13.8** ± 0.6	–	–	**3.23**	0.0020139 ± 0.0090	**6.9** ± 0.09
	edge			0.281463	0.000680	0.026502	0.281442 ± 0.000014	**-10.9** ± 0.5	–	–	**3.04**	0.0020143 ± 0.0090	**7.1** ± 0.09
24.1	centre	**1629** ± 50	1.65	0.281430	0.000793	0.029649	0.281406 ± 0.000018	**-12.2** ± 0.6	–	–	**3.12**	0.0020134 ± 0.0086	**6.6** ± 0.09
	edge			0.281405	0.000770	0.026143	0.281381 ± 0.000016	**-13.0** ± 0.6	–	–	**3.18**	0.0020133 ± 0.0071	**6.6** ± 0.07
25.1	centre	**1664** ± 46	2.27	0.281476	0.000814	0.031949	0.281450 ± 0.000016	**-9.8** ± 0.6	–	–	**3.00**	0.0020147 ± 0.0101	**7.3** ± 0.10
	edge			0.281446	0.000551	0.017234	0.281429 ± 0.000011	**-10.5** ± 0.4	–	–	**3.05**	0.0020145 ± 0.0088	**7.2** ± 0.09

NOTES: (a) Each δO^{18} uncertainty (1σ) represents the sum of counting statistics errors for each individual spot and the external error based on all standards analysed during the session, which were added in quadrature
(b) Background corrected raw ratios corrected for measured Faraday offsets and yields
(c) Normalized to a Pengali value of 5.3‰

This Report documents the Hf and O isotopic compositions of magmatic and inherited zircons from several felsic magmatic supersuites in the Capricorn Orogen of Western Australia. The results of this study permit the differentiation history of this portion of late Archean to Proterozoic orogenic crust, and provide a unique insight into the processes that led to 'cratonization' of continental lithosphere. This has been an important geological process on Earth since the Archean, which has led to the long-term stability of the continents. The data show that cratonization is driven by deep crustal melting with the transfer of melts to shallower regions resulting in a strongly chemically stratified crust, with a refractory, dehydrated lower portion overlain by a complementary enriched upper portion. The isotope data also identify a previously unknown crustal reservoir in the Capricorn Orogen that may represent the remnants of an Ophthalmian-age magmatic arc.

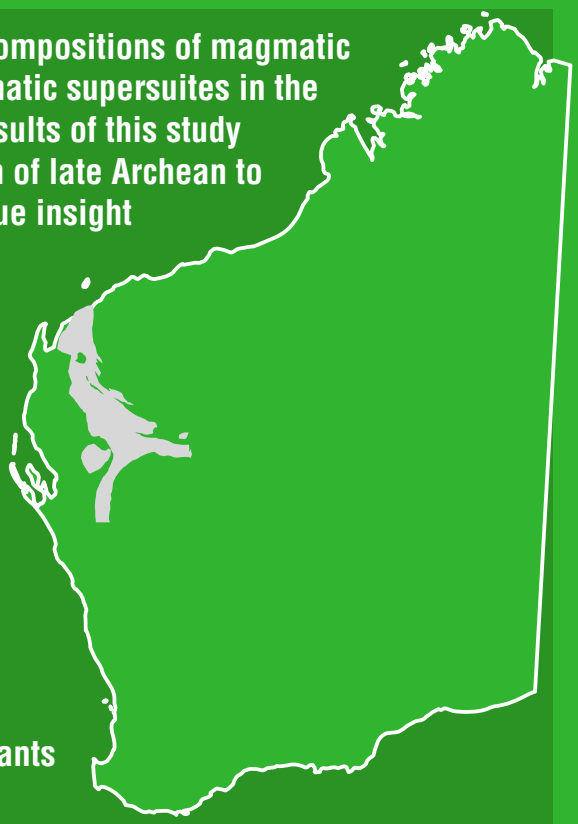

Further details of geological products and maps produced by the Geological Survey of Western Australia are available from:

Information Centre
Department of Mines and Petroleum
100 Plain Street
EAST PERTH WA 6004
Phone: (08) 9222 3459 Fax: (08) 9222 3444

www.dmp.wa.gov.au/GSWApublications